

Hydroacoustic Evaluation of the Effects of Spill Treatments on Fish Passage at Ice Harbor Dam in 2003



R. A. Moursund
K. D. Ham
P. S. Titzler
F. Khan

FINAL REPORT
31 March 2004

Prepared for
the U.S. Army Corps of Engineers
Walla Walla District
Walla Walla, Washington
under Contract DACW68-02-D-0001
Task Order No. 05

Battelle
The Business of Innovation

LEGAL NOTICE

This report was prepared by Battelle Memorial Institute (Battelle) as an account of sponsored research activities. Neither Client nor Battelle nor any person action on behalf of either:

MAKES ANY WARRANTY OR REPRESENTATION, EXPRESS OR IMPLIED, with respect to the accuracy, completeness, or usefulness of the information contained in this report, or that the use of any information, apparatus, process, or composition disclosed in this report may not infringe privately owned rights; or

Assumes any liabilities with respect to the use of, or for damages resulting from the use of, any information, apparatus, process, or composition disclosed in this report.

Reference herein to any specific commercial product, process, or service by trade name, trademark, manufacture or otherwise, does not necessarily constitute or imply its endorsement, recommendation, or favoring by Battelle. The views and opinions of authors expressed herein do not necessarily state or reflect those of Battelle.

Hydroacoustic Evaluation of the Effects of Spill Treatments on Fish Passage at Ice Harbor Dam in 2003

R. A. Moursund
K. D. Ham
P. S. Titzler
F. Khan

31 March 2004

Prepared for
the U.S. Army Corps of Engineers
Walla Walla District
Walla Walla, Washington
under Contract DACW68-02-D-0001

Battelle, Pacific Northwest Division
P.O. Box 999
Richland, Washington 99352

Summary

Battelle Pacific Northwest Division conducted this study in 2003 for the U.S. Army Corps of Engineers, Walla Walla District (Corps) to evaluate downstream fish passage at Ice Harbor Dam. The initial goal of this fixed-aspect hydroacoustic study was to estimate fish passage efficiency (FPE) for two spill treatments, nominally plunging vs. skimming flow conditions where the spill meets the water in the tailrace. However, in response to early survival test results, test conditions were altered midway through the summer to test a bulk spill pattern. This bulk spill pattern (spilling normal quantities through fewer gates) was compared to a no spill condition during the remainder of summer only. Each spill treatment for all tests was assigned to the first or last two consecutive days within four day blocks.

The passage monitoring period extended from 15 April to 15 July. The transition from spring to summer occurred June 7 based on when the dominant species and run in the Smolt Monitoring Program at Lower Monumental Dam switched from steelhead (*Oncorhynchus mykiss*) and yearling Chinook (*O. tshawytscha*) to subyearling Chinook (*O. tshawytscha*). Flows were near normal, on average, with a spring freshet peak on May 31. All blocks were accepted for the statistical analysis, acknowledging that the dam operations as attained were a typical application of the planned treatment conditions.

Fish passage efficiency was consistently high at this project, approximately 95%. The spillway was a major passage route with 54% of the fish utilizing this route with about 50% of the river flow during the day. Higher spill proportions at night resulted in 70% of fish utilizing this route. Fish passage efficiency was statistically different between BiOp and Spill50 treatments in both spring and summer periods, and also between BulkBiOp and NoSpill treatments tested in summer. Fish guidance efficiency (FGE), however, did not differ significantly among treatments for any of the combinations tested. The spill treatment test results are summarized below in Table S.1.

As a basis for maximizing project survival at Ice Harbor Dam, we've shown that route-specific passage and project-wide passage performance metrics differ among operational treatments. The biological significance of these metrics will become clearer when the results of concurrent studies of route specific survival are published. The fish trajectory information and vertical distributions immediately upstream of the Tainter gates will be useful in designing direct survival studies that rely on hose releases to introduce fish into spill routes. Finally, the horizontal distributions of fish passage across all treatments suggest that a Removable Spillway Weir or similar structure would be most effective at or near spill Bay 3.

Table S.1. Mean Fish Passage Metrics for the Spill Treatments During Spring and Summer Seasons

	FPE	SPE	SPS	FGE
Spring (BiOp Spill50)	97.4% 94.3% ^(a)	81.4% 56.0%*	1.12 1.01	85.1% 85.6%
Summer (BiOp Spill50)	96.9% 92.7%	76.4% 65.4%	1.07 1.27*	81.5% 77.8%
Summer (BulkBiOp NoSpill)	98.8% 87.7%*			93.2% 87.7%

(a) Indicates a statistically significant difference (ANOVA, $\alpha = 0.05$).

Acknowledgments

We sincerely acknowledge the cooperation, assistance, and hard work of the following:

U.S. Army Corps of Engineers staff:

Mark Smith for overall project oversight; Mark Plummer and Bill Rose for their research coordination activities at the dam; Scott Sutliff for operations management; Ice Harbor Dam control room operators for tag out clearances and outage coordination; mechanical staff (riggers and electricians) for their support at the dam; and Mike Remington for dive safety coordination. Thanks to all of the above for their common commitment to safety.

Battelle staff:

Susan Thorsten for server administration, data management, and backups; Eric Robinson for database management and support; Jessica Vucelick for data management and collection at the dam; Matt Bleich and Nathan Phillips for installation support. Chris Cook, John Serkowski, and Marshall Richmond created the spillway computational fluid dynamics model used in the fish trajectory visualizations.

Mevatec staff:

Peter Johnson led the Mevatec team with Kiel Bouchard and Shon Zimmerman in the field for equipment installation. Michale Botu, Robert Warrington, Fenya Kashergen, and Kathleen Cullen were the 24/7 system monitors at the project.

Divers:

Global Diving and Salvage, Inc. installed and removed the powerhouse transducers.

Mobile Crane:

Lampson International provided on-site mobile crane support.

Contents

Summary	iii
Acknowledgments.....	v
1.0 Introduction.....	1.1
1.1 Background	1.1
1.2 Previous Studies	1.1
1.3 Study Goals and Objectives	1.2
1.4 Study Site Description.....	1.2
1.5 Report Organization	1.2
2.0 Methods.....	2.1
2.1 Study Design	2.1
2.2 Hydroacoustic Sampling System.....	2.2
2.3 Powerhouse Sampling	2.3
2.4 Spillway Sampling	2.4
2.5 Data Processing	2.4
2.5.1 Dam Operations	2.4
2.5.2 Autotracking	2.5
2.5.3 Detectability and Effective Beam Widths.....	2.5
2.5.4 Spatial and Temporal Expansion	2.5
2.6 Data Analysis	2.6
2.6.1 Organization.....	2.6
2.6.2 Performance Measures.....	2.6
3.0 Results.....	3.1
3.1 Study Conditions	3.1
3.1.1 River Discharge and Temperature	3.1
3.1.2 Species Composition and Run Timing	3.2
3.1.3 Dam Operations	3.3
3.2 Seasonal Fish Passage	3.5
3.2.1 Passage Metrics.....	3.5
3.2.2 Daily Trends	3.6
3.2.3 Seasonal Diel Passage.....	3.9

3.2.4	Horizontal Distributions	3.9
3.2.5	Continuous Spill Curves	3.10
3.3	BiOp vs. Spill50 Treatment Effects	3.12
3.3.1	Analysis of Variance.....	3.14
3.3.2	Diel Trends by Treatment	3.16
3.3.3	Horizontal Distribution by Treatment.....	3.17
3.4	BulkBiOp vs. NoSpill Treatment Effects	3.18
3.4.1	Analysis of Variance.....	3.19
3.4.2	Diel Trends by Treatment	3.20
3.4.3	Horizontal Distributions by Treatment	3.20
3.5	Fish Trajectories.....	3.21
3.5.1	Spillway Trajectories, Vertical Distributions, and Flows	3.21
3.5.2	Spring vs. Summer Vertical Distributions by Spill Gate Opening	3.26
3.5.3	Powerhouse Trajectories and Vertical Distributions	3.28
4.0	Discussion	4.1
4.1	General Fish Passage.....	4.1
4.2	Fish Passage During Spill Treatments.....	4.1
4.3	Fish Trajectories and Vertical Distributions at the Spillway.....	4.3
4.4	Potential RSW Placement	4.3
5.0	Conclusion	5.1
6.0	References.....	6.1
	Appendix A – Statistical Synopsis.....	A.1
	Appendix B – Effective Beam Widths.....	B.1
	Appendix C – Hourly Spill by Block.....	C.1
	Appendix D – Fish Trajectories by Spill Gate Opening	D.1
	Appendix E – Vertical Distributions by Season and Diel Period	E.1
	Appendix F – System Calibrations	F.1
	Appendix G – Equipment Diagrams.....	G.1
	Appendix H – (See attached CD)	

Figures

1.1	Ice Harbor Dam Configuration and Bathymetry	1.3
2.1	Plan View of the Powerhouse and Spillway Showing Each System and Transducer Locations	2.2
2.2	Side View of the Intake Transducer Aiming Angles and Sampling Volumes	2.3
2.3	Spillway Transducer Mount Deployment	2.4
3.1	Daily River Discharge, Spill, and Temperature for 2003 and the 10-yr Average	3.1
3.2	Species Composition Data from the Lower Monumental Dam Smolt Monitoring Facility	3.2
3.3	Lower Monumental Dam Smolt Monitoring Program and Hydroacoustic Estimate Comparison of Run Timing	3.3
3.4	Correlation Scatterplot for Adjusted Lower Monumental Dam Smolt Monitoring Index vs. Hydroacoustic Estimate	3.3
3.5	Turbine Unit Operating Preference	3.4
3.6	Graphical Representation of the Regular BiOp Spill Pattern and the BulkBiOp Spill Pattern	3.4
3.7	Hourly River Discharge Through the Powerhouse and Spillway for the Season.....	3.5
3.8	Fish Passage Efficiency and Spill Passage Efficiency in Spring Summer and Day Night.....	3.6
3.9	Spill Passage Effectiveness and Fish Guidance Efficiency in Spring Summer and Day Night	3.6
3.10	Daily Fish Passage Efficiency Trend Across the Season	3.7
3.11	Daily Spill Passage Efficiency Trend Across the Season	3.7
3.12	Daily Spill Passage Effectiveness Trend Across the Season	3.8
3.13	Daily Fish Guidance Efficiency Trend for the Entire Powerhouse Across the Season.....	3.8
3.14	Diel Passage During the Spring and Summer	3.9
3.15	Horizontal Distribution of Fish Passage and Flow During the Spring and Summer.....	3.10
3.16	Spring and Summer Fish Guidance Efficiency by Unit.....	3.10
3.17	Fish Passage Efficiency vs. Percent Spill by Season and Diel Period	3.11
3.18	Spill Passage Efficiency vs. Percent Spill by Season and Diel Period.....	3.11

3.19	Spill Passage Effectiveness vs. Percent Spill by Season and Diel Period.....	3.12
3.20	Fish Guidance Efficiency vs. Continuous Percent Spill by Season and Diel Period	3.12
3.21	Example Hourly Spill by Block Plots	3.13
3.22	Fish Passage Efficiency and Spill Passage Efficiency by Block.....	3.14
3.23	Spill Passage Effectiveness and Fish Guidance Efficiency by Block	3.14
3.24	Fish Passage Efficiency and Spill Passage Efficiency by Treatment.....	3.16
3.25	Spill Passage Effectiveness and Fish Guidance Efficiency by Treatment	3.16
3.26	Diel Passage During the Spring BiOp and Spill50 Treatments for the 11 Available Blocks...	3.17
3.27	Diel Passage During the Summer BiOp and Spill50 Treatments for the 4 Selected Blocks....	3.17
3.28	Horizontal Passage and Flow Distribution in Spring During the BiOp and Spill50 Treatments for the 11 Available Blocks.....	3.18
3.29	Horizontal Passage and Flow Distribution in Summer During the BiOp and Spill50 Treatments for the 4 Available Blocks.....	3.18
3.30	Fish Passage Efficiency and Fish Guidance Efficiency Trends by Block.....	3.19
3.31	Fish Passage Efficiency and Fish Guidance Efficiency by Treatment for Summer BulkBiOp vs. NoSpill.....	3.19
3.32	Diel Passage During the Summer BulkBiOp Spill Period and the NoSpill Period.....	3.20
3.33	Horizontal Passage and Flow Distribution in Summer During the BulkBiOp Spill Period and the NoSpill Period	3.21
3.34	Spill Bay Plots Feature Legend.....	3.22
3.35	Fish Trajectories, Vertical Distribution, Flows, and Release Pipe Locations for 3-ft Gate in Spring	3.23
3.36	Fish Trajectories, Vertical Distribution, Flows, and Release Pipe Locations for 6-ft Gate in Spring	3.23
3.37	Fish Trajectories, Vertical Distribution, Flows, and Release Pipe Locations for 9-ft Gate in Spring	3.24
3.38	Fish Trajectories, Vertical Distribution, Flows, and Release Pipe Locations for 3-ft Gate in Summer.....	3.24
3.39	Fish Trajectories, Vertical Distribution, Flows, and Release Pipe Locations for 6-ft Gate in Summer.....	3.25

3.40	Fish Trajectories, Vertical Distribution, Flows, and Release Pipe Locations for 9-ft Gate in Summer.....	3.25
3.41	Vertical Distribution of Fish Abundance at Guided and Unguided Deployments.....	3.26
3.42	Vertical Distribution of Fish Abundance at 1- and 2-ft Gate Openings.....	3.26
3.43	Vertical Distribution of Fish Abundance at 3- and 4-ft Gate Openings.....	3.27
3.44	Vertical Distribution of Fish Abundance at 5- and 6-ft Gate Openings.....	3.27
3.45	Vertical Distribution of Fish Abundance at 7- and 8-ft Gate Openings.....	3.27
3.46	Vertical Distribution of Fish Abundance at a 9-ft Gate Opening.....	3.28
3.47	Powerhouse Trajectories and Vertical Distribution	3.28
4.1	Historic River Channel in the Forebay of Ice Harbor Dam	4.4

Tables

S.1	Mean Fish Passage Metrics for the Spill Treatments During Spring and Summer Seasons	iii
2.1	Nominal Treatment Schedule.....	2.1
2.2	Test Hypotheses	2.2
3.1	The Number of Treatment Blocks Available in Each Treatment and Season Combination....	3.13
3.2	ANOVA Results for Fish Passage Efficiency and Spill Passage Efficiency in Spring for the 11 Available Blocks	3.15
3.3	ANOVA Results for Spill Passage Effectiveness and Fish Guidance Efficiency in Spring for the 11 Available Blocks.....	3.15
3.4	ANOVA Results for Fish Passage Efficiency and Spill Passage Efficiency in Summer for the 4 Available Blocks.....	3.15
3.5	ANOVA Results for Spill Passage Effectiveness and Fish Guidance Efficiency in Summer for the 4 Available Blocks	3.15
3.6	ANOVA Results for Fish Passage Efficiency and Fish Guidance Efficiency in Summer for the 5 Available Blocks.....	3.19
4.1	Spring ANOVA Summary	4.2
4.2	Summer ANOVA Summary	4.2

1.0 Introduction

This report presents results of a hydroacoustic evaluation of juvenile salmonid passage funded by the Walla Walla District of the U.S. Army Corps of Engineers and conducted at Ice Harbor Dam by a team of researchers led by Battelle Pacific Northwest Division. This study was a comparison of the effect of two spill treatments on fish passage. The District funded other parallel research on juvenile salmonids at this location in 2003, including a radio telemetry study by the National Oceanic and Atmospheric Administration, National Marine Fisheries Service (NOAA Fisheries), a direct survival study by Normandeau, and a sensor fish study also by Battelle.

1.1 Background

The U.S. Army Corps of Engineers is committed to improving fish passage and increasing survival rates for fish passing its hydroelectric projects on the Snake and Columbia Rivers. At Ice Harbor Dam, this strategy entails the use of spill and implementation of submerged traveling screens (STS) as parts of a juvenile bypass system (JBS). The conversion of the ice and trash sluiceway to become the collection channel of the juvenile bypass system occurred in 1995 and 1996. The implementation of a spillway weir is now under consideration for Ice Harbor Dam.

Previous survival studies at Ice Harbor Dam showed poor survival at the spillway, and thus the spillway became the focus of this research. Based on physical hydraulic models from the USACE Waterways Experiment Station, spill conditions were generalized into two categories: skimming or plunging flows. The spill amounts mandated by the biological opinion (BIOP, NMFS 2000) are likely to result in plunging flows under common tailrace conditions. Since river managers cannot regulate the tailrace water elevations at Ice Harbor Dam (it is free flowing until near the confluence of the Columbia), one possibility was that the flow deflectors were causing fish to be injured at higher rates than at other dams where tailrace conditions are more likely to produce skimming flows. By changing the amount of water spilled, it might be possible to alter how fish pass through the flow deflector area. Skimming flows may exhibit better survival if they result in safer passage at the flow deflectors than under plunging flow conditions. In order to evaluate this assumption, both direct and indirect methods of survival estimation studies were undertaken along with a study to determine how many fish use these passage routes under various operational conditions. This study addressed the latter.

1.2 Previous Studies

Project passage estimates have been made previously with both hydroacoustic and radio tag methodologies. Hydroacoustic studies were conducted 1982, 1983, 1986, 1987, and 1995. Early studies focused on the efficiency of the ice and trash sluiceway at passing juvenile salmonids. The 1995 study focused on testing baffle extensions in front of the ice and trash sluiceway for enhancing fish passage through that route. By 1996, the current juvenile bypass system was installed which included standard length submersible traveling screens and a collection channel housed in the former ice and trash sluiceway.

1.3 Study Goals and Objectives

The goal of this study was to collect critical information for the U.S. Army Corps of Engineers spill passage program to optimize project passage. Initially, dam operations were structured to measure the proportion of downstream migrants utilizing the various passage routes during only two spill treatments. These test conditions later evolved into an additional two spill treatment test for the summer. Ultimately, this information can be combined with survival estimates to optimize downstream fish passage at Ice Harbor Dam. Specific objectives for this study were to:

- Estimate the proportion of juvenile salmon passing the dam through each passage route, and in relation to discharge.
- Test for significant differences in fish passage efficiency, spill passage efficiency/effectiveness, and fish guidance efficiency (FGE) for skimming vs. plunging spill treatments.
- Present the horizontal distributions of fish passage at the spillway and powerhouse by diel period, spill level, and spill treatment with emphasis on potential placement of a Removable Spillway Wier (RSW).
- Present the temporal passage patterns for the turbine and spillway for the two spill treatments.

1.4 Study Site Description

Ice Harbor Dam is a run-of-the-river hydroelectric facility located at Snake River mile 9.7. Major structures include a navigation lock on the north shore, a powerhouse on the south shore, and a spillway in between. Of the 2,822-ft overall length, the 671-ft powerhouse contains 6 turbine units while the 590-ft spillway contains 10 Tainter gates. Standard length STS are installed at all of the turbine unit intakes. The ice and trash sluiceway has been permanently walled off for use as the collection channel of the juvenile bypass system. The 10-yr average (1993-2002) forebay elevation during the fish passage season is 438 ft above mean sea level. A juvenile fish facility and egress for the juvenile bypass system is located on the south shore. Turbine units are numbered 1 to 6 from south to north. Spill bays are numbered from 1 to 10 also from south to north. Each turbine unit is divided into three intakes, identified as A, B, and C, beginning from the south. The thalweg, or historic river channel, is near the junction of the powerhouse and spillway (Figure 1.1).

1.5 Report Organization

This report has several sections. The study and explanation of the research are put into context in the Introduction. The Methods section describes the equipment used and sampling scheme. Within Results, the environmental and operational characteristics during the study are shown in Study Conditions. Results are apportioned into a Seasonal Fish Passage section and two Treatment sections. The Seasonal Fish Passage section reports on fish passage efficiency (FPE) and other project-wide fish passage metrics. The two Spill Treatment Effects sections examine in detail the relationship of spill levels with fish passage. The results are then brought together in the Discussion section and summarized in the Conclusion section. References and Appendices comprise the final two sections.

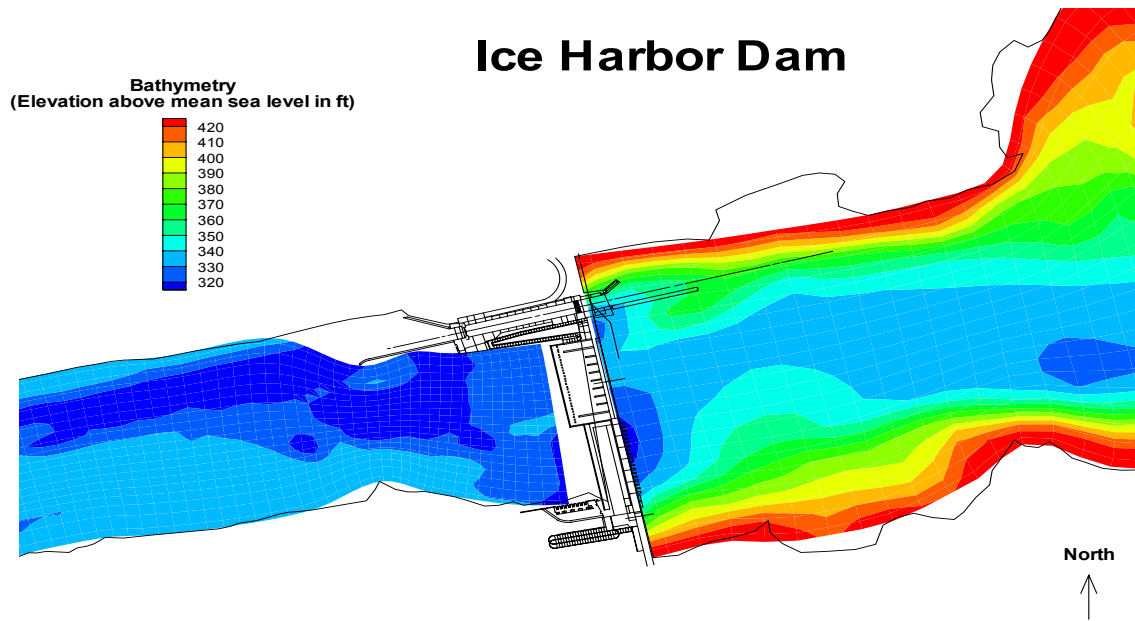


Figure 1.1. Ice Harbor Dam Configuration and Bathymetry

2.0 Methods

Fixed-aspect hydroacoustic methods were used to estimate fish passage through all routes. Single-beam and split-beam transducers were deployed to estimate fish passage rates and distributions. This approach uses the acoustic screen model to determine passage rates. At each type of passage route, split-beam transducer deployments were used to estimate the average backscattering cross-section of fish for detectability modeling and the direction of fish travel through sampling volumes to assess the assumptions of the acoustic screen model. The transducer sampling volumes were strategically aimed to minimize ambiguity in ultimate fish passage routes and the potential for multiple detections. Hourly estimates of passage through individual routes were combined to evaluate passage performance across varied spatial and temporal scales of interest and in relation to flow.

2.1 Study Design

Spill was manipulated during this study for the purpose of testing two sets of paired treatment comparisons. A stratified block design was used with four-day blocks. Each treatment was in place for two days in an alternating sequence. Each treatment day began at 0500 h and ended at 0459 h. Nighttime extended from 1900 h through 0459 h. Data collection occurred from 15 April through 15 July, 2003. The first set of paired treatments were nominally either skimming spill (50% for 24 hrs, referred to as Spill50) or plunging spill (45 kcfs daytime with 100% up to 100 kcfs at night, referred to as BiOp) (Table 2.1). The second set of paired treatments occurred during the summer only and was comprised of a bulk spill pattern (at BiOp flows, referred to as BulkBiOp) or no spill (referred to as NoSpill). Null and alternate hypotheses for testing are shown in Table 2.2.

Table 2.1. Nominal Treatment Schedule. The season switched from spring to summer at the red line (shown below) between blocks 11 and 12.

Month	Day	Block	Test	Month	Day	Block	Test	Month	Day	Block	Test
April	23		BIOP	May	27	9	BIOP	June	30	18	NoSpill
April	24		BIOP	May	28	9	SP50	July	1	18	NoSpill
April	25		BIOP	May	29	9	SP50	July	2	19	BULK
April	26	1	BIOP	May	30	10	BIOP	July	3	19	BULK
April	27	1	SP50	May	31	10	BIOP	July	4	19	NoSpill
April	28	2	BIOP	June	1	10	SP50	July	5	20	BULK
April	29	2	BIOP	June	2	10	SP50	July	6	20	BULK
April	30	2	SP50	June	3	11	BIOP	July	7	20	NoSpill
May	1	2	SP50	June	4	11	BIOP	July	8	20	NoSpill
May	2	3	BIOP	June	5	11	SP50	July	9	21	BULK
May	3	3	BIOP	June	6	11	SP50	July	10	21	NoSpill
May	4	3	SP50	June	7	12	BIOP	July	11	22	BULK
May	5	3	SP50	June	8	12	BIOP	July	12		Bulk*
May	6	4	BIOP	June	9	12	SP50	July	13		SURV
May	7	4	BIOP	June	10	12	SP50	July	14		SURV
May	8	4	SP50	June	11	13	BIOP	July	15		SURV
May	9	4	SP50	June	12	13	BIOP	July	16		NoSpill
May	10	5	BIOP	June	13	13	SP50	July	17		Bulk*
May	11	5	BIOP	June	14	13	SP50	July	18		Bulk*
May	12	5	SP50	June	15	14	BIOP	July	19		Bulk*
May	13	5	SP50	June	16	14	BIOP	July	20		Bulk*
May	14	6	BIOP	June	17	14	SP50	July	21		Bulk*
May	15	6	BIOP	June	18	14	SP50	July	22		Bulk*
May	16	6	SP50	June	19	15	BIOP	July	23		Bulk*
May	17	6	SP50	June	20	15	BIOP	July	24		Bulk*
May	18	7	BIOP	June	21	15	SP50				
May	19	7	BIOP	June	22	15	SP50				
May	20	7	SP50	June	23	16	BIOP				
May	21	7	SP50	June	24	17	BULK				
May	22	8	BIOP	June	25	17	BULK				
May	23	8	BIOP	June	26	17	NoSpill				
May	24	8	SP50	June	27	17	NoSpill				
May	25	8	SP50	June	28	18	BULK				
May	26	9	BIOP	June	29	18	BULK				

* Did not spill over 24-hr period

2.3 Powerhouse Sampling

One single-beam system and two split-beam systems were used to monitor the turbine intakes. One intake within each of the six units were randomly selected and monitored. Pairs of 6° single-beam transducers were deployed at units 2C and 5A, and pairs of 6° split-beam transducers were deployed at units 1A, 3B, 4C, and 6B. Split-beam systems sampled at a rate of 25 pings per second, slow multiplexing 1 transducer at 88-sec intervals, 10 times per hour. Single-beam systems sampled at a rate of 25 pings per second, slow multiplexing 1 transducer at 58-sec intervals, 10 times per hour.

Intake transducer mounts were designed to fit between the trash rack vertical members (Figure 2.2). This design allowed divers to secure the mount to the bottom of the trash rack of each intake from the forebay side of the trash racks. This strategy eliminated the need for more costly and time-consuming penetration dives. Transducer, mount, and cable assemblies were sent down with the diver. The diver then pushed the mount between the vertical trash rack members and secured them to a horizontal member via an existing drain hole. Prior to each transducer mount deployment, a 73-ft 2-in. long by 2-in. diameter schedule 40 PVC pipe was deployed through trash rack drain holes that run the entire vertical length of the trash rack. The pipes provided a way to route and protect the telemetry cables from debris and trash raking. Each pipe was cut so that the bottom end sat just above the head of the transducer.

STS intake deployments consisted of two single-beam or split-beam transducers, mounted at an elevation of 129 ft. One of the two transducers in each intake was intended to sample guided fish and was aimed up and above the STS screen tip at 35° from the plane of the trash rack, looking downstream. The second transducer which sampled the unguided volume was aimed directly at the STS screen tip at 63° from the plane of the trash rack (Figure 2.2).

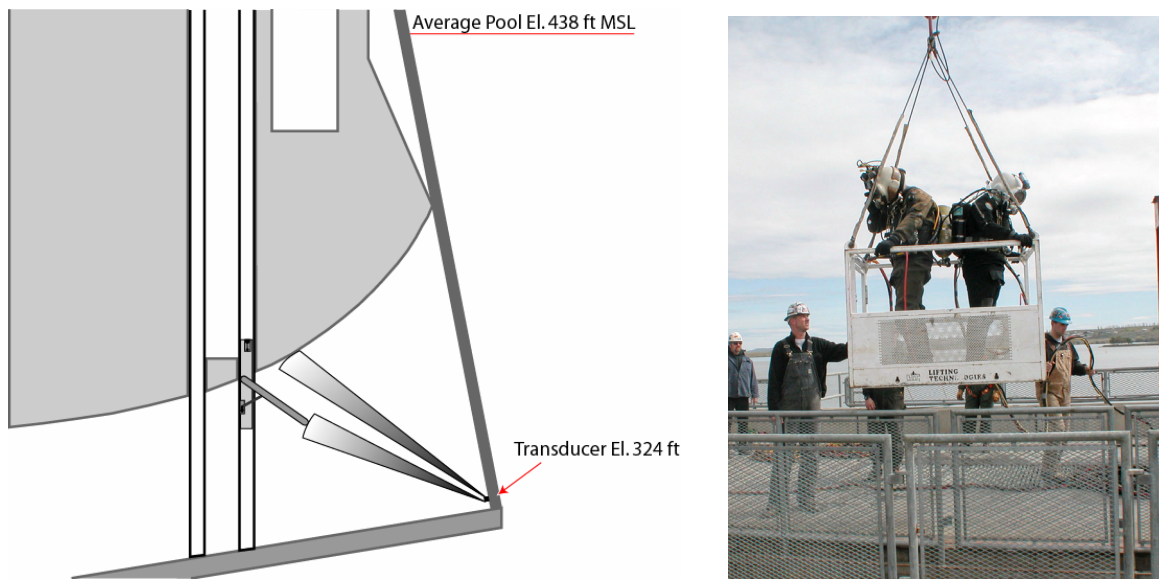


Figure 2.2. Side View of the Intake Transducer Aiming Angles and Sampling Volumes

2.4 Spillway Sampling

One single-beam and two split-beam systems were used to monitor the spillway. Every spill bay was monitored. Each mount was offset in either a north (n), middle (m), or south (s) position to reduce any bias caused by non-uniform distribution within each bay. 10° single-beam transducers were deployed at spill bays 7s and 9m. 10° split-beam transducers were deployed at spill bays 1s, 2n, 3m, 4n, 5s, 6m, 8n, and 10s. The single-beam system sampled at a rate of 25 pings per second, slow multiplexing each transducer at 58-sec intervals, 10 times per hour. The split-beam systems sampled at a rate of 25 pings per second, slow multiplexing each transducer at 88-second intervals, 10 times per hour.

All single-beam and split-beam transducers were deployed from poles mounted on the downstream side of the stop log slots in the spillway. From an elevation of 258 ft, they were aimed 2° downstream from vertical, putting the beam as close to the Tainter gate as possible. The resulting sampling volume assured that fish were committed to passage when detected (Figure 2.3).

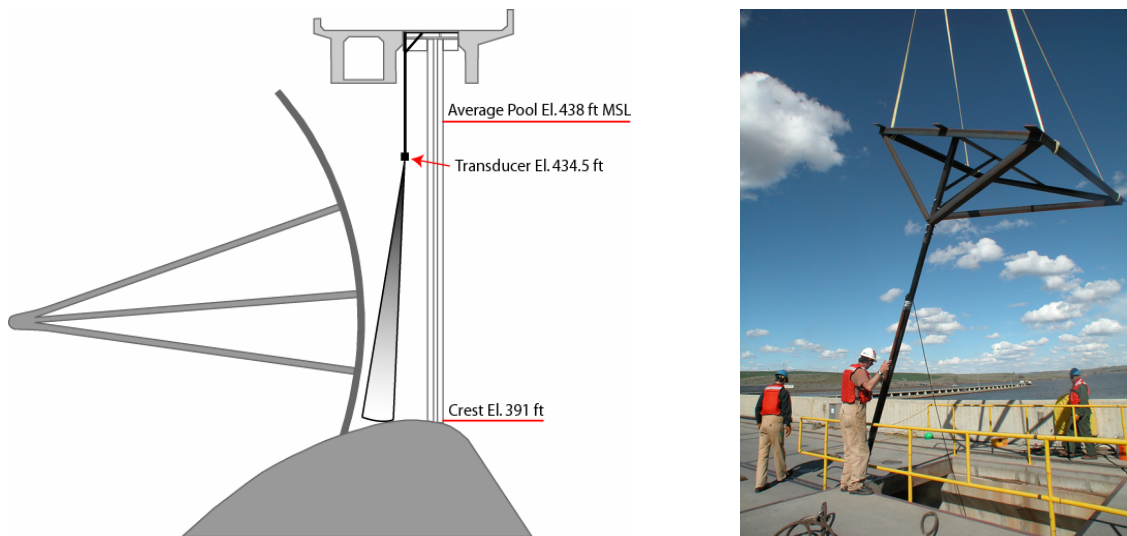


Figure 2.3. Spillway Transducer Mount Deployment. Both the single- and split-beam transducers were mounted in identical configurations.

2.5 Data Processing

This section describes the data processing steps used to produce the fish passage estimates. The output of sounders and transducers are in volts, not passage estimates. Understanding the data processing methods is important to understanding the nature, and quality, of the data.

2.5.1 Dam Operations

Dam operations data were collected by the District on a 5-min basis (24/7) from data acquisition systems. This data was transferred and loaded into the fish passage database. The data had very few periods of missing data, with only 18 of the 5-min intervals missing out of 26208 possible (>99.9% complete). The entire season of dam operations data is included with the raw hourly passage data in Appendix H.

2.5.2 Autotracking

The data produced by both single- and split-beam transducers were processed with autotracking software, which was initially developed by the Portland District and received major revision by Battelle in 2001. The autotracker identifies linear features in echograms. Linear traces that meet minimum criteria are saved as tracks. These criteria were based upon fields contained in the track statistics output by the autotracker. Additional filters eliminate tracks that do not match the criteria established for fish committed to passing. These post-tracking filters were developed to eliminate tracks having characteristics inconsistent with a smolt-sized fish committed to passing the dam by the monitored route. The filtered tracks estimate the number of fish passing the sample volume covered by the effective beam of a transducer.

2.5.3 Detectability and Effective Beam Widths

Split-beam data of smolt movements (e.g., trajectory and speed distributions) through the beam were used as an input to a detectability model. The detectability model also originated from the Portland District. The detectability model simulates individual echoes for fish passing through a transducer beam. The fish movement and echo characteristics are simulated to match those measured in split-beam transducers. A simulated fish is tabulated as detected if enough echoes in a series exceed a minimum number of consecutive echoes and echo strength. The proportion of fish detected in the beam is used to compute an effective beam width. The effective beam width more accurately quantifies how well a beam is able to detect fish than the nominal beam width. Effective beam widths are computed for each meter because track characteristics such as angle and speed that can change with distance from the transducer.

2.5.4 Spatial and Temporal Expansion

Under the acoustic screen model, the number of tracks within the beam is expanded spatially and temporally to estimate total passage through a single passage route. Detected fish are adjusted for detectability and expanded for space and time not sampled. Hourly passage was estimated by expanding the fish that passed through the beam for the cross-sectional area sampled (Equation 1) and sampled fraction per hour (Equation 2). All remaining analyses and response variables derive from these fundamental data. Appendix I is a comma-delimited matrix of the raw hourly passage data on the CD included with this report.

$$W_{ij} = \frac{I_j}{2R_i \tan\left(\frac{\theta_j}{2}\right)} \quad (1)$$

where,

W_{ij} is the i^{th} weighted fish at the j^{th} location

I_j is the width (m) at the j^{th} location

R_i is the midrange (m) of the i^{th} fish

θ_j is the effective beam width of the transducer at the j^{th} location

$$X_{jh} = \left(\frac{K}{k} \right) \sum_{i=1}^{n_{jh}} W_{ijh} \quad (2)$$

where,

X_{jh} is the fish passage at the j^{th} location in the h^{th} hour

W_{ijh} is the i^{th} weighted fish at the j^{th} location in the h^{th} hour

n_{jh} is the number of fish at the j^{th} location in the h^{th} hour

K is the total number of sampling intervals in the hour

k is the number of intervals sampled in the hour

2.6 Data Analysis

Data analysis consisted of estimating fish passage and integrating that with flow and other conditions for specific time periods and passage routes. These general analysis results were then summarized to address specific questions of interest. Care has been taken to account for both spatial and temporal variation in the sampling. The variances were calculated and carried through to the final estimates. The detailed statistical methods are contained in Appendix A.

2.6.1 Organization

The analysis is divided into sections based on the scope of inference for each section. Seasonal fish passage estimates are presented for each season in the first section. Treatment effects are dealt with in the following sections. A series of analyses of variance (ANOVAs) were run on the various fish passage metrics such as fish passage efficiency, spill passage efficiency, and spill passage effectiveness. Graphical presentations were used to illustrate treatment effects on metrics for smaller time scales, such as trends among days or blocks.

2.6.2 Performance Measures

The following fish passage metric terms are used extensively in this report. Understanding of the definitions presented here is critical for interpretation of the results of the study. Fish passage efficiency is the proportion of fish that passed through non-turbine routes at the dam as a whole (Equation 3). Spill passage efficiency (SPE) is the proportion of fish that passed via the spillway (Equation 4). Both fish passage efficiency and spill passage efficiency are unit-less ratios that are reported as a percentage to avoid confusion with spill effectiveness. Spill passage effectiveness (SPS) is the ratio of the proportion of fish passing over the spillway vs. the proportion of water passing over the spillway (Equation 5). It is intended to describe the effectiveness that a particular passage route is at passing fish per unit of water. If fish passed the spillway in the same proportion as water, then spill passage effectiveness would equal 1. Fish guidance efficiency is the percentage of fish guided into the juvenile bypass system by the intake screens (Equation 6). It is intended to be a measure of screen performance.

$$FPE \equiv \frac{X_{guided} + X_{spillway}}{X_{guided} + X_{unguided} + X_{spillway}} \quad (3)$$

$$SPE \equiv \frac{X_{spillway}}{X_{guided} + X_{unguided} + X_{spillway}} \quad (4)$$

$$SPS \equiv \frac{SPE}{Q_{spillway} / (Q_{powerhouse} + Q_{spillway})} \quad (5)$$

$$FGE \equiv \frac{X_{guided}}{X_{guided} + X_{unguided}} \quad (6)$$

where,

X is the fish passage estimate for the subscripted route

Q is the flow of water through that route

3.0 Results

The presentation of results begins with environmental conditions of the study, such as river flow and run timing by species. Next, seasonal (spring and summer) estimates of fish passage are described. This includes seasonal and daily trends, but without reference to spill treatments. The next two sections deal exclusively with the analysis of the spill treatments, as the statistics used and inferences drawn from these sections are distinct. Fish trajectories and vertical distributions are described in the final section.

3.1 Study Conditions

The environmental and dam operational characteristics during the 2003 study are described in this section. These data set the stage and context for the fish passage results that follow. In general, the increase in river flows was slightly later than average this year with a notable peak in flow arriving in late May. The flows for the remainder of the season were somewhat below average.

3.1.1 River Discharge and Temperature

River discharge during the study period averaged 81 kcfs which was 89% of the 10-yr average. The minimum discharge was 29 kcfs on July 13 near the end of the study. The maximum discharge was 203 kcfs on May 31. Spring flows had a near normal average discharge (94% of the 10-yr average), but started slowly and ended with a bang. Summer flows were 82% of the 10-yr average and decreased rapidly, as expected. Spill averaged 47 kcfs (112% of the 10-yr average) with a range of 0 to 113 kcfs. Spill levels were normal except for the period from May 25 to June 5 when high flows occurred. Spring and summer spill levels were 123% and 97% of the 10-yr average, respectively. River temperature increased steadily over the study period, starting at 9.0°C, ending at 20.0°C, and averaged 14.0°C. River temperature over the study period was 99% of the 10-yr average (Figure 3.1). Mean forebay elevation was 438.5 ft msl and varied less than a foot with a range of 438.3 to 438.8 ft msl.

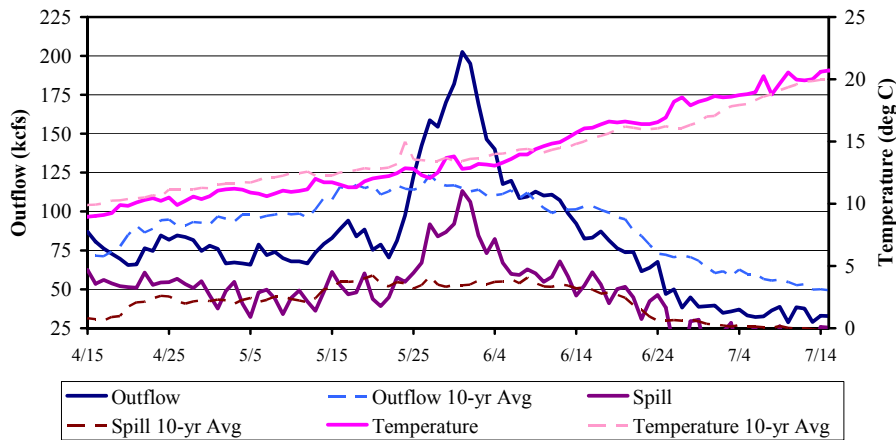


Figure 3.1. Daily River Discharge, Spill, and Temperature for 2003 (solid lines) and the 10-yr Average (dashed lines). Data from DART.

3.1.2 Species Composition and Run Timing

Species composition and run timing data for juvenile salmonids are presented below based on data from the Smolt Monitoring Program at Lower Monumental Dam. The division of spring and summer was based on the transition of dominance of the run from yearling Chinook to subyearling Chinook on June 4. We assumed a lag of 3 days to Ice Harbor dam, including one for sampling and 2 for travel time, so the summer period began June 7 at the sampling location. During spring, 71% of the downstream migrants were steelhead and 27% were steelhead as indicated by smolt monitoring data from the sampling site at Lower Monumental Dam. The numbers of coho, sockeye, and subyearling Chinook smolts were negligible at 1% or less. During summer, 86% of the downstream migrants were subyearling Chinook (Figure 3.2). The first adult shad fallback sighted in the juvenile bypass system this year was on June 27.

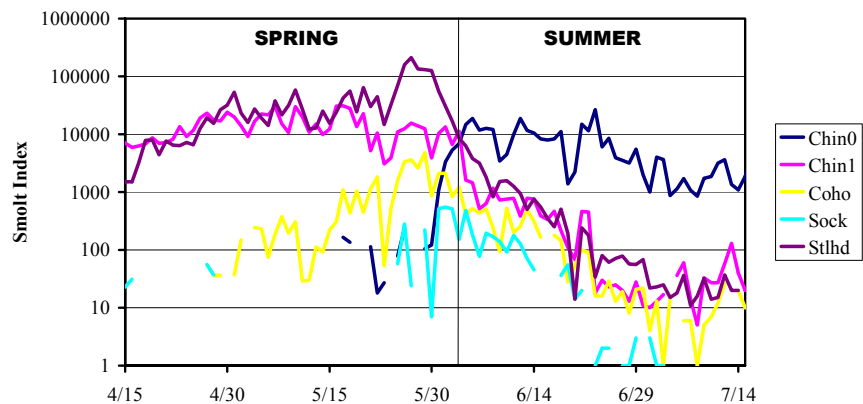


Figure 3.2. Species Composition Data from the Lower Monumental Dam Smolt Monitoring Facility. Data from DART. The vertical division marks the transition from spring to summer.

Trends in hydroacoustic estimates of passage were similar to those exhibited by the number of fish traveling in-river below Lower Monumental Dam as estimated from smolt monitoring program numbers. Smolt monitoring program estimates do not account for fish guidance efficiency or spill passage effectiveness other than 1, so we used the BiOp numbers from SIMPAS to adjust those estimates. For our purposes, we also had to account for the fact that bypassed fish at Lower Monumental Dam are transported, and not returned to the river. These adjustments yielded a daily estimate of the number of fish downstream of Lower Monumental Dam, which agreed fairly well with the hydroacoustic passage estimates a few days later at Ice Harbor (Figure 3.3 and Figure 3.4). Summer hydroacoustic estimates were generally higher than those computed from the Smolt Monitoring Program.

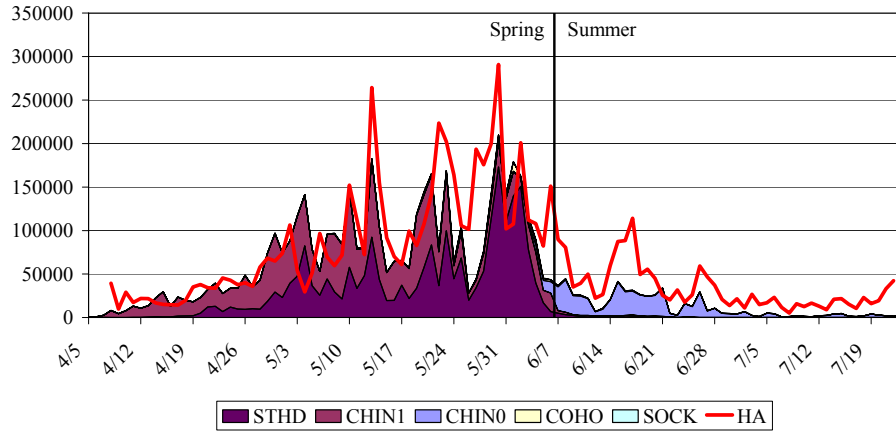


Figure 3.3. Lower Monumental Dam Smolt Monitoring Program and Hydroacoustic Estimate Comparison of Run Timing. The smolt monitoring program passage values have been adjusted to account for FGE, SPE, and transportation values from SIMPAS and to include a 3-day lag from Lower Monumental Dam to account for sampling time and travel time to Ice Harbor.

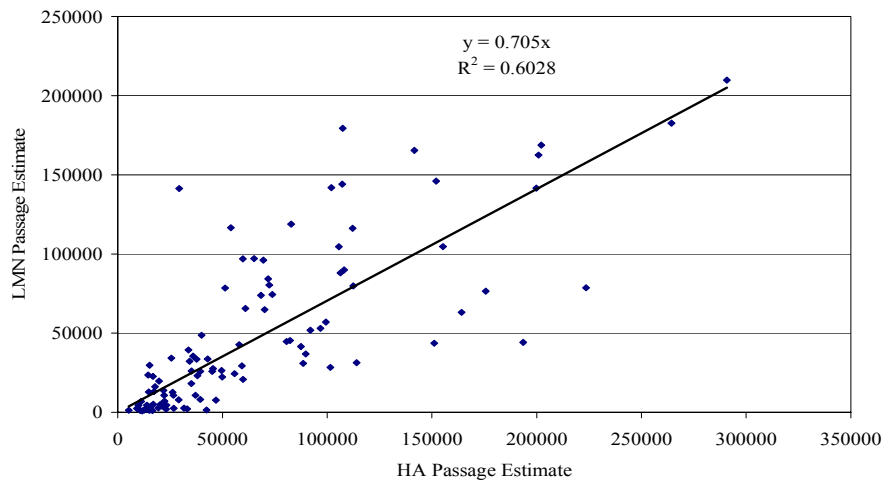


Figure 3.4. Correlation Scatterplot for Adjusted Lower Monumental Dam Smolt Monitoring Index vs. Hydroacoustic Estimate

3.1.3 Dam Operations

Daytime unit operating preference according to the Fish Passage Plan was: 1-3-6-4-5-2. Nighttime unit operating preference was: 3-1-6-4-5-2. This preference order is what was seen in the dam operations data. Units 1, 3, and 6 ran the most and unit 2 ran the least (Figure 3.5).

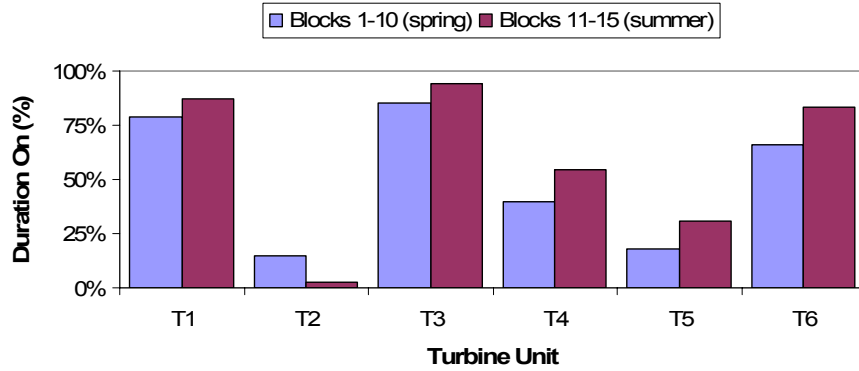


Figure 3.5. Turbine Unit Operating Preference. Duration on is based on hours that the unit was running over the total available for the study period.

The regular BiOp spill pattern for Ice Harbor Dam was nearly flat. The first bays to open are the end bays for adult attraction. As flows increase, these are held at 2 stops to maintain favorable hydraulic conditions at the fishway entrances. The interior eight bays are moved nearly in unison (Figure 3.6). The regular BiOp spill pattern was also in effect for the Spill50 treatment, but the proportion of total flow that was spilled differed from the BiOp Treatment. The BulkBiOp spill pattern, however, concentrated all flow in Bays 2-4 with a 6 stop minimum and a 10 stop maximum. Though the patterns differ, the proportion of total flow spilled during the BulkBiOp treatment were governed by the same guidelines as for the BiOp treatment.

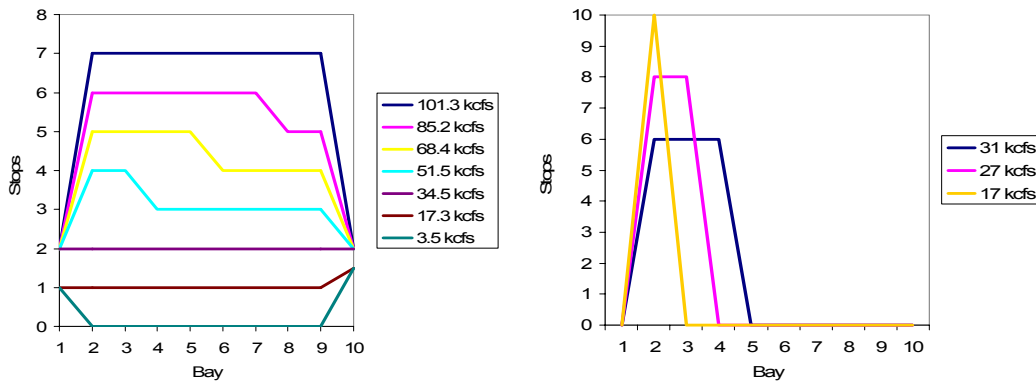


Figure 3.6. Graphical Representation of the Regular BiOp Spill Pattern (left) and the BulkBiOp Spill Pattern (right)

Hourly dam operations data illustrate the range of operations at the dam. Both powerhouse and spillway discharge reflect the spill treatment schedules. The prescribed BiOp spill to the gas cap at night is clearly seen with spill periods of 100% in both spring and summer. During the spring freshet, however, spill levels were gas limited and excess flow was run through the powerhouse (Figure 3.7).

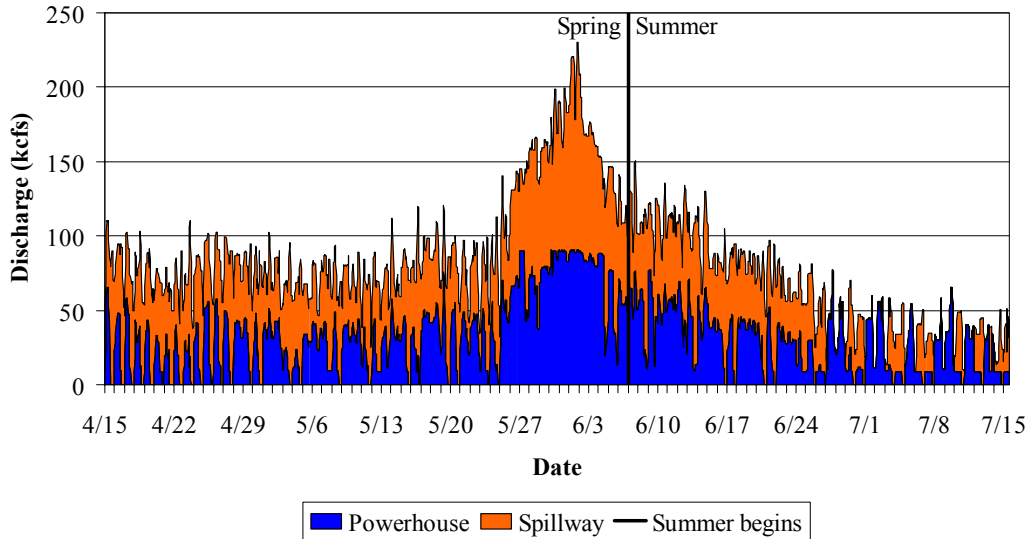


Figure 3.7. Hourly River Discharge Through the Powerhouse and Spillway for the Season

3.2 Seasonal Fish Passage

This section describes fish passage at the dam over the entire sampling season. The intent is to illustrate the influence that varying river conditions and species composition may have, independent of spill treatments. Fish passage metrics are based on actual dam operations. All days and all blocks are included, without regard to whether spill treatment conditions were met. The influence of spill treatments cannot be eliminated, and may be evident in this section, especially in diel trends. This section will break metrics out by season (spring|summer) and diel period (day|night). The statistical analysis of the treatment blocks are addressed in the next two sections.

3.2.1 Passage Metrics

The following fish passage metrics are calculated for season and diel period separately. No treatments or blocks are taken into account. Fish passage efficiency was approximately 95% in spring and summer, and did not differ much between day and night (Figure 3.8). Overall spill passage efficiency was approximately 54% during the day and 70% at night with similar results for spring and summer. Overall spill passage effectiveness averaged between 1.0 and 1.2, with slightly higher values during the summer and during the day (Figure 3.9). Fish guidance efficiency was slightly lower at night during the summer, but did not differ greatly between spring and summer.

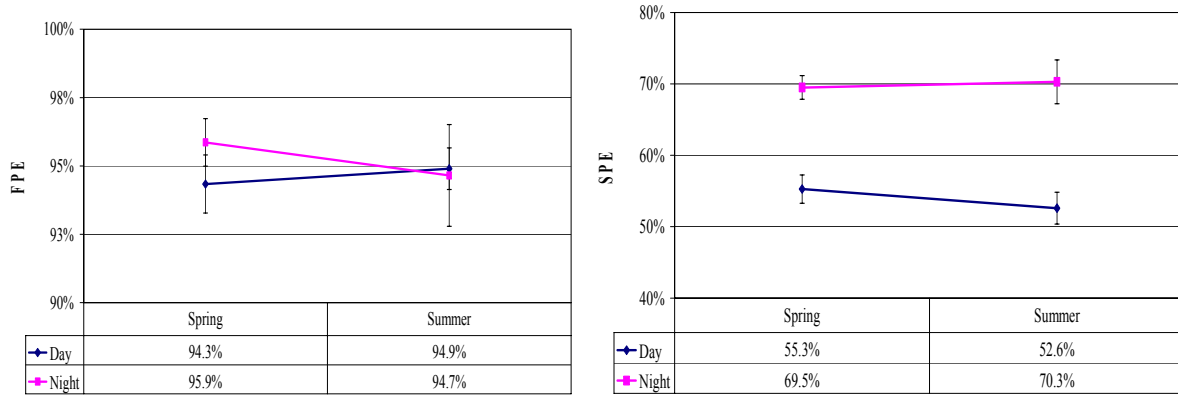


Figure 3.8. Fish Passage Efficiency (FPE, left) and Spill Passage Efficiency (SPE, right) in Spring|Summer and Day|Night. Error bars are 95% confidence intervals based on measurement uncertainty (Equation A29, Appendix A).

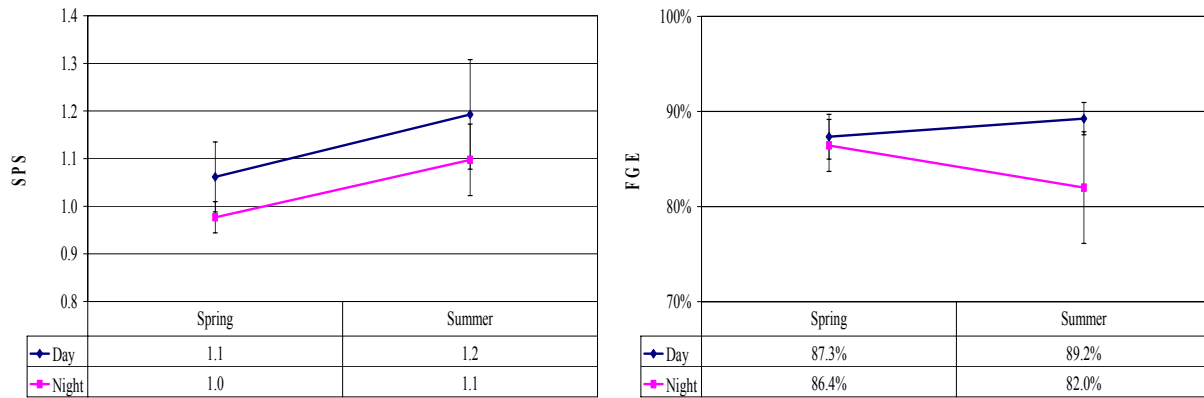


Figure 3.9. Spill Passage Effectiveness (SPS, left) and Fish Guidance Efficiency (FGE, right) in Spring|Summer and Day|Night. Error bars are 95% confidence intervals based on measurement uncertainty (Equation A29, Appendix A).

3.2.2 Daily Trends

Trends in fish passage metrics across the entire sampling season are shown in this section. Treatments in effect for each day are shown simply to avoid the need for duplicating these graphics and to make the reader aware of their potential influence. Survival flows were set for other studies in progress during the sampling period and are plotted here to identify periods excluded from analysis in this study. Fish passage metrics were relatively constant during the season (Figure 3.10 through Figure 3.13). The influences of treatment conditions and of high flows near the end of the spring period are both evident in these figures. The NoSpill treatment results in zeros or extremely low values for the spill metrics (SPE and SPS). The peak flow near the end of the spring period resulted in lower spill proportions to avoid exceeding dissolved gas limits. Those lower spill proportions resulted in lower values for the spill metrics.

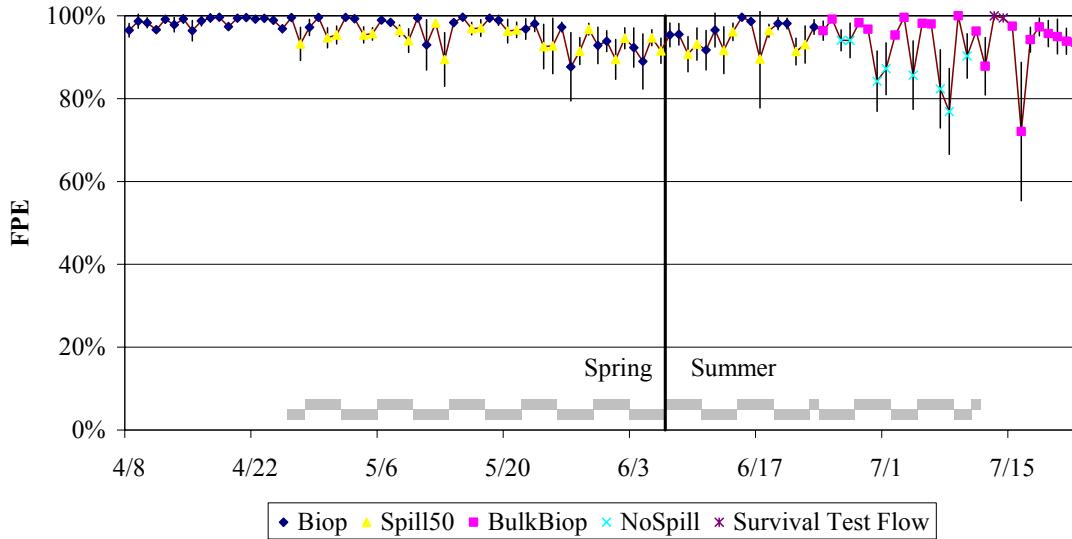


Figure 3.10. Daily Fish Passage Efficiency (FPE) Trend Across the Season. The series of alternating gray rectangles delineate study blocks. Error bars are 95% confidence intervals based on measurement uncertainty (Equation A29, Appendix A).

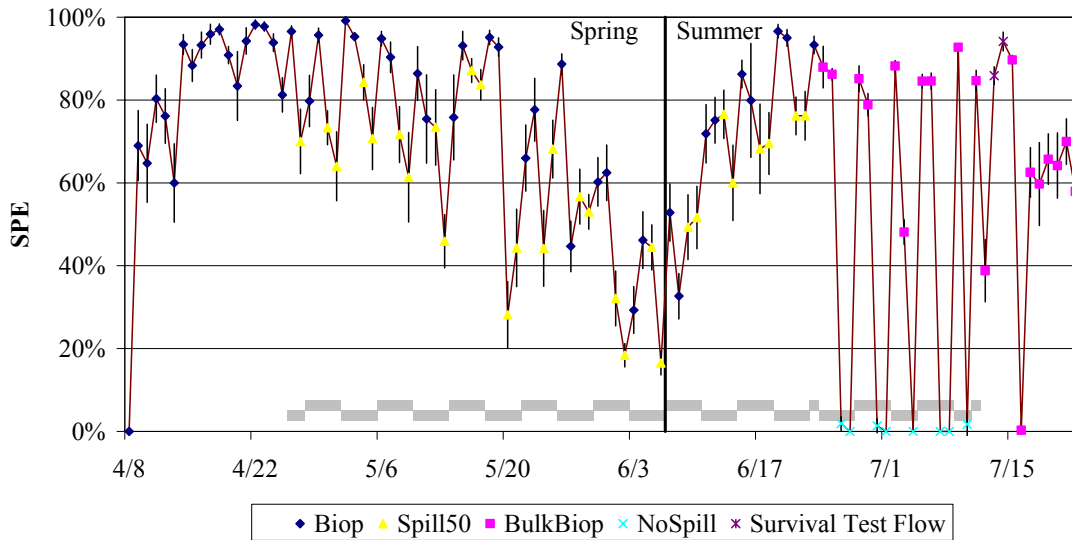


Figure 3.11. Daily Spill Passage Efficiency (SPE) Trend Across the Season. The series of alternating gray rectangles delineate study blocks. Error bars are 95% confidence intervals based on measurement uncertainty (Equation A29, Appendix A).

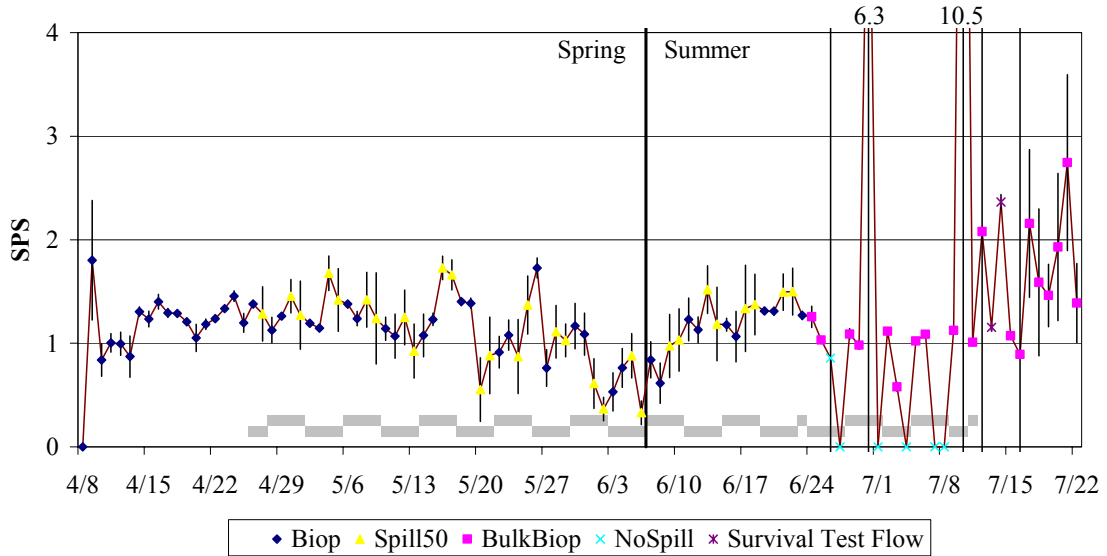


Figure 3.12. Daily Spill Passage Effectiveness (SPS) Trend Across the Season. The series of alternating gray rectangles delineate study blocks. Error bars are 95% confidence intervals based on measurement uncertainty (Equation A29, Appendix A).

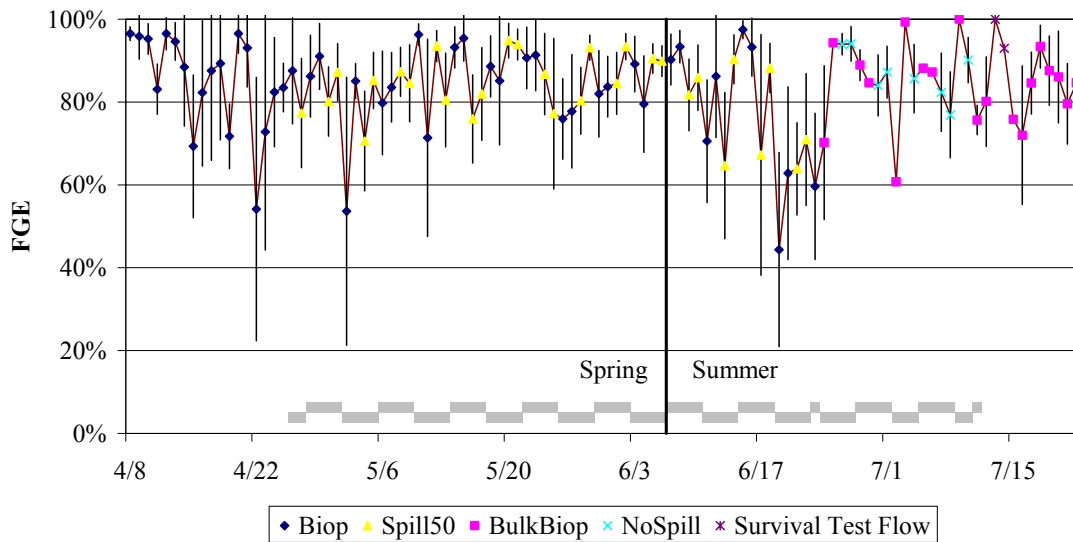


Figure 3.13. Daily Fish Guidance Efficiency (FGE) Trend for the Entire Powerhouse Across the Season. The series of alternating gray rectangles delineate study blocks. Error bars are 95% confidence intervals based on measurement uncertainty (Equation A29, Appendix A).

3.2.3 Seasonal Diel Passage

Passage trends over the 24-hour day revealed the influence of spill proportion manipulations related to the treatments and fish passage behavior. The specific effects of spill treatments are addressed in Section 3.3. The majority of passage occurred during the nighttime hours in both spring (59%) and summer (53%) (Figure 3.14). Higher proportions of the total flow were spilled at night. The nighttime peak in passage is less pronounced in summer, as is the spill proportion at night.

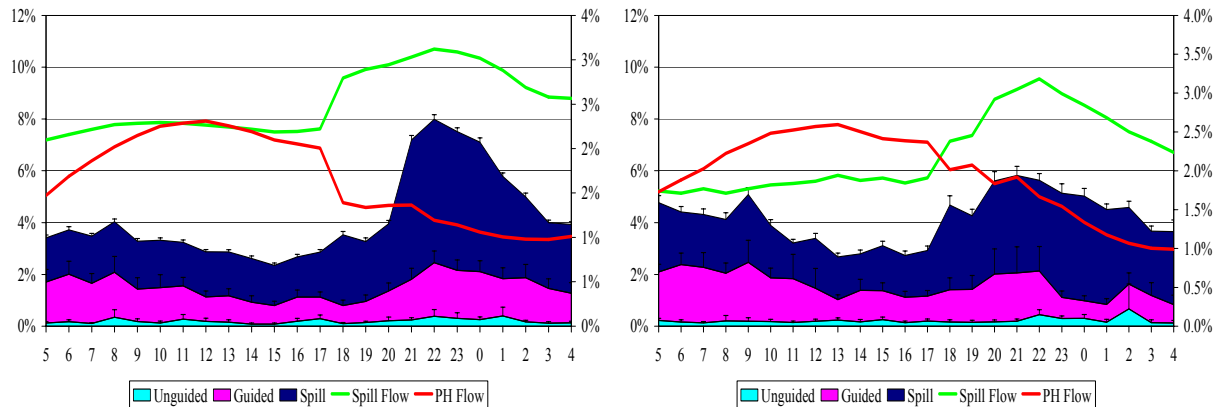


Figure 3.14. Diel Passage During the Spring (left) and Summer (right). All spill treatments were pooled. Error bars are 95% confidence intervals based on measurement uncertainty (Equation A29, Appendix A).

3.2.4 Horizontal Distributions

On the following graphs the column chart portion is the fish passage by unit across the entire dam, and the line chart portion is the flow of water by unit. At both the powerhouse and spillway, fish tended to pass in greatest number near the thalweg but also passed in high proportion at bays and units nearest the shore (Figure 3.15). This pattern may be referred to as a crown pattern. Fish guidance efficiency at individual turbine intakes was highly variable, but unit performance was consistent from spring to summer. Fish guidance efficiency was slightly lower at night than during the day (Figure 3.16). During summer, when subyearling Chinook predominate, fish guidance efficiency was lower than during spring when steelhead and yearling Chinook make up the bulk of the run.

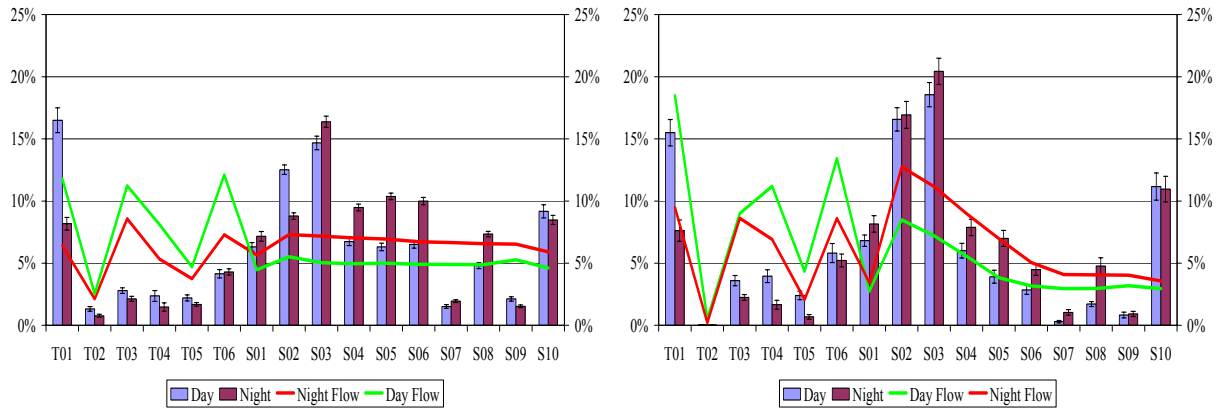


Figure 3.15. Horizontal Distribution of Fish Passage and Flow During the Spring (left) and Summer (right). Error bars are 95% confidence intervals based on measurement uncertainty (Equation A29, Appendix A).

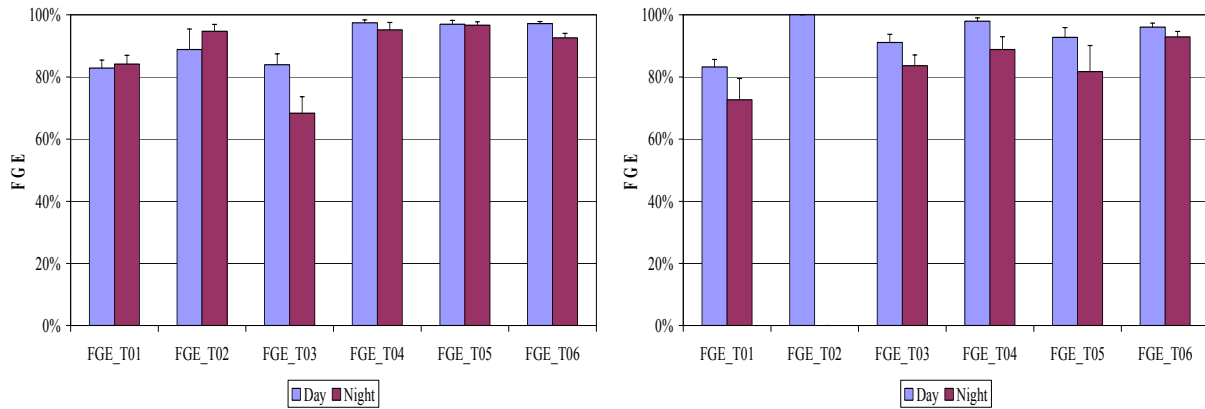


Figure 3.16. Spring (left) and Summer (right) Fish Guidance Efficiency (FGE) by Unit. Error bars are 95% confidence intervals based on measurement uncertainty (Equation A29, Appendix A).

3.2.5 Continuous Spill Curves

Although spill treatment conditions were generally met, periods did occur with spill proportions outside the planned treatments. As a result, it was possible to more fully evaluate the relationship between spill proportion and the passage performance metrics. The additional information is useful, with the caveat that it cannot substitute for a more direct study of spill proportion. Actual proportions are mostly clumped near the planned treatment spill proportions. The amount of time that spill differed widely from the planned treatments was insufficient to account for the influence of factors such as diel period and temporal trends in passage across the sampling season. The data, given these limitations, still provide a basic understanding of the trend of passage performance metrics across spill proportions.

Fish passage efficiency generally increased with the proportion of spill, as expected, with more fish proportionately passing via the spillway. Fish passage efficiency was also generally higher during the day than at night for similar percent spill (Figure 3.17).

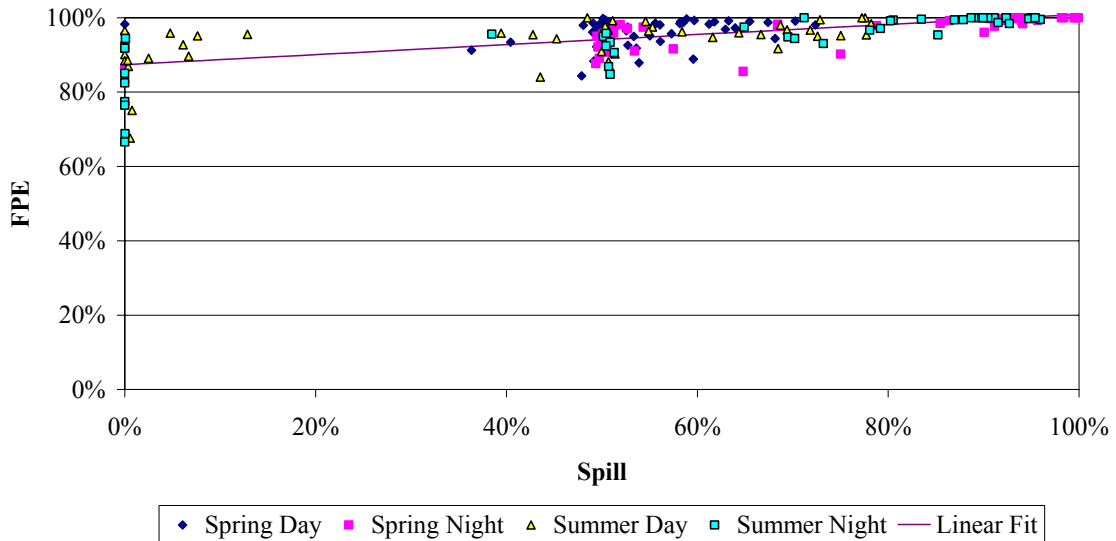


Figure 3.17. Fish Passage Efficiency vs. Percent Spill by Season and Diel Period. The curve fit is linear.

Even in the absence of spill, fish passage efficiency cannot drop below fish guidance efficiency, so the trend does not approach zero. Spill passage efficiency increased with the proportion of spill, but there was a great deal of variation at 50% spill. Seasonal and diel influences do not appear to explain the majority of this variation. Spill passage effectiveness decreased rapidly toward 1 with increasing spill proportion (Figure 3.18 and Figure 3.19, respectively). Fish guidance efficiency generally decreased with increasing spill, suggesting that spill may have more influence over fish that would otherwise be guided (Figure 3.20). Differences in these metrics among spring and summer or day and night were not clearly evident.

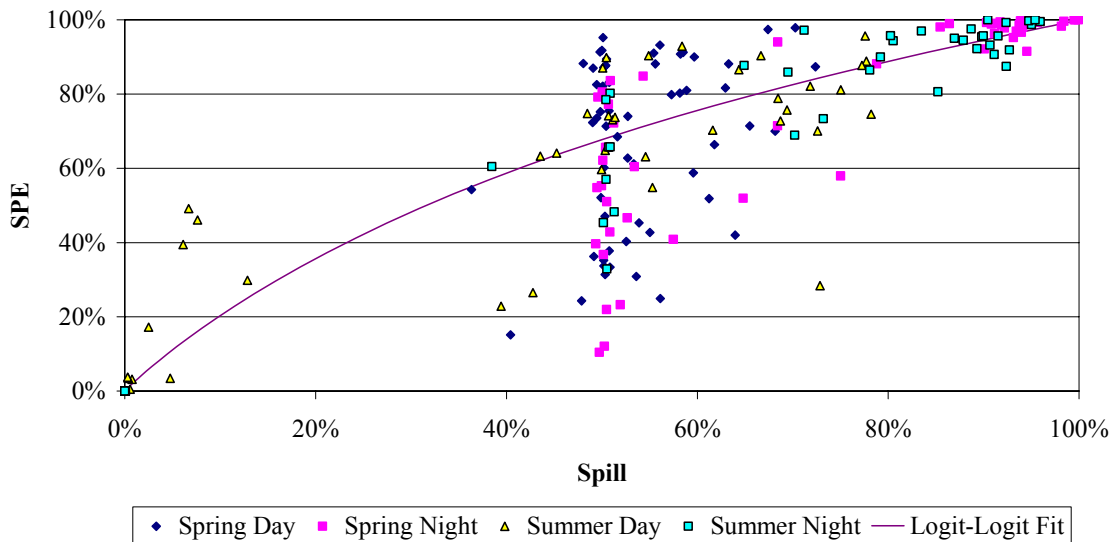


Figure 3.18. Spill Passage Efficiency vs. Percent Spill by Season and Diel Period. The curve fit is logit-logit, which forces the line through both 0,0 and 100,100.

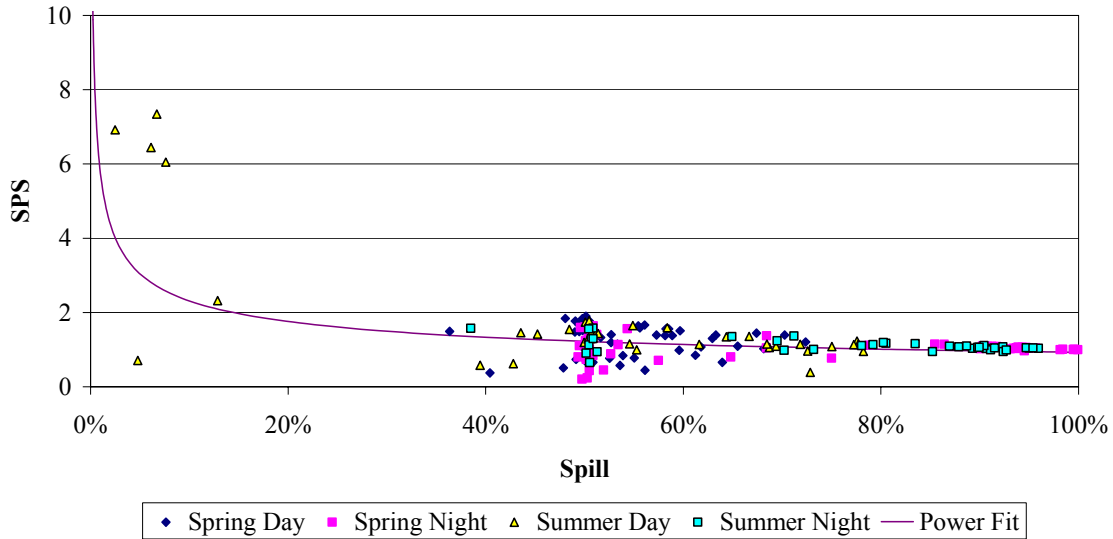


Figure 3.19. Spill Passage Effectiveness vs. Percent Spill by Season and Diel Period. The power curve fit is based on the premise that spill effectiveness should approach infinity where all fish pass via an amount of water that approaches 0, and asymptote to 1 where all of the fish pass when all of the water is spilled.

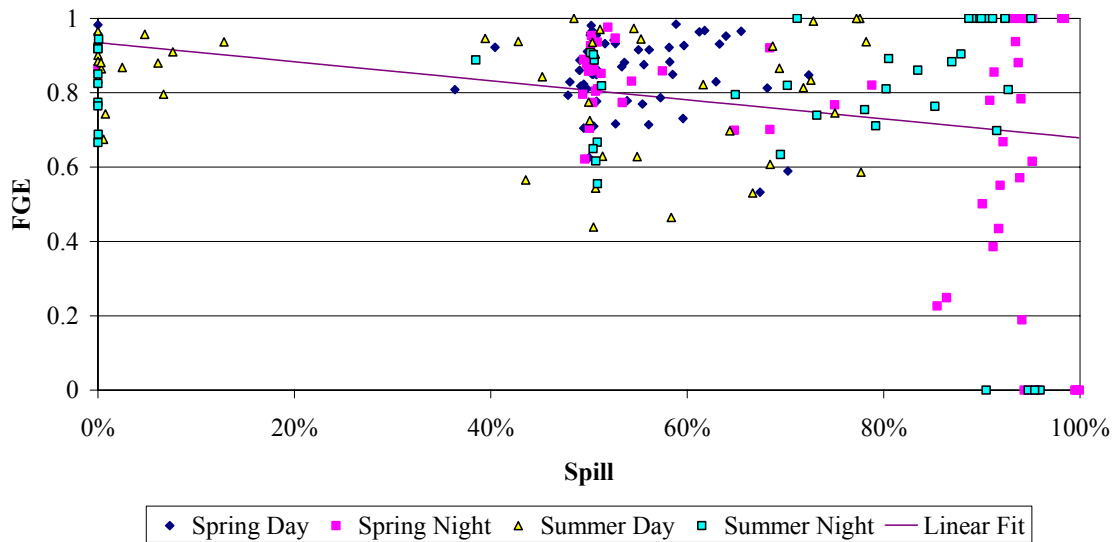


Figure 3.20. Fish Guidance Efficiency vs. Continuous Percent Spill by Season and Diel Period. The curve fit is linear.

3.3 BiOp vs. Spill50 Treatment Effects

The fish passage metric responses to the first set of spill treatments are described in this section. Table 3.1 illustrates how treatments were arranged across the seasons. The treatments were nominally either skimming spill (50% for 24 hrs, referred to as Spill50) or plunging spill (45 kcfs daytime with

Table 3.1. The Number of Treatment Blocks Available in Each Treatment and Season Combination

	BiOp	Spill50	BulkBiOp	NoSpill
Spring	11	11		
Summer	4	4	5	5

100% up to 100 kcfs at night, referred to as BiOp). In spring, 11 blocks were available and all were used in the analysis, though the first block contained only one day of each treatment. In summer, only four blocks were available for this pair of treatments and all were used in the analysis. Summer blocks include only the first part of the summer passage season, after which another set of treatments was implemented. The results from this second set of treatments are described in detail in Section 3.4. The number of available blocks and the season into which they fell are summarized in Table 3.1.

This pair of treatments extended through block 15, and operators did an excellent job of meeting the 50% spill treatment conditions. The primary difference between Spill50 and BiOp was during the nighttime hours where the BiOp called for 100% spill up to 100 kcfs. During daytime hours both treatment specifications resulted in spill proportions of approximately 50%. During block 9 and 10, total flows exceeded the 100 kcfs spill cutoff (the gas cap) and therefore spill was less than 100% during the BiOp treatment at night (Figure 3.21). Appendix C contains the complete set of hourly spill by block plots with which to examine block fidelity.

Trends within season show the influence of high flows near the end of the spring season and the start of the summer season on spill metrics but little else that might bias the treatment comparison (Figure 3.22 and Figure 3.23). Trends across blocks reveal persistent differences for fish passage efficiency and spill passage efficiency in spring and for spill passage effectiveness in summer. The ANOVA methods are specified in detail in Appendix A. The results refute the null hypothesis that project fish passage during skimming (50%) spill does not differ from that during BiOp (gas cap) spill, at least for fish passage efficiency and spill passage efficiency in spring and spill passage effectiveness in summer. We can, therefore, accept the alternate hypothesis that project fish passage during skimming (50%) spill differs from that during BiOp (gas cap) spill. The statistical inferences from the data presented in this section are

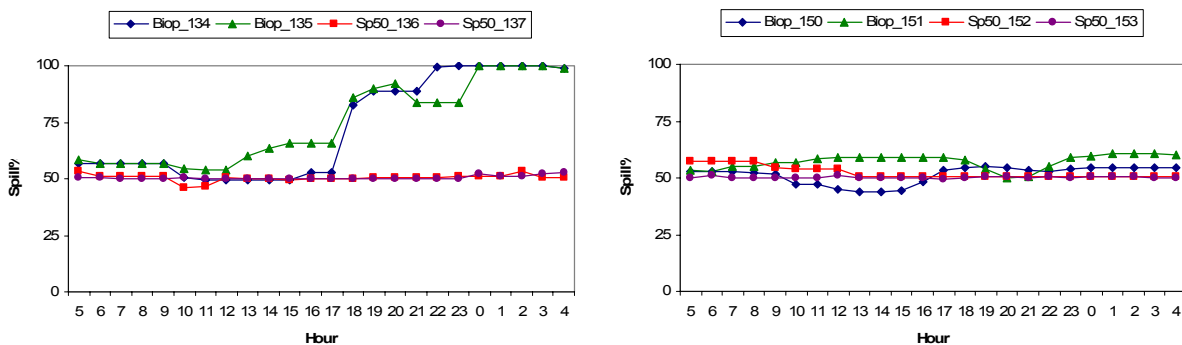


Figure 3.21. Example Hourly Spill by Block Plots. Each colored line represents a treatment day. Block 6 (left) was typical for the spring and summer blocks. Block 10 (right) was during high flows in which BiOp spill was approximately the same as Spill50 due to reaching the gas cap. Excess flows during that period were run through the powerhouse.

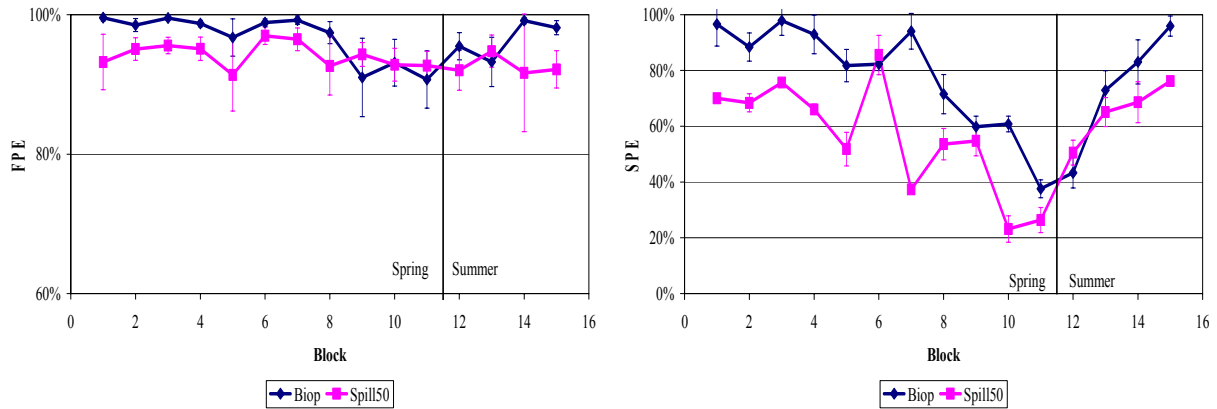


Figure 3.22. Fish Passage Efficiency (FPE, left) and Spill Passage Efficiency (SPE, right) by Block. Error bars are 95% confidence intervals based on measurement uncertainty (Equation A29, Appendix A).

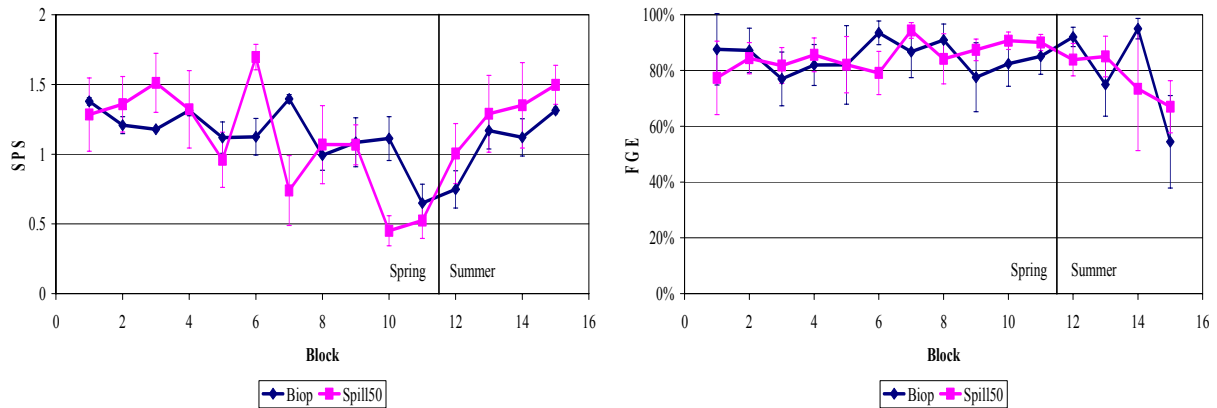


Figure 3.23. Spill Passage Effectiveness (SPS, left) and Fish Guidance Efficiency (FGE, right) by Block. Error bars are 95% confidence intervals based on measurement uncertainty (Equation A29, Appendix A).

limited to this pair of treatment effects. Statistical power to detect differences among treatments during the summer season will be low due to the small number of blocks.

3.3.1 Analysis of Variance

A two-way analysis of variance was performed on all the fish passage performance measures for both spring and summer. The data was arcsine transformed (FGE, FPE, SPE) or ln-transformed (SPS) prior to analysis to stabilize the variance (Appendix A). Fish passage efficiency was significantly different between treatments in spring but not in summer ($\alpha = 0.05$). Spill passage efficiency was significantly different between treatments in spring, but not in summer. In both seasons the block effect was statistically significant, possibly as a result of the influence of high flows and changing spill proportions. Spill passage effectiveness was significantly different among treatments in summer, but not in spring. In summer the block effect was also statistically significant, possibly as a result of high flows and their effect on spill proportions for the BiOp treatment. None of the other fish passage performance metrics

were significantly different among treatments (Table 3.2 through Table 3.5). ANOVA results for passage metrics under BiOp and Spill50 treatments in spring and summer are plotted in Figure 3.24 and Figure 3.25. In those figures we would expect combinations that differ significantly in the ANOVA test to have confidence intervals that do not include the mean of the other treatment.

Table 3.2. ANOVA Results for Fish Passage Efficiency (FPE, left) and Spill Passage Efficiency (SPE, right) in Spring for the 11 Available Blocks

FPE	df	SS	MS	F	p	SPE	df	SS	MS	F	P
Block	10	0.0682	0.0068	2.2100	0.1134	Block	10	0.842	0.084	4.393	0.014
Treatment	1	0.0332	0.0332	10.7800	0.0082	Treatment	1	0.427	0.427	22.285	0.001
Error	10	0.0308	0.0031			Error	10	0.192	0.019		
Total _{Cor}	21	0.1322				Total _{Cor}	21	1.461			

Table 3.3. ANOVA Results for Spill Passage Effectiveness (SPS, left) and Fish Guidance Efficiency (FGE, right) in Spring for the 11 Available Blocks

SPS	df	SS	MS	F	P	FGE	df	SS	MS	F	P
Block	10	1.561	0.156	2.186	0.117	Block	10	0.044	0.004	0.638	0.755
Treatment	1	0.059	0.059	0.822	0.386	Treatment	1	0.000	0.000	0.036	0.853
Error	10	0.714	0.071			Error	10	0.069	0.007		
Total _{Cor}	21	2.334				Total _{Cor}	21	0.114			

Table 3.4. ANOVA Results for Fish Passage Efficiency (FPE, left) and Spill Passage Efficiency (SPE, right) in Summer for the 4 Available Blocks

FPE	df	SS	MS	F	P	SPE	df	SS	MS	F	P
Block	3	0.0047	0.0016	0.3090	0.8196	Block	3	0.221	0.074	5.838	0.091
Treatment	1	0.0187	0.0187	3.6610	0.1516	Treatment	1	0.030	0.030	2.368	0.221
Error	3	0.0153	0.0051			Error	3	0.038	0.013		
Total _{Cor}	7	0.0388				Total _{Cor}	7	0.288			

Table 3.5. ANOVA Results for Spill Passage Effectiveness (SPS, left) and Fish Guidance Efficiency (FGE, right) in Summer for the 4 Available Blocks

SPS	df	SS	MS	F	P	FGE	df	SS	MS	F	P
Block	3	0.255	0.085	22.715	0.015	Block	3	0.1293	0.0431	1.8554	0.3122
Treatment	1	0.063	0.063	16.824	0.026	Treatment	1	0.0044	0.0044	0.1880	0.6939
Error	3	0.011	0.004			Error	3	0.0697	0.0232		
Total _{Cor}	7	0.330				Total _{Cor}	7	0.2033			

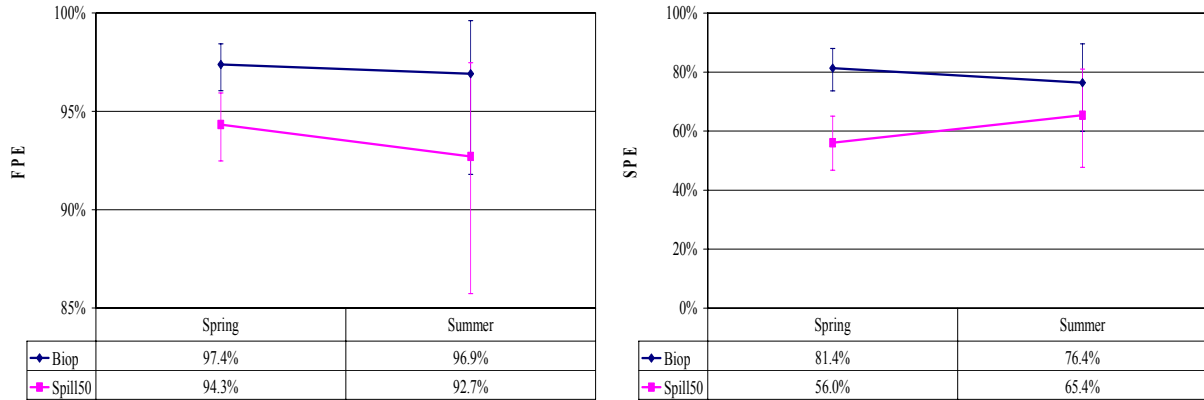


Figure 3.24. Fish Passage Efficiency (FPE, left) and Spill Passage Efficiency (SPE, right) by Treatment. Error bars are 95% confidence intervals based on ANOVA MSE (Equation A30, Appendix A).

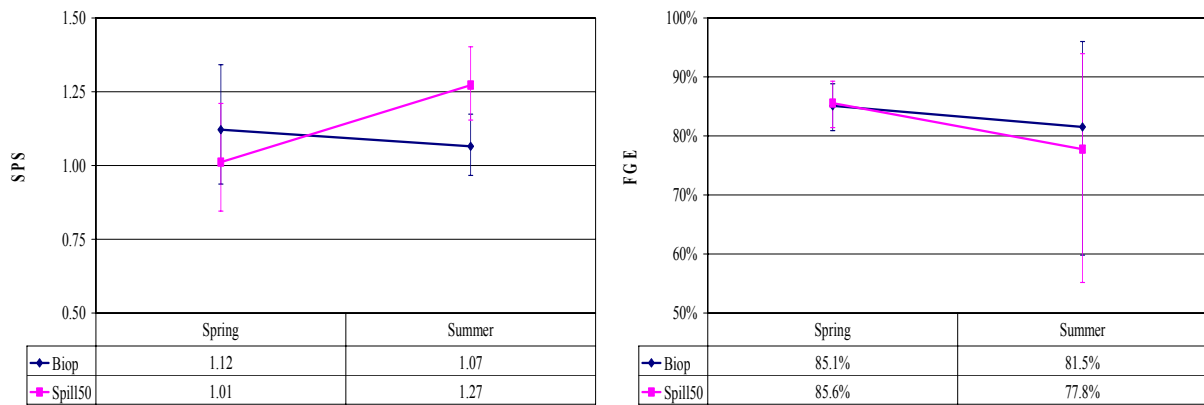


Figure 3.25. Spill Passage Effectiveness (SPS, left) and Fish Guidance Efficiency (FGE, right) by Treatment. Error bars are 95% confidence intervals based on ANOVA MSE (Equation A30, Appendix A).

3.3.2 Diel Trends by Treatment

Because these spill treatments differed primarily in the proportion of water spilled at night, the presentation of fish passage by route and by hour of the day are informative. On the following graphs, flow through the powerhouse and spillway are also shown. The plots of flow show that overall discharge was relatively consistent among treatments during the day, and that a greater proportion of total flow was spilled at night during the BiOp treatment than during Spill50 treatment.

During the spring, overall passage trends are similar among treatments, but differences are evident in which routes fish are passing (Figure 3.26 and Figure 3.27). Peak passage during both treatments occurs around 2100 h to 2200 h. During the BiOp treatment, spill passage predominates, but a much greater proportion of passage during Spill50 at night is through the juvenile bypass (guided). Unguided fish are also more common during the Spill50 treatment at night, resulting in lower fish passage efficiency than for BiOp. Unguided fish are less common during the day during all treatments and seasons, indicating

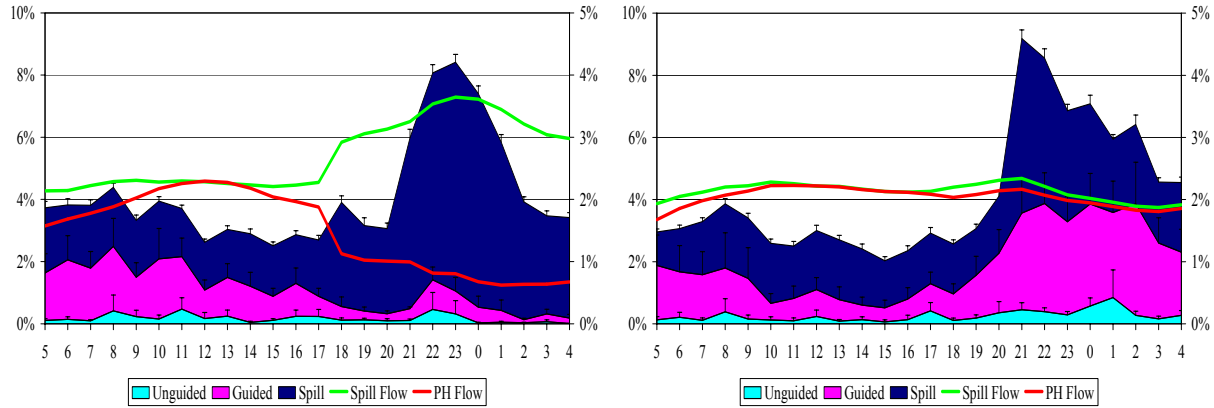


Figure 3.26. Diel Passage During the Spring BiOp (left) and Spill50 (right) Treatments for the 11 Available Blocks. Error bars are 95% confidence intervals based on measurement uncertainty (Equation A29, Appendix A).

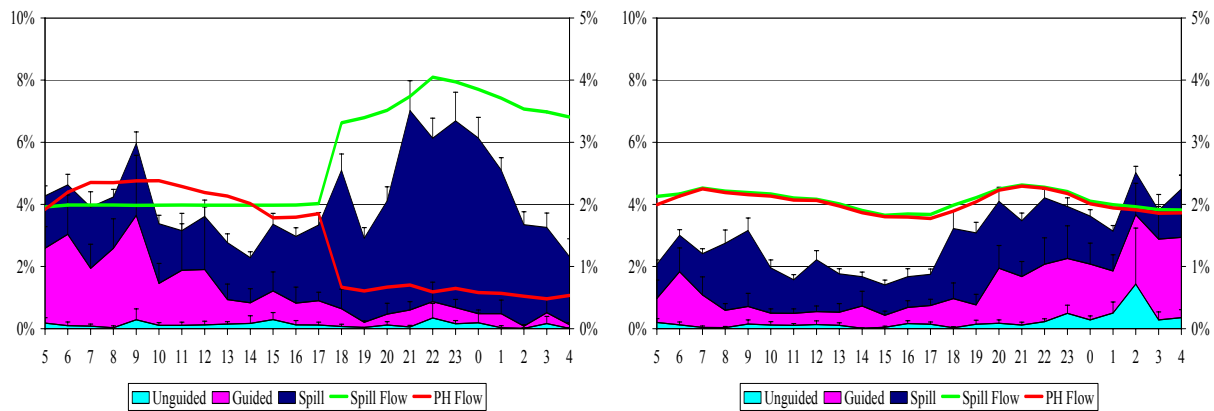


Figure 3.27. Diel Passage During the Summer BiOp (left) and Spill50 (right) Treatments for the 4 Selected Blocks. Error bars are 95% confidence intervals based on measurement uncertainty (Equation A29, Appendix A).

that fish guidance efficiency is high during the day. Of interest is the first peak of spillway passage at 1800 h, which is more evident in the BiOp treatment in both spring and summer. This peak suggests that fish may have been holding in the forebay during the day until the spillway opened.

3.3.3 Horizontal Distribution by Treatment

In the following charts (Figure 3.28 and Figure 3.29), the column elements represent fish passage through each unit. The line elements are the water flow through each unit by treatment. In general, more fish passed through units near the thalweg or nearest either shoreline in a crown pattern during either treatment. The horizontal distribution of fish passage is not closely correlated with the flows through each unit. Another general trend is that fewer fish passed the powerhouse than the spillway. The trend would be further exaggerated if adjusted for flow. This is evident in the figures because spill passage proportion at a unit often exceeds flow proportion for that unit. The opposite is true at the powerhouse.

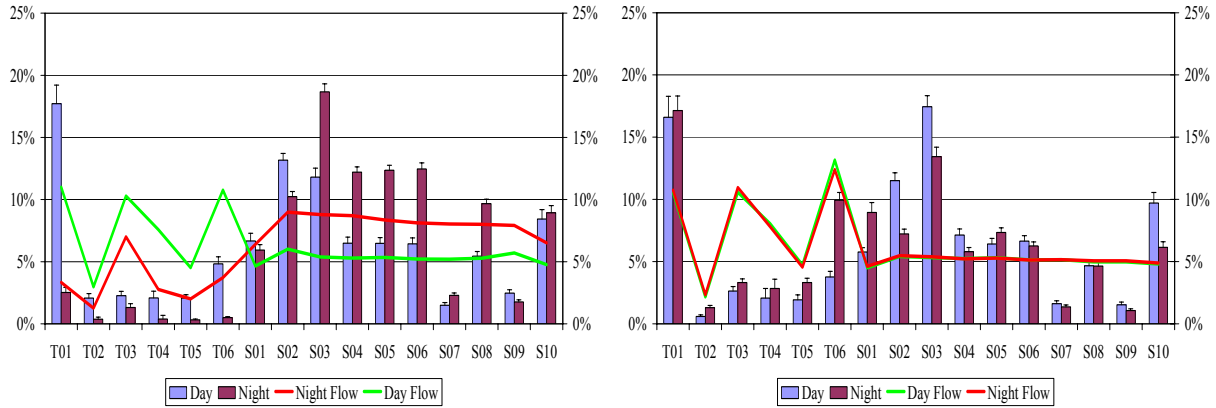


Figure 3.28. Horizontal Passage and Flow Distribution in Spring During the BiOp (left) and Spill50 Treatments for the 11 Available Blocks. Error bars are 95% confidence intervals based on measurement uncertainty (Equation A29, Appendix A).

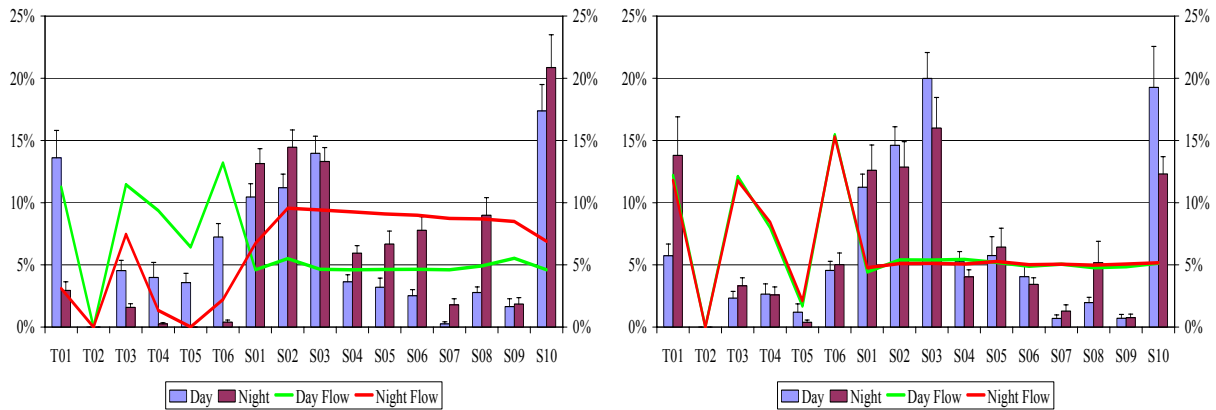


Figure 3.29. Horizontal Passage and Flow Distribution in Summer During the BiOp (left) and Spill50 (right) Treatments for the 4 Available Blocks. Error bars are 95% confidence intervals based on measurement uncertainty (Equation A29, Appendix A).

3.4 BulkBiOp vs. NoSpill Treatment Effects

Due to the no spill condition for this summer treatment comparison, the spill metrics (SPE and SPS) were not included in the analysis. Fish passage efficiency and fish guidance efficiency, however, are compared. In all blocks, fish passage efficiency under BulkBiOp treatment conditions was greater than under the NoSpill treatment. Fish guidance efficiency was generally higher for BulkBiOp, but not consistently so for all blocks (Figure 3.30).

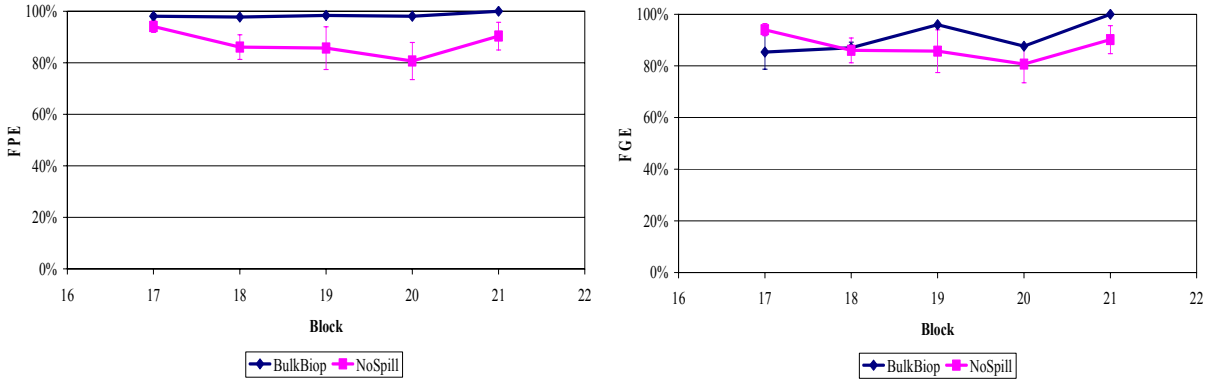


Figure 3.30. Fish Passage Efficiency (FPE) and Fish Guidance Efficiency (FGE) Trends by Block. Error bars are 95% confidence intervals based on measurement uncertainty (Equation A29, Appendix A).

3.4.1 Analysis of Variance

The analysis of variance shows a significant treatment effect ($\alpha = 0.05$) in fish passage efficiency but not in fish guidance efficiency (Table 3.6). The block effect was not statistically significant for either metric. Fish passage efficiency for the NoSpill treatment was approximately 87% versus 98% for the BulkBiOp pattern spill. The confidence intervals reflect the consistency among blocks. Fish guidance efficiency for the NoSpill treatment was approximately 87% versus 91% for the BulkBiOp treatment. Fish guidance efficiency confidence intervals are wide relative to treatment differences, reflecting the lack of statistically significant difference in fish guidance efficiency among treatments (Figure 3.31).

Table 3.6. ANOVA Results for Fish Passage Efficiency (FPE, left) and Fish Guidance Efficiency (FGE, right) in Summer for the 5 Available Blocks

FPE	Df	SS	MS	F	p	FGE	Df	SS	MS	F	p
Block	4	0.026	0.007	1.759	0.299	Block	4	0.074	0.018	1.198	0.433
Treatment	1	0.152	0.152	41.070	0.003	Treatment	1	0.022	0.022	1.438	0.297
Error	4	0.015	0.004			Error	4	0.061	0.015		
Total _{Cor}	9	0.193				Total _{Cor}	9	0.157			

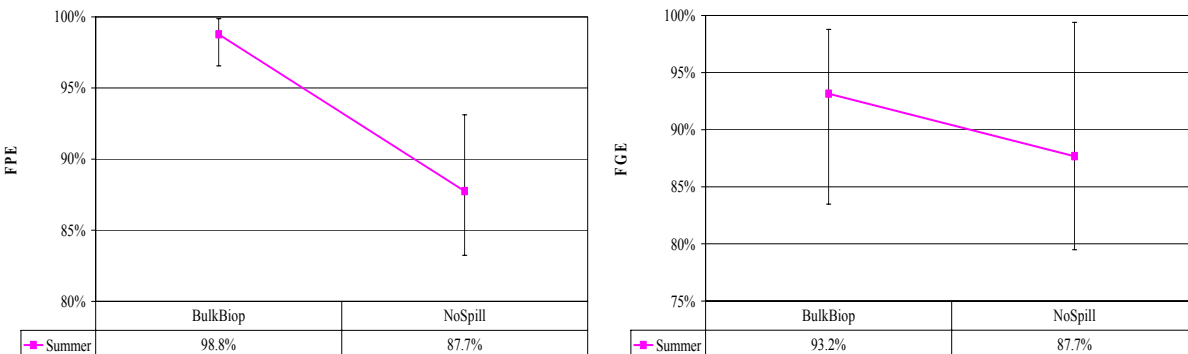


Figure 3.31. Fish Passage Efficiency (left) and Fish Guidance Efficiency (right) by Treatment for Summer BulkBiOp vs. NoSpill. Error bars are 95% confidence intervals based on ANOVA MSE (Equation A30, Appendix A).

The small number of blocks in this test greatly increases the potential for a single block to influence the results. The potential for false negative or false positive results increases as sample size decreases. The limited coverage of the blocks across the summer season limits the inference of these results to that period.

3.4.2 Diel Trends by Treatment

Under BulkBiOp spill, there is a pulse of guided fish when the powerhouse begins operation around 0500 h (Figure 3.32). This unexpected result suggests fish are holding in the forebay until powerhouse operations commence. Also under BulkBiOp, the evening peak in passage appears less pronounced and later than for the previous comparison of BiOp and Spill50 treatments (Figure 3.26 and Figure 3.27). Under NoSpill conditions the evening peak in passage is as pronounced as that seen in BiOp and Spill50 treatments, even though spill is absent. A peak in unguided passage around 2200 h follows soon after the peak in overall passage, resulting in low fish passage efficiency for the NoSpill treatment at night.

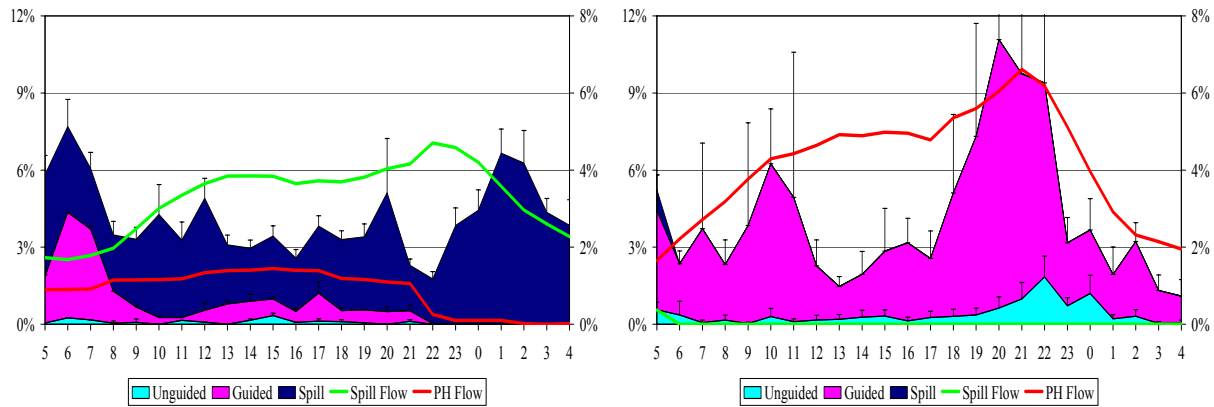


Figure 3.32. Diel Passage During the Summer BulkBiOp Spill Period (left) and the NoSpill Period (right). Error bars are 95% confidence intervals based on measurement uncertainty (Equation A29, Appendix A).

3.4.3 Horizontal Distributions by Treatment

During BulkBiOp spill, most of the river flow is sent over the spillway. Most of the fish approaching the dam during BulkBiOp spill passed through the spillway. Furthermore, fish passed Bay 3 in a greater proportion than water (Figure 3.33, left), but otherwise passage proportion appeared to be consistent with flow proportion. During the NoSpill treatment condition, fish passed via the end units (1 and 6) in a greater proportion than water (Figure 3.33, right). Spill bays 2, 3, and 4 were opened briefly during the NoSpill treatment, but neither flows nor passage through those bays amounted to more than a small fraction of the total.

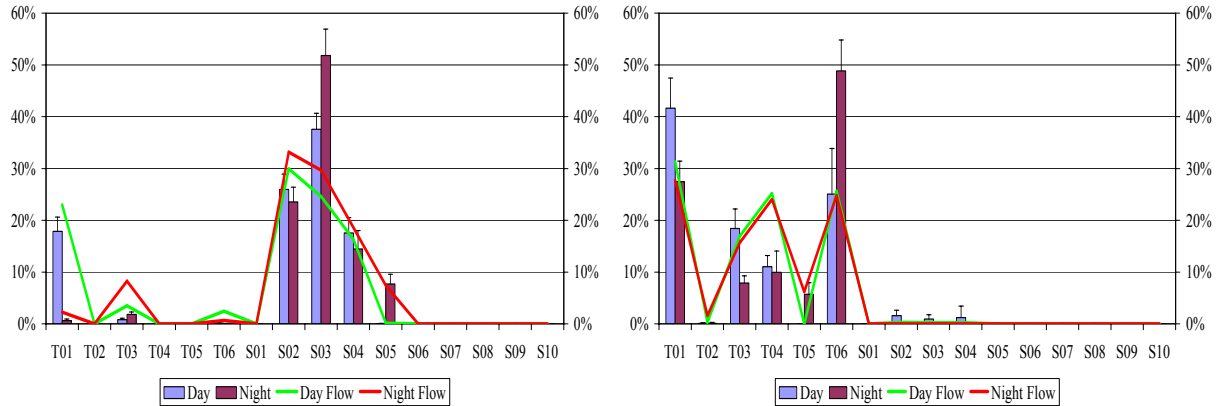


Figure 3.33. Horizontal Passage and Flow Distribution in Summer During the BulkBiOp Spill Period (left) and the NoSpill Period (right). Error bars are 95% confidence intervals based on measurement uncertainty (Equation A29, Appendix A).

3.5 Fish Trajectories

3.5.1 Spillway Trajectories, Vertical Distributions, and Flows

The following series of pictures show the spatial relationships between fish trajectories, fish distributions within the water column, and flows at selected spill gate openings. The data is further divided into spring and summer along the run timing transition date of June 4 (Smolt Monitoring Program data). Features of the plot include the forebay elevation of 438 ft, the top of the spillway crest at elevation 391 ft, and the hydroacoustic transducer at elevation 436 ft. The series of circles and vectors are a combination plot of fish vertical abundance and trajectories along the middle of the hydroacoustic beam. The relative abundance of fish within these 1-m range bins from the transducer is color coded in the circles relative to the right-hand side vertical contour legend. The fish vectors are on the same scale as the axes, so that 1 ft of distance along the vector is equivalent to 1 ft/s (the horizontal axis, while not shown, is also at the same scale as the vertical axis). The nominal beamwidth of the transducer is also plotted, and describes the hydroacoustic sample volume (Figure 3.34).

The fish distribution and trajectory data shown represents only those tracks meeting the criteria for fish expected to pass the dam via the spillway. In addition, distribution estimates have been corrected for detectability within the beam. The fish speed and direction data were collected with split-beam transducers, while the vertical distribution data represents a combination of single- and split-beam data across the entire spillway. Factors other than spill gate opening and season, such as treatments and diel period, have been pooled. The flow field was constructed from a computational fluid dynamics model (CFD) by Battelle to represent the flow through the centerline of a single spill bay—it is two dimensional and static. The flow field contour key is horizontally oriented across the top of the graph, and the flow vectors have been reduced to a 1/5th scale.

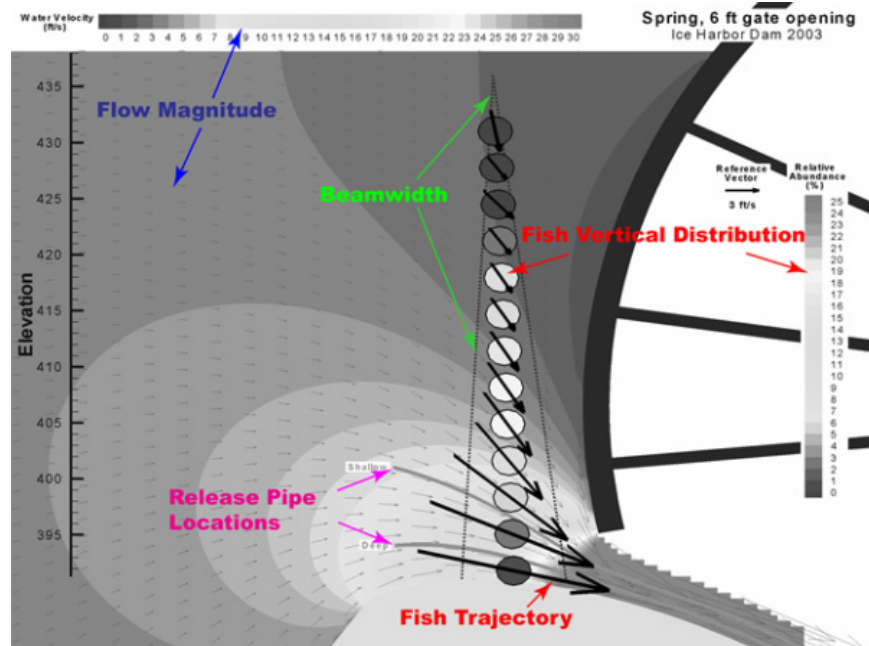


Figure 3.34. Spill Bay Plots Feature Legend

The purple lines were formed as forward streamtraces into the CFD flow field from the release points used in a concurrent study of direct survival: the shallow release point was 10 ft above the crest at elevation 401 ft, and the deep release point was 3 ft above the crest at elevation 394 ft. Representative gate openings of 3, 6, and 9 ft are shown below (Figures 3.35 through 3.40). Appendix D contains plots in 1-ft gate opening increments.

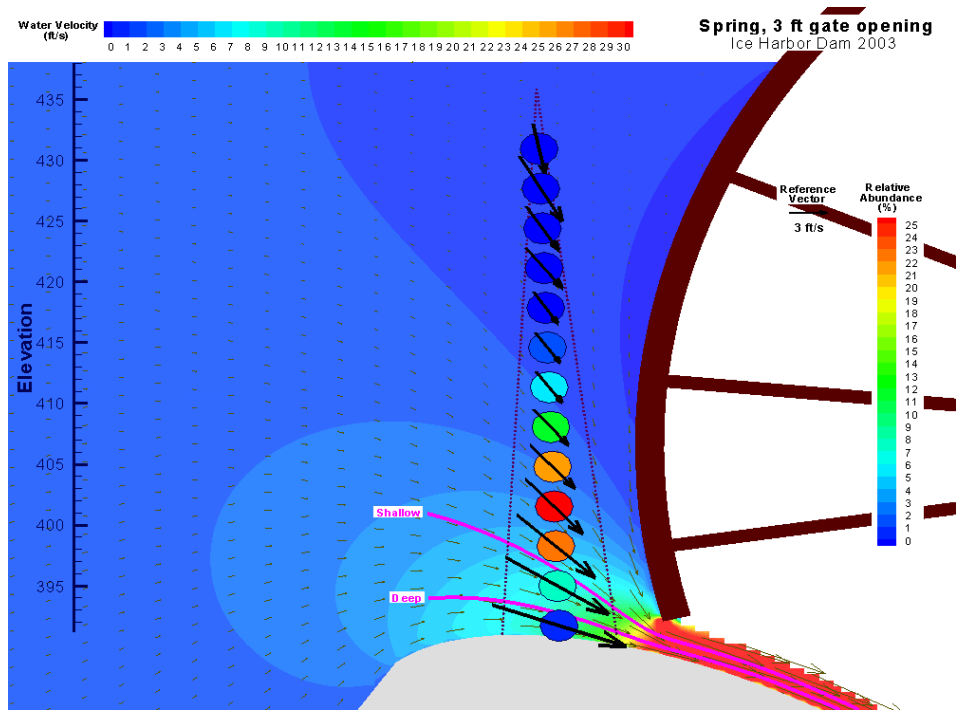


Figure 3.35. Fish Trajectories, Vertical Distribution, Flows, and Release Pipe Locations for 3-ft Gate in Spring

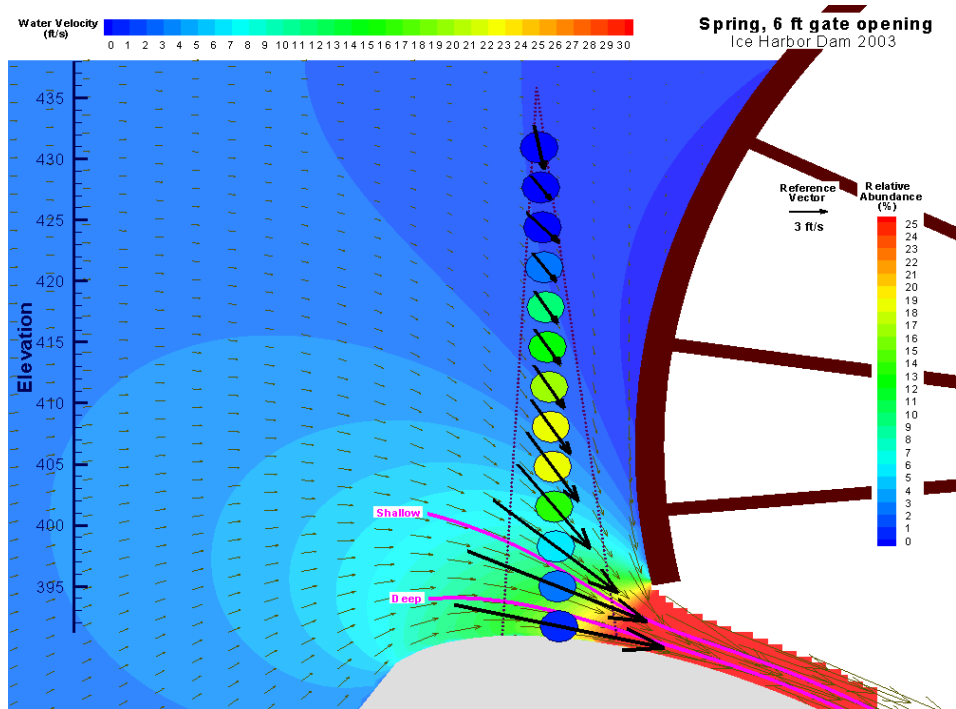


Figure 3.36. Fish Trajectories, Vertical Distribution, Flows, and Release Pipe Locations for 6-ft Gate in Spring

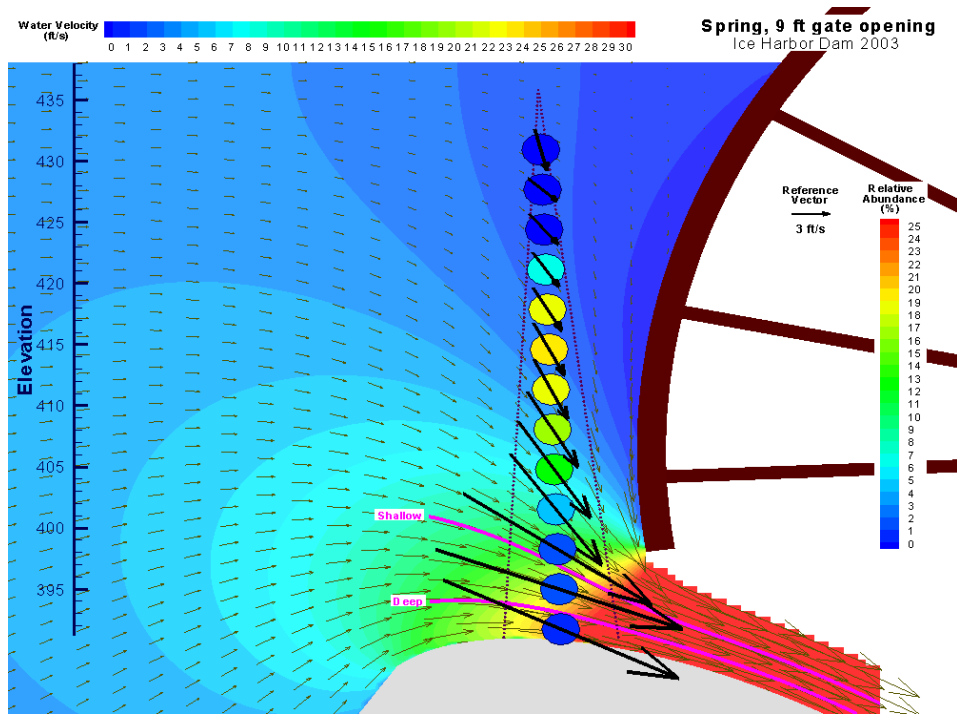


Figure 3.37. Fish Trajectories, Vertical Distribution, Flows, and Release Pipe Locations for 9-ft Gate in Spring

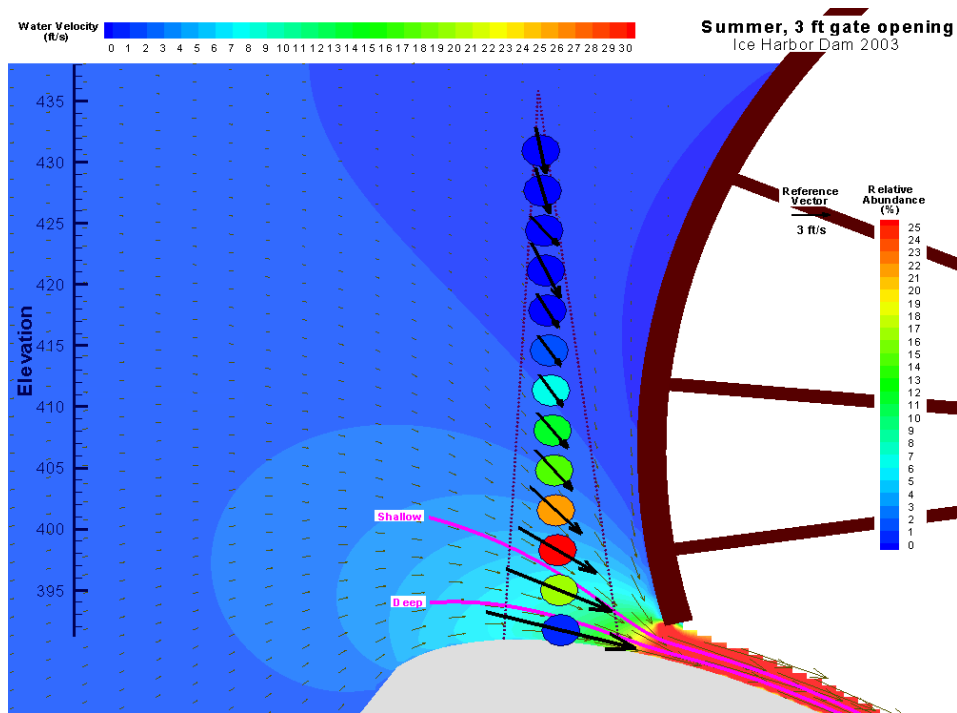


Figure 3.38. Fish Trajectories, Vertical Distribution, Flows, and Release Pipe Locations for 3-ft Gate in Summer

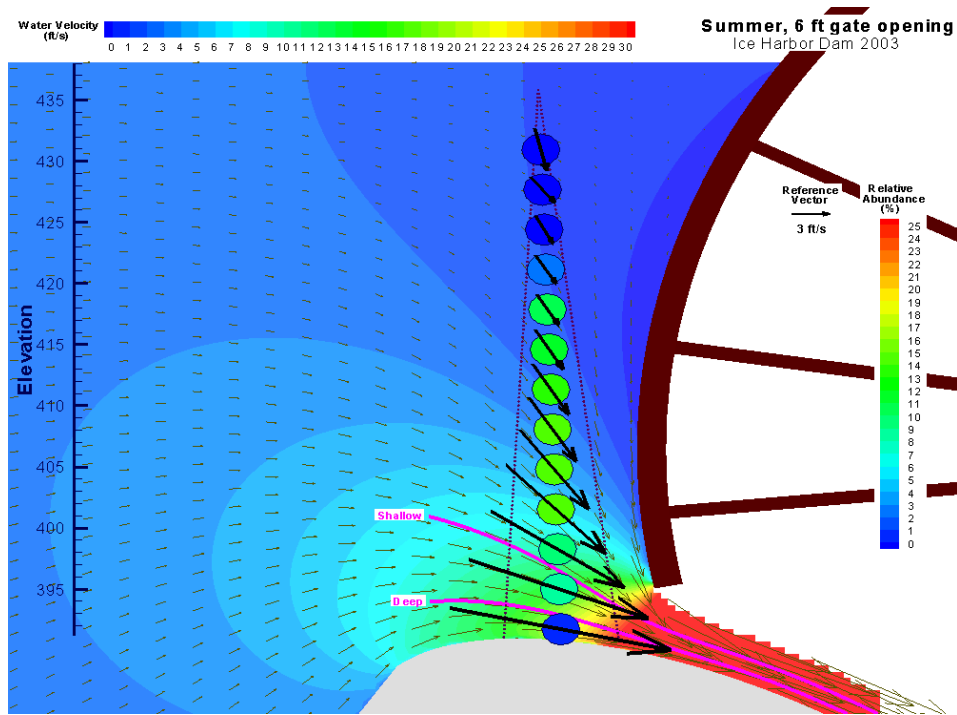


Figure 3.39. Fish Trajectories, Vertical Distribution, Flows, and Release Pipe Locations for 6-ft Gate in Summer

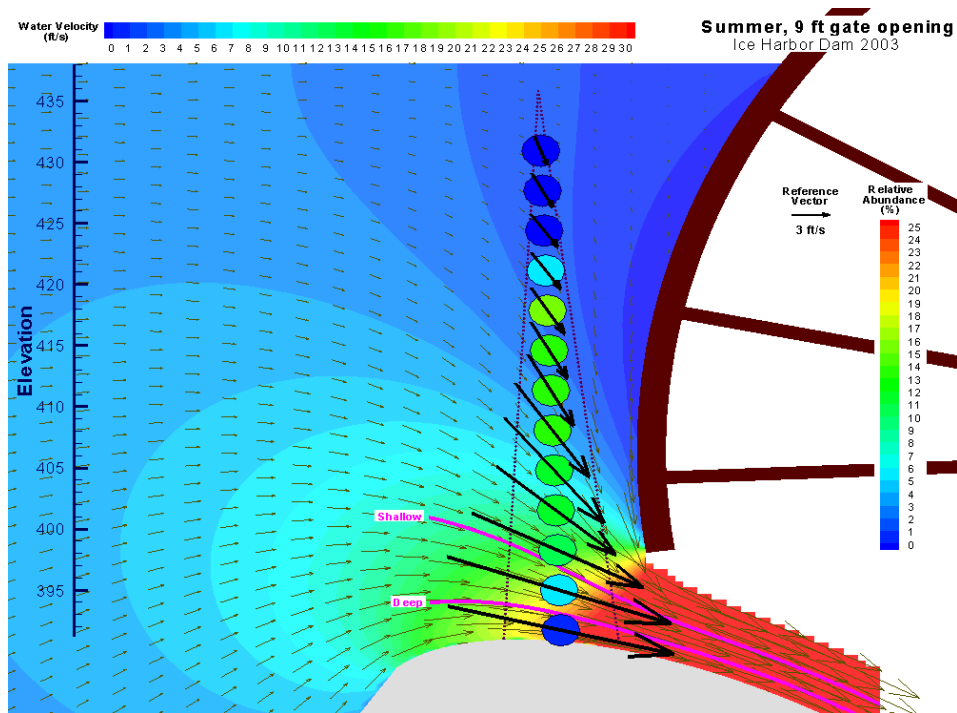


Figure 3.40. Fish Trajectories, Vertical Distribution, Flows, and Release Pipe Locations for 9-ft Gate in Summer

3.5.2 Spring vs. Summer Vertical Distributions by Spill Gate Opening

The following series of graphs (Figures 3.41 through 3.46) directly compare the fish vertical distribution by season for guided, unguided and spill by spill gate opening. The spillway did operate briefly at higher gate openings, but there were insufficient fish data during those periods to create informative distributions. The distributions in both spring and summer at guided and unguided locations indicate a tendency for passage nearer the ceiling of the turbine intake (Figure 3.41). Trends at low flows/gate openings show a slight difference between seasons. This difference widens, and continues to widen, until the 8-ft gate opening. At the highest gate opening, 9 ft, this difference shrank—presumably due to the quantity of water entraining fish from further away. Recall that vertical axis elevation 436 ft is the location of the transducer, and elevation 391 ft is the top of the spillway crest. Appendix E contains additional plots of vertical distributions broken out by season and diel period.

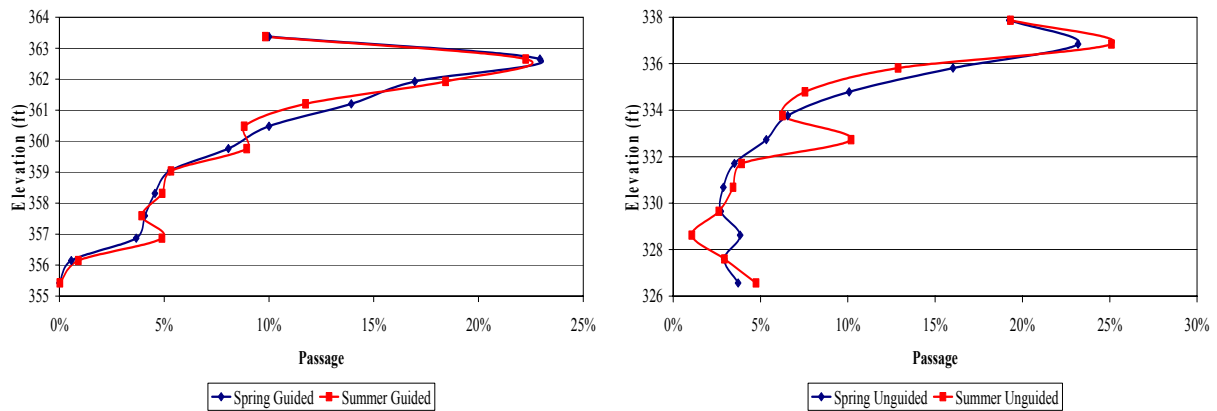


Figure 3.41. Vertical Distribution of Fish Abundance at Guided and Unguided Deployments

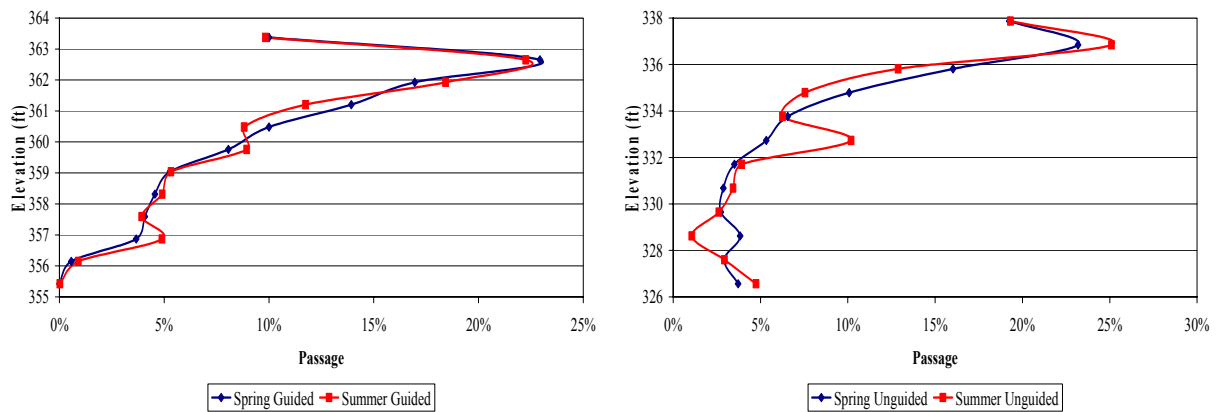


Figure 3.42. Vertical Distribution of Fish Abundance at 1- and 2-ft Gate Openings

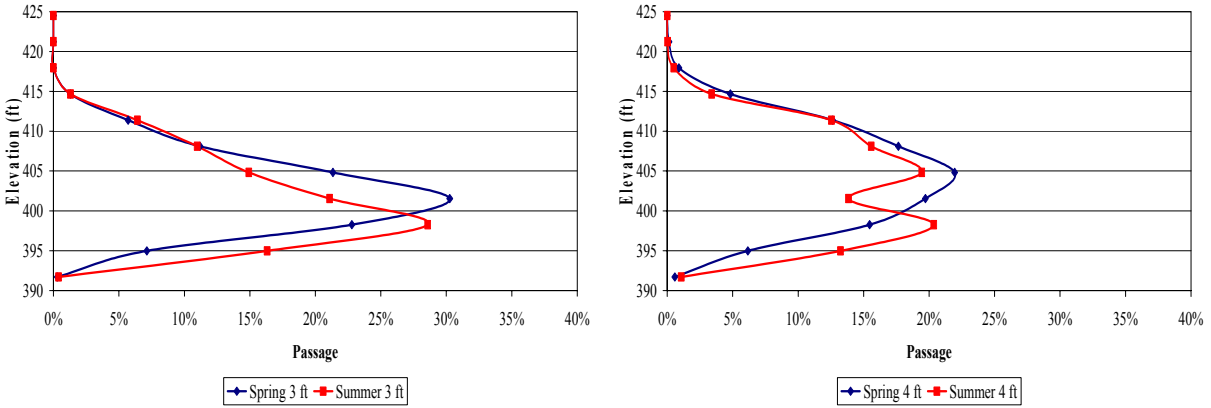


Figure 3.43. Vertical Distribution of Fish Abundance at 3- and 4-ft Gate Openings

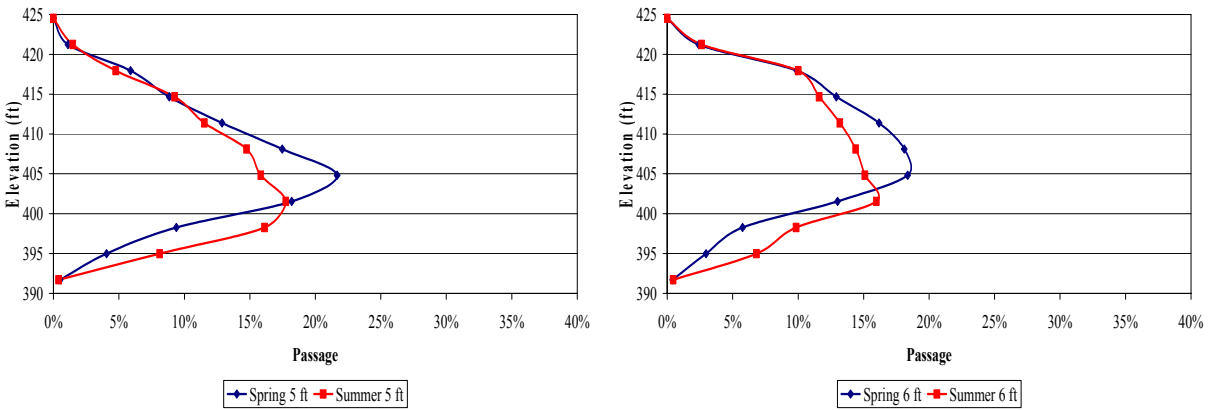


Figure 3.44. Vertical Distribution of Fish Abundance at 5- and 6-ft Gate Openings

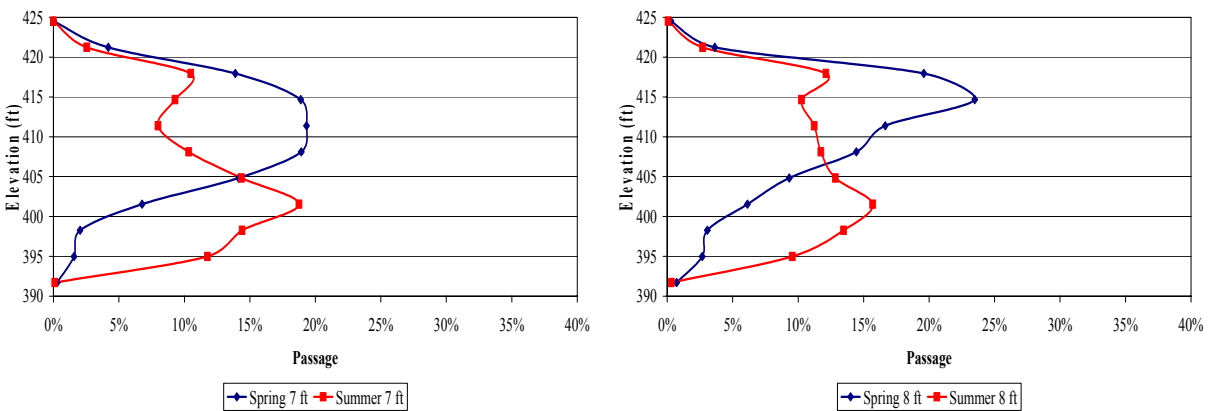


Figure 3.45. Vertical Distribution of Fish Abundance at 7- and 8-ft Gate Openings

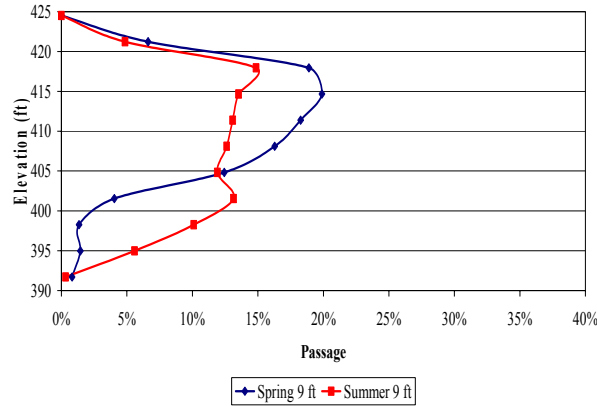


Figure 3.46. Vertical Distribution of Fish Abundance at a 9-ft Gate Opening

3.5.3 Powerhouse Trajectories and Vertical Distributions

Fish were distributed near the turbine intake ceiling, and as expected most of the unguided fish passed near the screen tip. While detailed flow information was not available for this report, trajectories match the expectations of vectors both parallel to the intake walls and perpendicular to the intake screen. Because of its shallow aiming angle, the unguided sample volume showed these expected changes from near the intake floor to the screen tip. The trajectories of fish were nearly identical during both spring and summer. This is especially true where there are more samples, higher in the water column (Figure 3.47).

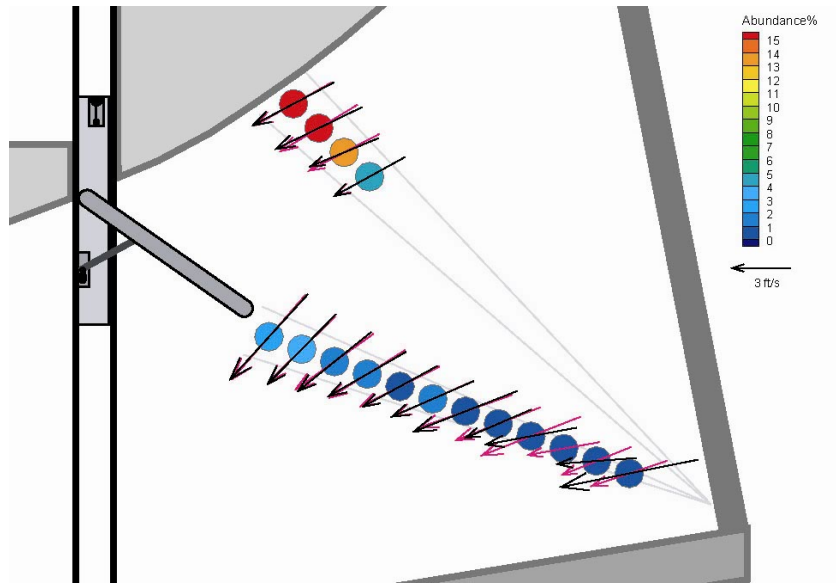


Figure 3.47. Powerhouse Trajectories and Vertical Distribution. Pink vectors are spring, black are summer.

4.0 Discussion

This section begins with the study conditions, which provide the river environment context for the study. Then the general fish passage results are discussed. These results contain where and when fish passed the dam regardless of dam operations, and are based on the inclusive data set. Next, how the spill treatments affected fish passage is discussed for the two sets of treatment. Then, implications of the fish trajectory and vertical distribution data are discussed. Finally, data for the potential placement of an RSW is addressed.

4.1 General Fish Passage

River flows during this sample period were near the 10-yr average, with peak flows occurring near the end of the spring period. Steelhead and yearling Chinook salmon were the most abundant spring migrants. During the summer study period, nearly all of the downstream migrants were subyearling Chinook. Spill treatments were altered day and night with spill proportion and their influence is evident in some of the seasonal comparisons.

Project fish passage efficiency was high in both spring and summer periods. Daily trends showed the influence of spill treatments, but the tendency of fish to pass in greater numbers at night was evident during all treatments. Horizontal distributions were consistent with proportion of flow through a route, except that fish pass in greater proportion than flow at the spillway, relative to the powerhouse. Fish passage efficiency increased slightly with increasing proportion of spill. For all seasons and diel periods, a greater proportion of fish passed via the spillway than proportion of flow. Spill passage relationships with spill proportion showed similar trends among seasons and diel periods.

4.2 Fish Passage During Spill Treatments

Passage differences among plunging (BiOp) versus skimming flow treatments (Spill50) were driven largely by nighttime differences in spill proportion. The BiOp treatment called for 100% night spill up to the gas cap, compared to 50% spill at night for the Spill50 treatment. Both treatments resulted in approximately 50% spill during the day. Because night is generally the time of greatest passage, we would expect the treatment differences to affect the majority of fish. The decision to curtail this treatment study due to other information and begin another treatment resulted in reduced statistical power for the summer ANOVA tests. That decision was based on information that suggested neither treatment was providing acceptable direct survival results. If that result is confirmed, passage comparisons among treatments become moot. Nevertheless, we have computed and reported ANOVA results with the caveat that the reader should be aware of the limited number of blocks in summer.

The fish passage efficiency and spill passage efficiency differed significantly among treatments only for spring (Table 4.1). Though not statistically significant, the trend among treatments in summer was the same as in spring for both fish passage efficiency and spill passage efficiency. Spill passage effectiveness differed significantly among treatments only in the summer. The trend among treatments in summer was the reverse of that in spring. Such inconsistency raises the question of whether statistical significance is a spurious result due to low sample size. A difference in the way species respond to the treatments cannot be ruled out on the basis of available information, so the question must remain unanswered. Fish

Table 4.1. Spring ANOVA Summary. The mean values for the BiOp treatment are shown in the upper left and the Spill50 treatment in the lower right of each square. Yellow highlighted squares indicate a statistically significant difference ($\alpha = 0.05$).

	FPE	SPE	SPS	FGE
Spring	BiOp 97.4% Spill50 94.3%	81.4% 56.0%	1.12 1.01	85.1% 85.6%
Summer	96.9% 92.7%	76.4% 65.4%	1.07 1.27	81.5% 77.8%

guidance efficiency differed little among these treatments regardless of season. Differences in horizontal distribution among BiOp and Spill50 treatments can be explained by the differing proportions of flow over the spillway at night.

The summer BulkBiOp vs. NoSpill treatment comparison was added in response to the in-season results from survival studies. BulkBiOp was intended to result in larger spillgate openings and more spill per bay for a given spill volume while maintaining the same total spill volume mandated by the BiOp. The NoSpill treatment addressed the high apparent injury rates at the spillway by directing all flow through the powerhouse. The BulkBiOp treatment differed more widely from the NoSpill treatment than did the previously compared treatments (BiOp vs. Spill50). The uncertainty surrounding the relative survival among passage routes means that the passage differences we report here will best be interpreted in the context of survival study results. Those results were not finalized as of this writing.

Fish passage efficiency was significantly higher for BulkBiOp than for NoSpill treatments (Table 4.2). We would generally expect fish passage efficiency to drop as spill is reduced, and this difference is consistent with that expectation. If spill survivals are low, however, high fish passage efficiencies may not provide the best overall survival. That determination will have to wait until the results of concurrent survival studies become available. Bypass survival will be critical to the survival performance of the NoSpill treatment, because the majority of fish in that treatment are guided and pass through the juvenile

Table 4.2. Summer ANOVA Summary. The mean values for the BulkBiOp treatment are shown in the upper left and the NoSpill treatment in the lower right of each square. Yellow highlighted squares indicate a statistically significant difference ($\alpha = 0.05$).

	FPE	FGE
Summer	BulkBiOp 98.8% NoSpill 87.7%	93.2% 87.7%

bypass system. Fish guidance efficiency did not differ significantly among treatments. Fish guidance efficiency during this period was high for both treatments, relative to the earlier spring and summer periods.

4.3 Fish Trajectories and Vertical Distributions at the Spillway

We were able to describe both the vertical distribution and trajectories of fish in the forebay immediately prior to passage under the Tainter gate. Based on preliminary sensor fish and direct survival data, a fish's location within the water column as it approaches the Tainter gate may be an important determinant in its ultimate survival. Fish trajectories paralleled flows both in direction and magnitude through the sample volume; however both trajectories and distributions also vary by spill gate opening. At low gate openings, fish must pass through an opening only a few feet high and their vertical distribution is compressed and deep. At higher gate openings, fish are distributed through more of the water column at the sample location and are drawn from higher in water column. In addition, vertical distributions differ by season and/or species composition. This difference is pronounced at 7- and 8-ft gate openings with the summer run of fish passing the sample volume deeper than the spring run.

4.4 Potential RSW Placement

The proportions of fish passing spill Bays 2 and 3 often exceeded the proportion of flow passing those routes. During BiOp flows, both Bays 2 and 3 were consistently effective at passing fish. During the BulkBiop treatment, Bay 3 outperformed adjacent bays. The preference for this portion of the dam can still be seen in the NoSpill treatment as most of the fish passed through Unit 6. Their location is consistent with the location of the historical river channel, or thalweg (Figure 4.1). Relatively high passage through Unit 1 was also a trend consistent through season and treatment condition. If these fish are orienting relative to the bank of the river, they might not be strongly influenced by an RSW located on the spillway.

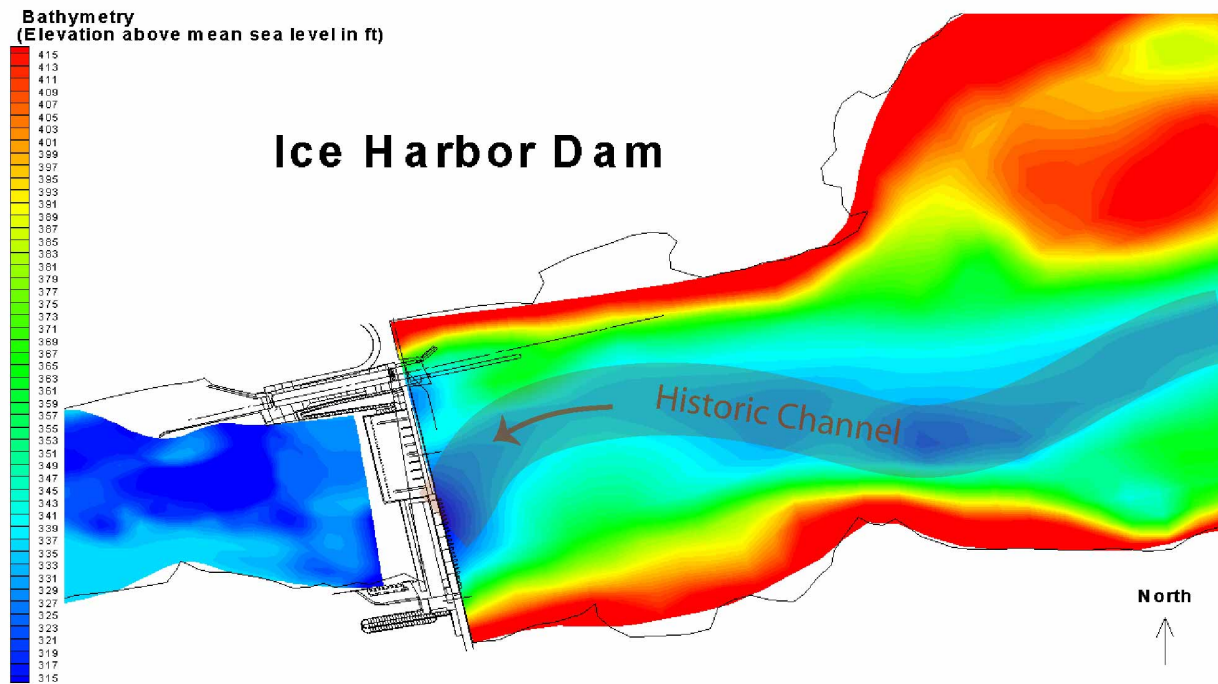


Figure 4.1. Historic River Channel in the Forebay of Ice Harbor Dam

5.0 Conclusion

The original question of interest for this study was whether and/or how two spill operations, BiOp vs. Spill50, influenced downstream fish passage. This was based on the assumption that the skimming flows in the tailrace created during 50% spill were beneficial to smolt survival. Based on preliminary results from other studies, these assumptions changed during the course of this study. Rapid adaptation by the Corps and regional entities altered the research direction at Ice Harbor Dam to include a BulkBiop vs. NoSpill test in the summer.

Comparing the BiOp to Spill50, fish passage efficiency decreased 3.1% in spring and 4.2% in summer. While this was statistically significant in the spring (but not in the summer likely due to small sample size), it may or may not be biologically significant. The decrease in fish passage efficiency was due to fewer fish utilizing the spillway passage route. Since the two treatments had the same daytime operations, this decrease occurred during nighttime passage. Whether this decrease in spill flows was beneficial to overall project survival can only be answered with results from concurrent survival studies.

The BulkBiop to NoSpill comparison has a limited inference from testing only in the summer and with a limited number of blocks. Even during this short period, though, fish passage efficiency decreased from 98.8% to 87.7% in the absence of spill and was statistically different. This was an expected decrease with no spill at the project, as fish passage efficiency becomes dependent solely on fish guidance efficiency. The survival benefit to this treatment will also become clearer when survival study results are published.

Variation in fish trajectory and vertical distributions at the spillway by spill gate opening and by season should be taken into account when making inferences from other field studies. For planning purposes of a potential Removable Spillway Weir, spill Bay 3 was the most consistent at passing more fish per volume of water than other bays. This was regardless of spill treatment, spill pattern, or season.

6.0 References

- BioSonics, Inc. 1996. *Acoustic Evaluation of the Surface Bypass and Collection System at Ice Harbor Dam in 1995*. Prepared for the U.S. Army Corps of Engineers, Walla Walla District by BioSonics, Inc., Seattle, Washington.
- Johnson L, C Noyes, and R McClure. 1984. *Hydroacoustic Evaluation of the Efficiencies of the Ice and Trash Sluiceway and Spillway at Ice Harbor Dam for Passing Downstream Migrating Juvenile Salmon and Steelhead, 1983*. Prepared for the U.S. Army Corps of Engineers, Walla Walla District by BioSonics, Inc., Seattle, Washington.
- Johnson L, C Noyes, and G Johnson. 1982. *Hydroacoustic Evaluation of the Efficiency of the Ice Harbor Dam Ice and Trash Sluiceway and Spillway for Passing Downstream Migrating Juvenile Salmon and Steelhead, 1982*. Prepared for the U.S. Army Corps of Engineers, Walla Walla District by BioSonics, Inc., Seattle, Washington.
- Love RH. 1977. "Target strength of an individual fish at any aspect." *Journal of the Acoustical Society of America* 62:1397-1403.
- Moursund RA, KD Ham, and PS Titzler. 2003. *Hydroacoustic Evaluation of Downstream Fish Passage at John Day Dam in 2002*. PNWD-3236, prepared for the U.S. Army Corps of Engineers, Portland District, Portland, Oregon.
- Skalski JR, A Hoffman, BH Ransom, and TW Steig. 1993. "Fixed-location hydroacoustic monitoring designs for estimating fish passage using stratified random and systematic sampling." *Canadian Journal of Fisheries and Aquatic Sciences* 50:1208-1221.
- Zar JH. 1999. *Biostatistical Analysis*. Prentice-Hall: Upper Saddle River, New Jersey.

Appendix A
Statistical Synopsis

Statistical Methods for Hydroacoustic Data Analysis at Ice Harbor Dam 2003

1.0 Introduction

The purpose of this synopsis is to describe the statistical methods used in the analysis of the 2003 hydroacoustic study at Ice Harbor Dam. The study will estimate fish passage through the powerhouse (i.e., turbines) and spillway during the spring and summer smolt outmigration. These estimates of fish passage will be used to estimate various measures of fish passage performance including the following:

- a. Fish passage efficiency (FPE)
- b. Spill passage efficiency (SPE)
- c. Spill passage effectiveness (SPS)
- d. Fish guidance efficiency (FGE)

These performance measures will be compared under two different spill treatments conducted during the course of this study.

2.0 Transducer Deployment and Sampling Scheme

This section describes the hydroacoustic sampling schemes that were used to estimate smolt passage at the powerhouse and spillway at Ice Harbor Dam in 2003.

2.1 Sampling at Powerhouse

The Ice Harbor powerhouse is comprised of 6 turbine units, each with 3 turbine intake slots (i.e., A, B, and C). Standard-length submerged traveling screens (STS) are installed in all slots. One intake within each of the 6 units were randomly selected and monitored. A pair of transducers (Figure A1) was used within an intake slot to monitor guided and unguided fish passage. One single-beam system and two split-beam systems were used to monitor the turbine intakes. Pairs of 6° single-beam transducers were deployed at units 2C and 5A, and pairs of 6° split-beam transducers were deployed at units 1A, 3B, 4C, and 6B (Figure 2). Split-beam

systems sampled at a rate of 25 pings per second, slow multiplexing 1 transducer at 88-sec intervals, 10 times per hour. Single-beam systems sampled at a rate of 25 pings per second, slow multiplexing 1 transducer at 58-sec intervals, 10 times per hour.

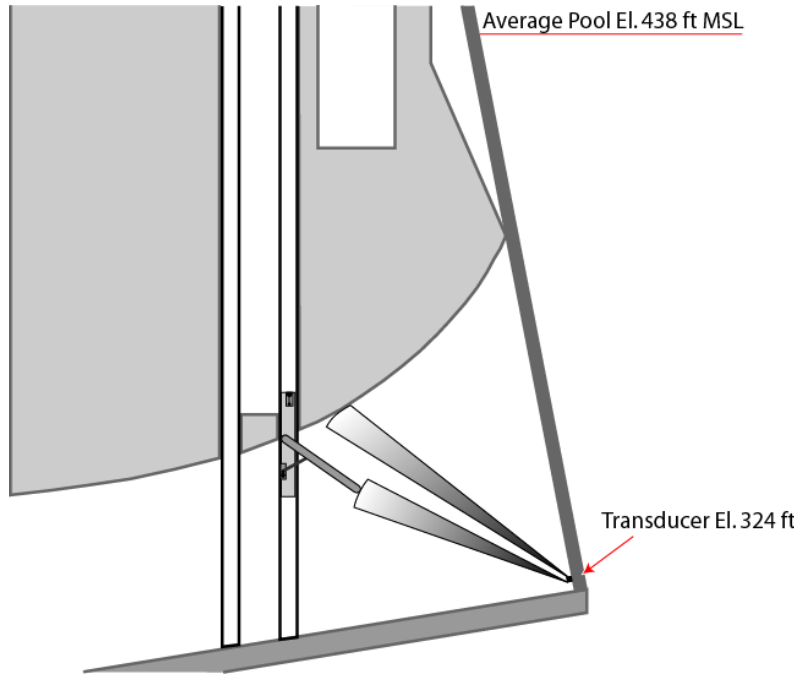


Figure A1. Deployment of Hydroacoustic transducers at STS intakes.

2.2 Sampling at Spillway

There are 10 spillbays at Ice Harbor Dam. Every spill bay was monitored. One downlooking-transducer monitored fish passage at each of the spillbays. One single-beam and two split-beam systems were used to monitor the spillway. Each mount was offset in either a north (n), middle (m), or south (s) position to reduce any bias caused by non-uniform distribution within each bay. 10° single-beam transducers were deployed at spill bays 7s and 9m. 10° split-beam transducers were deployed at spill bays 1s, 2n, 3m, 4n, 5s, 6m, 8n, and 10s. The single-beam system sampled at a rate of 25 pings per second, slow multiplexing each transducer at 58-sec intervals, 10 times per hour. The split-beam systems sampled at a rate of 25 pings per second, slow multiplexing each transducer at 88-second intervals, 10 times per hour.

3.0 Estimating Fish Passage

The following sections describe how the estimates of smolt passage will be calculated at the various locations at Ice Harbor Dam.

3.1 Powerhouse Passage – Unguided Fish

3.1.1 Total Powerhouse

The sampling at the powerhouse can be viewed as a two-stage sampling scheme. The first stage is the sampling of intake slots within a stratum composed of neighboring turbine units that were operating simultaneously. Typically, 3 consecutive turbine units would be grouped together to form a stratum, and it would be assumed that 3 of 9 intake slots were randomly selected for monitoring. Neighboring turbine units would be grouped into strata while still retaining the ability to calculate spatial sampling variances. The resulting variance estimates can generally be considered conservative for they often include more between-intake variance than expected under the original sampling design.

The unguided fish passage at the powerhouse (U) will be estimated by the quantity

$$\hat{U} = \sum_{i=1}^D \sum_{j=1}^{24} \sum_{k=1}^{K_{ij}} \left[\frac{A_{ijk}}{a_{ijk}} \left[\sum_{l=1}^{a_{ijk}} \hat{U}_{ijkl} \right] \right] \quad (\text{A1})$$

where

\hat{U}_{ijkl} = estimated fish passage in the l th intake slot ($l = 1, \dots, a_{ijk}$) within the k th turbine stratum ($k = 1, \dots, K_{ij}$) during the j th hour ($j = 1, \dots, 24$) on the i th day ($i = 1, \dots, D$);

a_{ijk} = number of intake slots actually sampled in the k th turbine stratum ($k = 1, \dots, K_{ij}$) during the j th hour ($j = 1, \dots, 24$) on the i th day ($i = 1, \dots, D$);

K_{ij} = number of turbine strata created during the j th hour ($j = 1, \dots, 24$) on the i th day
($i = 1, \dots, D$).

Because of the varying power loads over time, the number of spatial strata (i.e., K_{ij}) formed by post-stratification of adjacent turbine units may vary between hours ($j = 1, \dots, 24$) and days ($i = 1, \dots, D$).

The estimate of \hat{U}_{ijkl} is based on the assumption of simple random sampling within a slot-hour, in which case

$$\hat{U}_{ijkl} = \frac{B_{ijkl}}{b_{ijkl}} \sum_{b=1}^{b_{ijkl}} z_{ijklg} . \quad (\text{A2})$$

Combining Equations (A1) and (A2), the overall estimate of unguided fish passage during D days can be expressed as

$$\hat{U}_{ijkl} = \sum_{i=1}^D \sum_{j=1}^{24} \sum_{k=1}^{K_{ij}} \left[\frac{A_{ijk}}{a_{ijk}} \left[\frac{B_{ijkl}}{b_{ijkl}} \sum_{b=1}^{b_{ijkl}} z_{ijklg} \right] \right] \quad (\text{A3})$$

where

z_{ijklg} = expanded fish count in the g th sampling unit ($g = 1, \dots, b_{ijkl}$) in the l th intake slot
($l = 1, \dots, a_{ijk}$) within the k th turbine stratum ($k = 1, \dots, K_{ij}$) during the j th hour
($j = 1, \dots, 24$) on the i th day ($i = 1, \dots, D$);

b_{ijkl} = number of sampling units actually observed in the l th intake slot ($l = 1, \dots, a_{ijk}$)
within the k th turbine stratum ($k = 1, \dots, K_{ij}$) during the j th hour ($j = 1, \dots, 24$) on
the i th day ($i = 1, \dots, D$);

B_{ijkl} = total number of sampling units within the l th intake slot ($l = 1, \dots, a_{ijk}$) within the k th turbine stratum ($k = 1, \dots, K_{ij}$) during the j th hour ($j = 1, \dots, 24$) on the i th day ($i = 1, \dots, D$).

Nominally, $B_{ijkl} = 20, 40, 48$ or $60 \forall ijkl$ and $b_{ijkl} = 6$ or 10 , depending on location. Based on the assumption of simple random sampling

$$\widehat{Var}(\hat{U}_{ijkl}) = \frac{B_{ijkl}^2 \left(1 - \frac{b_{ijkl}}{B_{ijkl}}\right) s_{z_{ijkl}}^2}{b_{ijkl}} \quad (\text{A4})$$

where

$$s_{z_{ijkl}}^2 = \frac{\sum_{g=1}^{b_{ijkl}} (z_{ijklg} - \bar{z}_{ijkl})^2}{(b_{ijkl} - 1)}$$

and where

$$\bar{z}_{ijkl} = \frac{1}{b_{ijkl}} \sum_{g=1}^{b_{ijkl}} z_{ijklg} .$$

The variance of \hat{U} can then be estimated by the formula

$$\widehat{Var}(\hat{U}) = \sum_{i=1}^D \sum_{j=1}^{24} \sum_{k=1}^{K_{ij}} \left[\frac{A_{ijk}^2 \left(1 - \frac{a_{ijk}}{A_{ijk}}\right) s_{\hat{U}_{ijk}}^2}{a_{ijk}} + \frac{A_{ijk} \sum_{l=1}^{a_{ijk}} \widehat{Var}(\hat{U}_{ijkl})}{a_{ijk}} \right] \quad (\text{A5})$$

where

$$s_{\hat{U}_{ijk}}^2 = \frac{\sum_{l=1}^{a_{ijk}} (\hat{U}_{ijkl} - \hat{U}_{ijk})^2}{(a_{ijk} - 1)},$$

$$\hat{U}_{ijk} = \frac{1}{a_{ijk}} \sum_{l=1}^{a_{ijk}} \hat{U}_{ijkl}.$$

3.1.2 Single Turbine Unit

The estimator of unguided passage at a single turbine is as follows:

$$\hat{U}_k = \frac{3}{1} \sum_{i=1}^D \sum_{j=1}^{24} \left[\frac{B_{ijk} \sum_{g=1}^{b_{ijk}} z_{ijk}^g}{b_{ijk}} \right] \quad (\text{A6})$$

where

z_{ijk}^g = expanded fish passage in the g th sampling unit ($g = 1, \dots, b_{ijk}$) at the k th turbine unit during the j th hour ($j = 1, \dots, 24$) on the i th day ($i = 1, \dots, D$);

b_{ijk} = number of sampling intervals monitored at the k th turbine unit during the j th hour ($j = 1, \dots, 24$) on the i th day ($i = 1, \dots, D$);

B_{ijk} = total number of possible sampling intervals at the k th turbine unit during the j th hour ($j = 1, \dots, 24$) on the i th day ($i = 1, \dots, D$).

The variance of \hat{U}_k can be estimated by

$$\widehat{Var}(\hat{U}_k) = 9 \sum_{i=1}^D \sum_{j=1}^{24} \left[\frac{B_{ijk}^2 \left(1 - \frac{b_{ijk}}{B_{ijk}} \right) s_{z_{ijk}^g}^2}{b_{ijk}} \right] \quad (\text{A7})$$

where

$$s_{z_{ijk}}^2 = \frac{\sum_{g=1}^{b_{ijk}} (z_{ijk} - \bar{z}_{ijk})^2}{(b_{ijk} - 1)},$$

$$\bar{z}_{ijk} = \frac{\sum_{g=1}^{b_{ijk}} z_{ijk}}{b_{ijk}}.$$

It should be noted that the variance estimator (A7) will underestimate the true sampling variance at a specific turbine unit, because the intake-to-intake variance is not measured..

3.2 Powerhouse Passage – Guided Fish

3.2.1 Total Powerhouse

The post-stratification used in estimating unguided passage should be is the same as used to estimate guided passage at the powerhouse. Hence, the estimator for guided fish passage can be written as

$$\hat{G} = \sum_{i=1}^D \sum_{j=1}^{24} \sum_{k=1}^{K_{ij}} \left[\frac{A_{ijk}}{a_{ijk}} \left[\frac{B_{ijkl}}{b_{ijkl}} \sum_{g=1}^{b_{ijkl}} y_{ijklg} \right] \right] \quad (\text{A8})$$

where

y_{ijklg} = expanded fish passage in the g th sampling unit ($g = 1, \dots, b_{ijkl}$) in the l th intake slot ($l = 1, \dots, a_{ijk}$) within the k th turbine stratum ($k = 1, \dots, K_{ij}$) during the j th hour ($j = 1, \dots, 24$) on the i th day ($i = 1, \dots, D$).

The estimated variance of \hat{G} can then be expressed as

$$\widehat{Var}(\hat{G}) = \sum_{i=1}^D \sum_{j=1}^{24} \sum_{k=1}^{K_{ij}} \left[\frac{A_{ijk}^2 \left(1 - \frac{a_{ijk}}{A_{ijk}}\right) s_{G_{ijk}}^2}{a_{ijk}} + \frac{A_{ijk} \sum_{l=1}^{a_{ijk}} \widehat{Var}(\hat{G}_{ijkl})}{a_{ijk}} \right] \quad (\text{A9})$$

where

$$\begin{aligned} \widehat{Var}(\hat{G}_{ijkl}) &= \frac{B_{ijkl}^2 \left(1 - \frac{b_{ijkl}}{B_{ijkl}}\right) s_{y_{ijkl}}^2}{b_{ijkl}}, \\ s_{y_{ijkl}}^2 &= \frac{\sum_{g=1}^{b_{ijkl}} (y_{ijklg} - \bar{y}_{ijkl})^2}{(b_{ijkl} - 1)}, \\ \bar{y}_{ijkl} &= \frac{1}{b_{ijkl}} \sum_{g=1}^{b_{ijkl}} y_{ijklg}, \end{aligned}$$

and where

$$\begin{aligned} s_{\hat{G}_{ijk}}^2 &= \frac{\sum_{l=1}^{a_{ijk}} (\hat{G}_{ijkl} - \hat{G}_{ijk})^2}{(a_{ijk} - 1)}, \\ \hat{G}_{ijk} &= \frac{1}{a_{ijk}} \sum_{l=1}^{a_{ijk}} \hat{G}_{ijkl}. \end{aligned}$$

3.2.2 Single Turbine Unit

The estimator of guided passage at a single turbine is as follows:

$$\hat{G}_k = \frac{3}{1} \sum_{i=1}^D \sum_{j=1}^{24} \left[\frac{B_{ijk}}{b_{ijk}} \sum_{g=1}^{b_{ijk}} y_{ijk} \right] \quad (\text{A10})$$

where

y_{ijk} = expanded fish passage in the g th sampling unit ($g = 1, \dots, b_{ijk}$) at the k th turbine unit during the j th hour ($j = 1, \dots, 24$) on the i th day ($i = 1, \dots, D$);

b_{ijk} = number of sampling intervals monitored at the k th turbine unit during the j th hour ($j = 1, \dots, 24$) on the i th day ($i = 1, \dots, D$);

B_{ijk} = total number of possible sampling intervals at the k th turbine unit during the j th hour ($j = 1, \dots, 24$) on the i th day ($i = 1, \dots, D$).

The variance of \hat{G}_k can be estimated by

$$\widehat{Var}(\hat{G}_k) = 9 \sum_{i=1}^D \sum_{j=1}^{24} \left[\frac{B_{ijk}^2 \left(1 - \frac{b_{ijk}}{B_{ijk}} \right) s_{y_{ijk}}^2}{b_{ijk}} \right] \quad (\text{A11})$$

where

$$s_{y_{ijk}}^2 = \frac{\sum_{g=1}^{b_{ijk}} (y_{ijk} - \bar{y}_{ijk})^2}{(b_{ijk} - 1)},$$

$$\bar{y}_{ijk} = \frac{\sum_{g=1}^{b_{ijk}} z_{ijk}}{b_{ijk}}.$$

It should be noted that the variance estimator (A11) will underestimate the true sampling variance at a specific turbine unit.

3.3 Spillway Passage

The sampling at the Ice Harbor spillway can be envisioned as stratified random sampling within spillbay-hours. In which case, total spillway passage over D days can be estimated by the formula

$$\widehat{SP} = \sum_{i=1}^D \sum_{j=1}^{24} \sum_{k=1}^{10} \left[\frac{T_{ijk}}{t_{ijk}} \sum_{l=1}^{t_{ijk}} x_{ijkl} \right] \quad (\text{A12})$$

where

x_{ijkl} = expanded fish passage in the l th sampling interval ($l = 1, \dots, t_{ijk}$) during the j th hour ($j = 1, \dots, 24$) at the k th spillbay ($k = 1, \dots, 10$) on the i th day ($i = 1, \dots, D$);

T_{ijk} = total number of possible sampling units within the j th hour ($j = 1, \dots, 24$) at the k th spillbay ($k = 1, \dots, 10$) on the i th day ($i = 1, \dots, D$);

t_{ijk} = number of sampling units actually observed within the j th hour ($j = 1, \dots, 24$) at the k th spillbay ($k = 1, \dots, 10$) on the i th day ($i = 1, \dots, D$).

Nominally, $T_{ijk} = 30, 42$ or $48 \forall ijk$ and $t_{ijk} = 6$ or 10 depending on location.

The variance of \widehat{SP} can be estimated by the quantity

$$\widehat{Var}(\widehat{SP}) = \sum_{i=1}^D \sum_{j=1}^{24} \sum_{k=1}^{10} \left[\frac{T_{ijk}^2 \left(1 - \frac{t_{ijk}}{T_{ijk}} \right) s_{x_{ijk}}^2}{t_{ijk}} \right] \quad (\text{A13})$$

where

$$s_{x_{ijk}}^2 = \frac{\sum_{l=1}^{t_{ijk}} (x_{ijkl} - \bar{x}_{ijk})^2}{(t_{ijk} - 1)}$$

and where

$$\bar{x}_{ijk} = \frac{1}{t_{ijk}} \sum_{l=1}^{t_{ijk}} x_{ijkl} .$$

3.4 Estimating Missing Values

Occasionally throughout the sampling season, sample observations were missed when hydroacoustic equipment failed, log debris damaged equipment, or other unexpected events occurred. This loss of information typically occurred at only one or a few locations at a time. The majority of the data from many of these sites is still available when these lapses occurred.

Two specific missing-value scenarios make up a majority of the occurrences; these scenarios were:

1. In a turbine, the unguided turbine fish counts were missing, while the guided turbine fish counts were present.
2. Some spillbays were missing values, while concurrently, other spillbays were monitored.

Both approaches apply to the discussion.

Ratio or regression estimators can be used to estimate missing values on an hourly basis with associated variances (Snedecor and Cochran 1989: 165-167).

3.4.1 Regression Estimator

Figure A2 illustrates the typical scenario for missing values. Let

x_i = hourly passage estimate for the i th interval at a location with complete data,

y_i = hourly passage estimate for the i th interval at a location with missing values.

From hourly time intervals with complete data, a regression model of the form

$$y_i = \hat{\alpha} + \hat{\beta}x_i \quad (\text{A14})$$

is fitted using ordinary least squares. A missing y -value is then predicted by substituting into Equation (A14) the corresponding x -value where

$$\hat{y}_m = \hat{\alpha} + \hat{\beta}x_m. \quad (\text{A15})$$

The estimated variance for the predicted \hat{y}_m is computed according to the formula

$$\widehat{Var}(\hat{y}_m) = \text{MSE} \left(1 + \frac{1}{n} + \frac{(x_m - \bar{x})^2}{\sum_{i=1}^n (x_i - \bar{x})^2} \right) \quad (\text{A16})$$

where

n = number of observations used in estimating the regression line,

MSE = mean square for error resulting from the regression,

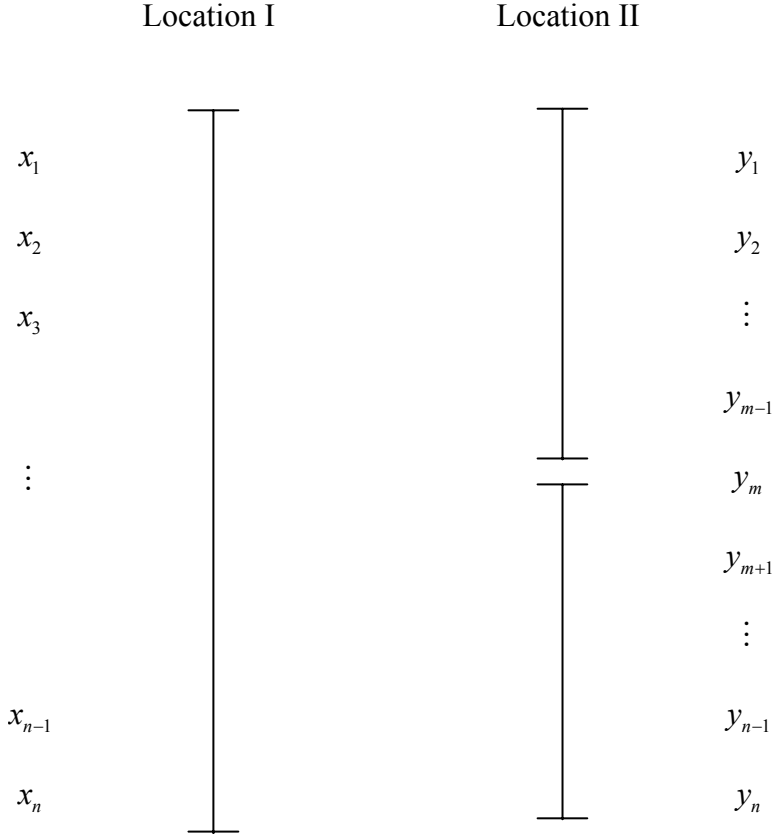
\bar{x} = mean value of x_i from the location with complete data,

x_m = value of x corresponding to the observation with a missing y -value,

\hat{y}_m = estimated missing value.

These results can be found in Snedecor and Cochran (1989: 165-167). The regression approach is most appropriate if the relationship is a straight-line not through the origin.

Figure A2. Schematic of missing value scenarios, where at one location (I) all values are completed and at another location (II) values are missing for an interval of time.



3.4.2 Ratio Estimator

Alternatively, if the relationship is a straight-line through the origin of the form

$$y_i = \beta x_i$$

then a ratio estimator can be used to estimate missing values. The ratio estimator can be written as

$$\hat{y}_m = \frac{\sum_{i=1}^n y_i}{\sum_{i=1}^n x_i} x_m \quad (\text{A17})$$

where the summations are over all paired observations where both the x and y values are present (i.e., n paired values). The variance of \hat{y}_m can be estimated by

$$\widehat{Var}(\hat{y}_m) = \frac{x_m^2 \sum_{i=1}^n (y_i - \hat{R}x_i)^2}{\bar{x}^2 n(n-1)}. \quad (\text{A18})$$

The method can be found in Cochran 1977 (pp. 153-156).

3.4.3 Interpolation Method

An estimate of a missing value can also be calculated by interpolating between neighboring values. Let y_m be a missing value for the m th hour, then it can be estimated by

$$\hat{y}_m = \frac{y_{m-1} + y_{m+1}}{2} \quad (\text{A19})$$

with interpolated variance

$$\widehat{Var}(\hat{y}_m) = \frac{\sum_{i=m-1}^{m+1} X_i^2 - \frac{\left(\sum_{i=1}^n X_i\right)^2}{n}}{(2-1)} \quad (\text{A20})$$

where

$\hat{y}_{m\pm 1}$ = passage one hour on either side of the m th hour with a missing value.

4.0 Estimating Passage Performance

4.1 Fish Passage Efficiency (FPE)

The fish passage efficiency (FPE) at Ice Harbor Dam will be estimated by the quotient

$$\widehat{FPE} = \frac{\widehat{SP} + \widehat{G}}{\widehat{SP} + \widehat{G} + \widehat{U}} \quad (\text{A21})$$

where

\widehat{SP} = estimated fish passage through the spillway,

\widehat{G} = estimated guided fish passage through the turbine routes,

\widehat{U} = estimated unguided fish passage through the turbine routes.

The denominator of Equation (A21) is an estimate of total project passage. The variance of \widehat{FPE} can be estimated by the quantity

$$\widehat{Var}(\widehat{FPE}) = \widehat{FPE}^2 (1 - \widehat{FPE})^2 \left[\frac{\widehat{Var}(\widehat{SP}) + \widehat{Var}(\widehat{G})}{(\widehat{SP} + \widehat{G})^2} + \frac{\widehat{Var}(\widehat{U})}{\widehat{U}^2} \right]. \quad (\text{A22})$$

4.2 Spill Efficiency (SPE)

Spill efficiency (SPE) at Ice Harbor Dam will be estimated by the quotient

$$\widehat{SPE} = \frac{\widehat{SP}}{\widehat{SP} + \widehat{G} + \widehat{U}}. \quad (\text{A23})$$

The variance of \widehat{SPE} can then be expressed as

$$\widehat{Var}(\widehat{SPE}) = \widehat{SPE}^2 (1 - \widehat{SPE})^2 \left[\frac{\widehat{Var}(\widehat{SP})}{\widehat{SP}^2} + \frac{\widehat{Var}(\widehat{G}) + \widehat{Var}(\widehat{U})}{(\widehat{G} + \widehat{U})^2} \right]. \quad (\text{A24})$$

4.3 Spill Effectiveness (SPS)

Spill effectiveness (SPS) at Ice Harbor Dam will be estimated by the function

$$\widehat{SPS} = \frac{\left(\frac{\widehat{SP}}{f_{SP}}\right)}{\left(\frac{\widehat{SP} + \widehat{G} + \widehat{U}}{f}\right)} = \left(\frac{f}{f_{SP}}\right) \widehat{SPE} \quad (\text{A25})$$

where

f = project-wide flow volume,

f_{SP} = spill flow volume.

The variance of \widehat{SPS} can be estimated by the quantity

$$\widehat{Var}(\widehat{SPS}) = \left(\frac{f}{f_{SP}}\right)^2 \cdot \widehat{Var}(\widehat{SPE}). \quad (\text{A26})$$

4.4 Fish Guidance Efficiency (FGE)

Fish guidance efficiency at Ice Harbor Dam will be estimated by the quotient

$$\widehat{FGE} = \frac{\widehat{G}}{\widehat{G} + \widehat{U}} \quad (\text{A27})$$

with an associated variance estimate of

$$\widehat{Var}(\widehat{FGE}) = \widehat{FGE}^2 (1 - \widehat{FGE})^2 \left[\frac{\widehat{Var}(\widehat{G})}{\widehat{G}^2} + \frac{\widehat{Var}(\widehat{U})}{\widehat{U}^2} \right], \quad (\text{A28})$$

The same formulas (A27) and (A28) can be used to estimate the FGE and its variance at a specific turbine unit or more specifically at a specific intake slot.

5.0 Confidence Interval Estimation

For all estimated passage and performance parameters (say, θ), confidence interval estimates were based on the assumption of asymptotic normality. Interval estimates were calculated according to the formula

$$\text{CI} \left(\hat{\theta} - Z_{1-\frac{\alpha}{2}} \sqrt{\widehat{\text{Var}}(\hat{\theta})} < \theta < \hat{\theta} + Z_{1-\frac{\alpha}{2}} \sqrt{\widehat{\text{Var}}(\hat{\theta})} \right) = 1 - \alpha \quad (\text{A29})$$

where

$$Z_{1-\frac{\alpha}{2}} = \text{standard normal deviate corresponding to the probability } P \left(|Z| < Z_{1-\frac{\alpha}{2}} \right) = 1 - \alpha .$$

For example, a Z-value of 1.96 is used to construct a 95% confidence interval. The interval estimate (A29) characterizes the statistical uncertainty associated with the measurement of a fish passage or performance parameter.

6.0 Test of Spill Regimes

The first set of spill regimes were nominally either skimming spill (50% for 24 hrs, referred to as Spill50) or plunging spill (45 kcfs daytime with 100% up to 100 kcfs at night, referred to as Biop). The second set of paired treatments occurred during the summer only and was comprised of a bulk spill pattern (at Biop flows, referred to as BulkBiop) or no spill (referred to as NoSpill). BulkBiop also spilled 45 kcfs daytime with 100% up to 100 kcfs at night, but concentrated that spill volume within fewer spill bays. A total of 22 blocks were planned between 26 April and 12 July 2003. Figure A3 has the planned schedule for the 2003 spill experiment.

Figure A3. Planned treatment and blocking schedule for the 2003 Ice Harbor experiment.

Month	Day	Block	Test	Month	Day	Block	Test	Month	Day	Block	Test
April	23		BIOP	May	27	9	BIOP	June	30	18	NoSpill
April	24		BIOP	May	28	9	SP50	July	1	18	NoSpill
April	25		BIOP	May	29	9	SP50	July	2	19	BULK
April	26	1	BIOP	May	30	10	BIOP	July	3	19	BULK
April	27	1	SP50	May	31	10	BIOP	July	4	19	NoSpill
April	28	2	BIOP	June	1	10	SP50	July	5	20	BULK
April	29	2	BIOP	June	2	10	SP50	July	6	20	BULK
April	30	2	SP50	June	3	11	BIOP	July	7	20	NoSpill
May	1	2	SP50	June	4	11	BIOP	July	8	20	NoSpill
May	2	3	BIOP	June	5	11	SP50	July	9	21	BULK
May	3	3	BIOP	June	6	11	SP50	July	10	21	NoSpill
May	4	3	SP50	June	7	12	BIOP	July	11	22	BULK
May	5	3	SP50	June	8	12	BIOP	July	12		Bulk*
May	6	4	BIOP	June	9	12	SP50	July	13		SURV
May	7	4	BIOP	June	10	12	SP50	July	14		SURV
May	8	4	SP50	June	11	13	BIOP	July	15		SURV
May	9	4	SP50	June	12	13	BIOP	July	16		NoSpill
May	10	5	BIOP	June	13	13	SP50	July	17		Bulk*
May	11	5	BIOP	June	14	13	SP50	July	18		Bulk*
May	12	5	SP50	June	15	14	BIOP	July	19		Bulk*
May	13	5	SP50	June	16	14	BIOP	July	20		Bulk*
May	14	6	BIOP	June	17	14	SP50	July	21		Bulk*
May	15	6	BIOP	June	18	14	SP50	July	22		Bulk*
May	16	6	SP50	June	19	15	BIOP	July	23		Bulk*
May	17	6	SP50	June	20	15	BIOP	July	24		Bulk*
May	18	7	BIOP	June	21	15	SP50	* Did not spill over 24-hr period			
May	19	7	BIOP	June	22	15	SP50				
May	20	7	SP50	June	23	16	BIOP				
May	21	7	SP50	June	24	17	BULK				
May	22	8	BIOP	June	25	17	BULK				
May	23	8	BIOP	June	26	17	NoSpill				
May	24	8	SP50	June	27	17	NoSpill				
May	25	8	SP50	June	28	18	BULK				
May	26	9	BIOP	June	29	18	BULK				

A two-way analysis of variance will be used to analyze the fish passage performance measures (i.e., FPE, SPE, and SPS). The ANOVA table will be of the form:

Source	DF	SS	MS	F
Total _{Cor}	$2B - 1$	SSTOT		
Blocks	$B - 1$	SSB		
Treatments	1	SST	MST	$F_{1,B-1} = \frac{MST}{MSE}$
Error	$B - 1$	SSE	MSE	

In the previous ANOVA table, B = number of blocks analyzed. Two-tailed tests of significance will be performed for each response variable. The fish passage measures will be arcsin- or ln-transformed prior to analysis to stabilize the variance and provide an additive model on the ln-scale.

Confidence interval estimates for the mean response for a treatment condition can be calculated from the ANOVA results as

$$CI \left(e^{\bar{x} \pm t_{B-1} \sqrt{\frac{MSE}{B}}} \right). \quad (A30)$$

In Equation (A30), \bar{x} is the sample mean based on the transformed performance measures used in the ANOVA analysis. The confidence interval is based on assuming the transformed values are normally distributed.

Appendix B
Effective Beam Widths

Appendix B

Effective Beam Widths

The effective beam width is calculated from a detectability model. Inputs to this model include fish speeds and trajectories as well as the sensitivity and beam pattern of each transducer. These come from split beam data of actual fish paths and from the equipment calibration process, respectively. The output forms the basis for expanding the fish counts. As shown below, the effective beam width varies by range, diel, and season. The charts below show the effective beam width used in this study.

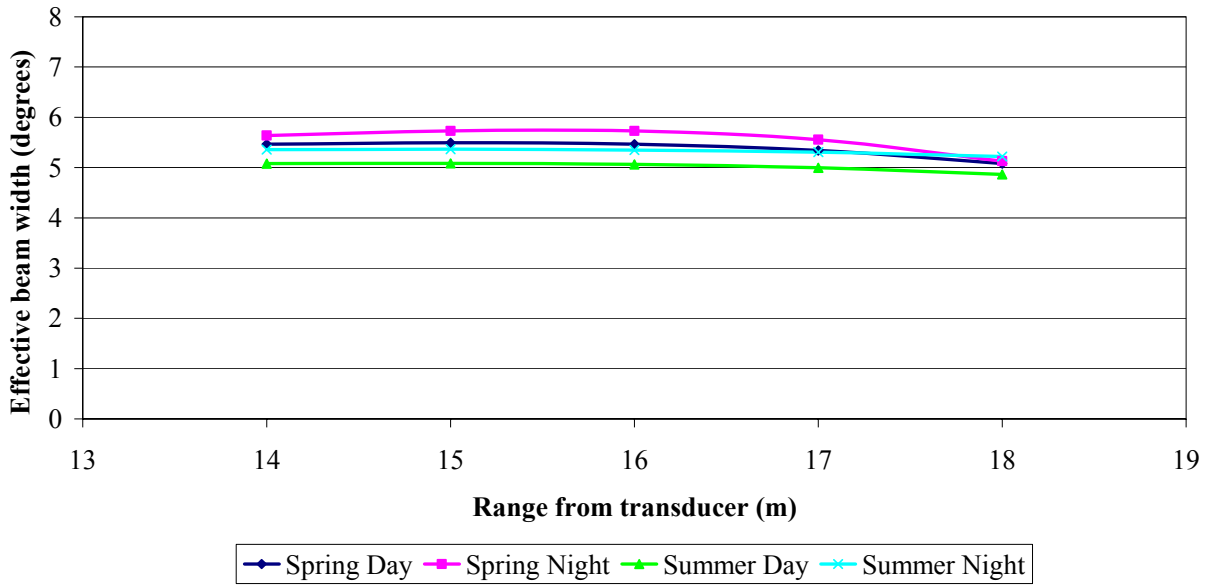


Figure 1. Guided

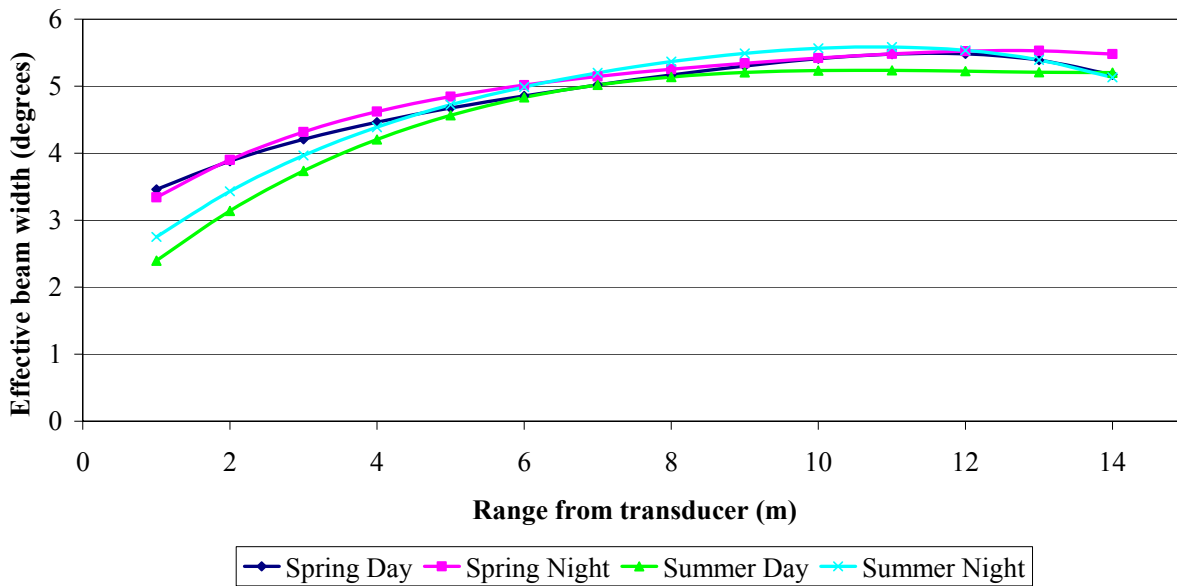


Figure 2. Unguided.

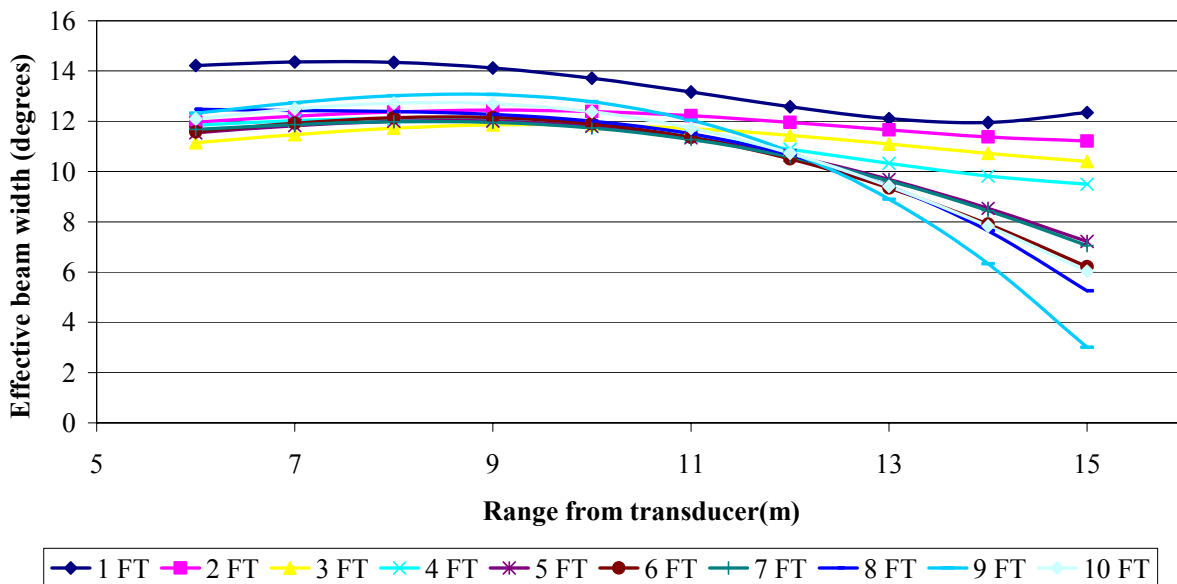


Figure 3. Spring day spill.

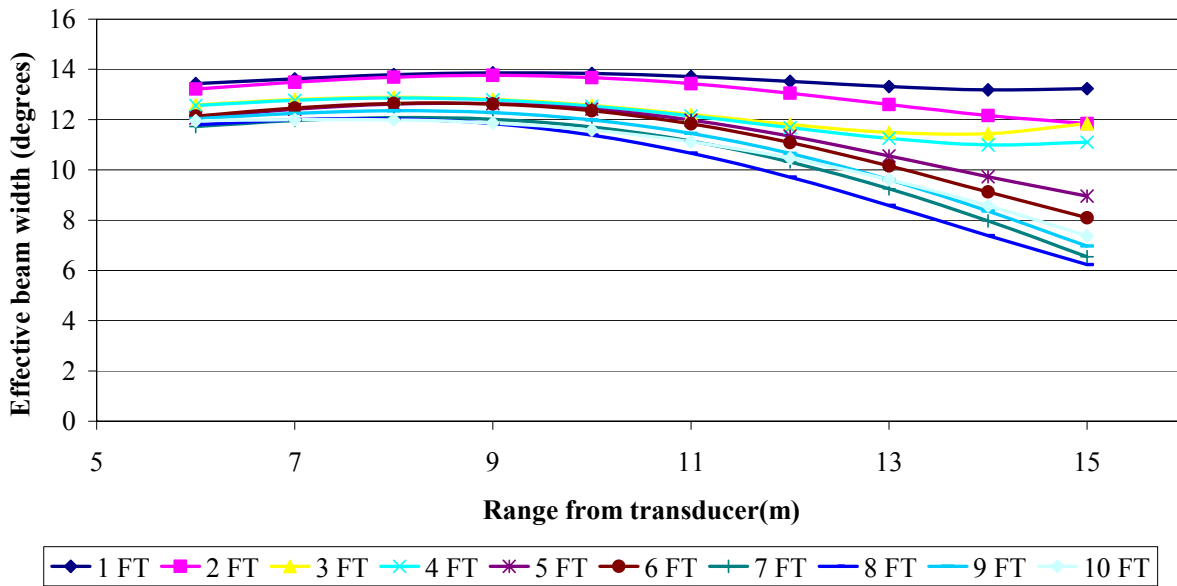


Figure 4. Spring night spill.

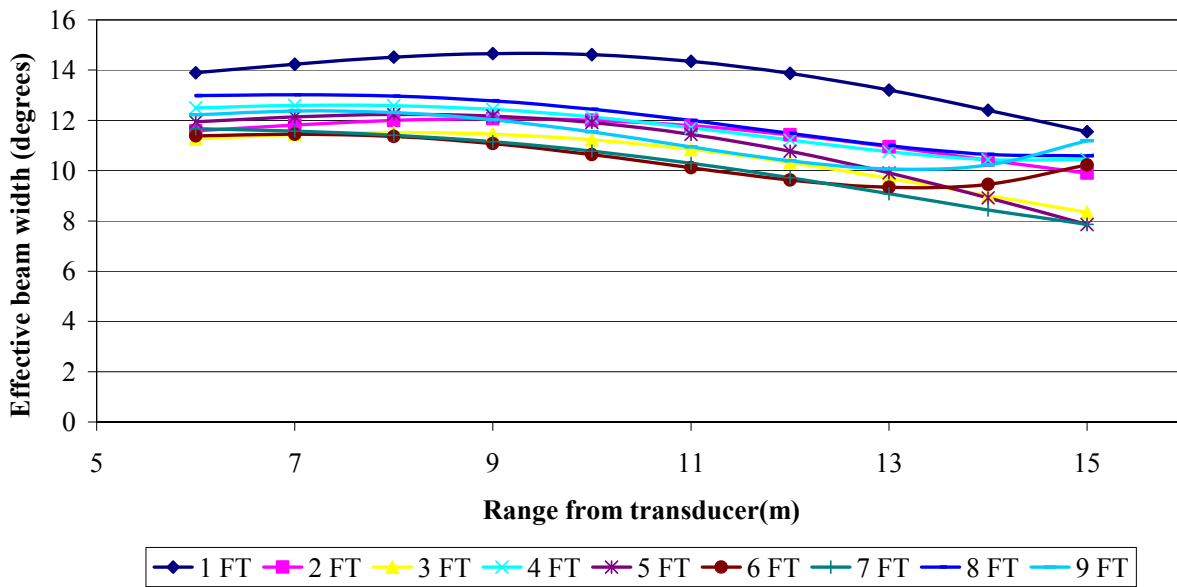


Figure 5. Summer day spill.

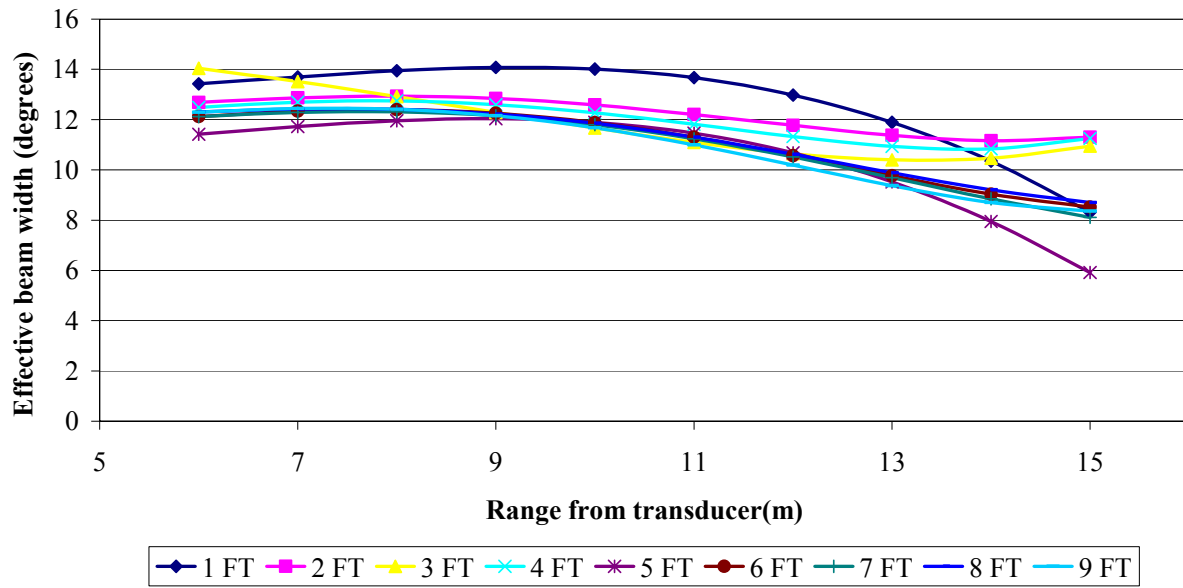


Figure 6. Summer night spill.

Appendix C
Hourly Spill by Block

Appendix C

Hourly Spill by Block

The spring Biop vs. Spill50 treatment tests occurred during blocks 1-11, for a total of 11 available blocks. The summer Biop vs. Spill50 treatment tests occurred during blocks 12-15, for a total of 4 available blocks. The summer Bulk vs. NoSpill treatment tests occurred during blocks 17-21, for a total of 5 available blocks. No blocks were censored from the analysis due to dam operations; however blocks 16 and 22 were not analyzed because both treatments were not represented. Summer begins at block 12 accounting for a 3-day lag from the Lower Monumental Dam smolt monitoring index.

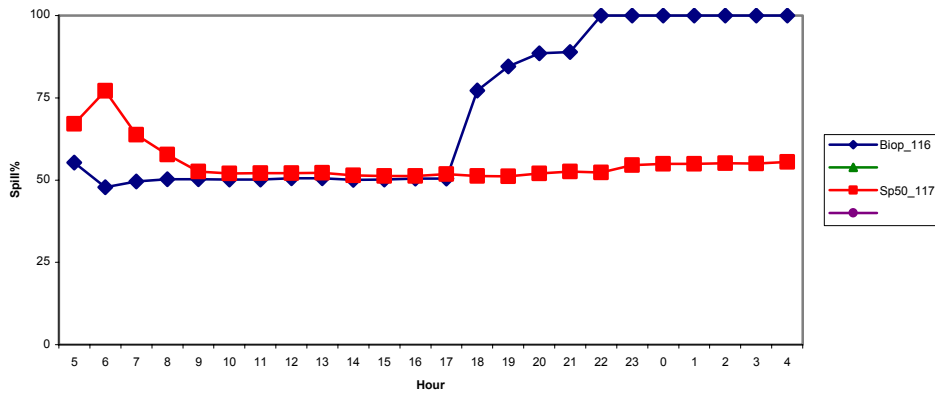


Figure 1. Percent spill during block 1 (spring Biop vs. Spill50).

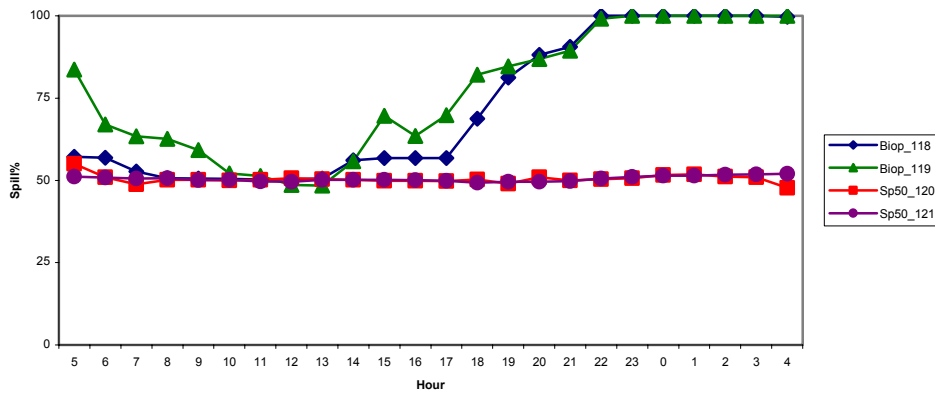


Figure 2. Percent spill during block 2 (spring Biop vs. Spill50).

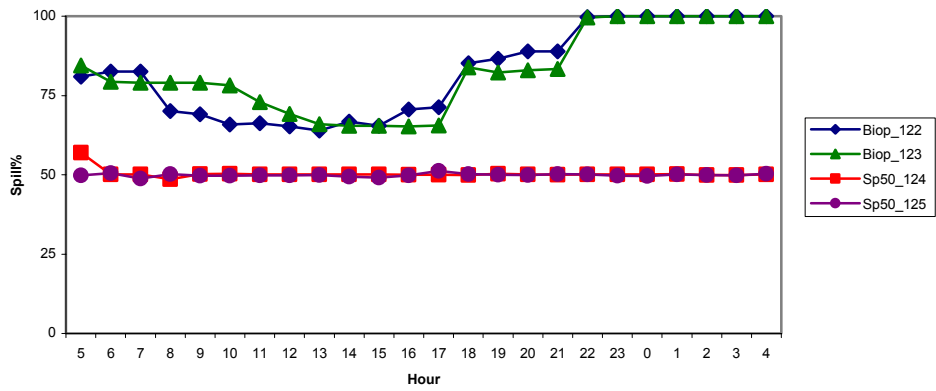


Figure 3. Percent spill during block 3 (spring Biop vs. Spill50).

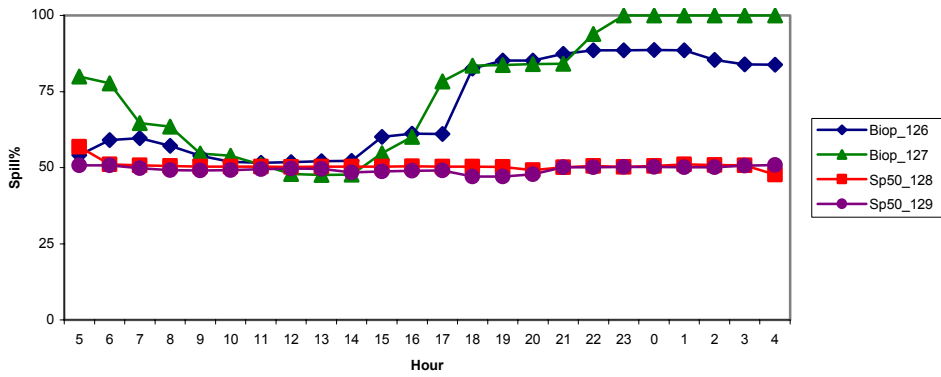


Figure 4. Percent spill during block 4 (spring Biop vs. Spill50).

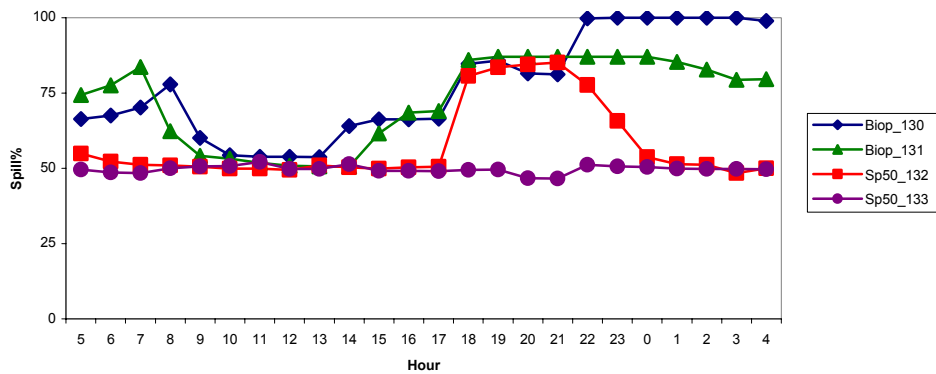


Figure 5. Percent spill during block 5 (spring Biop vs. Spill50).

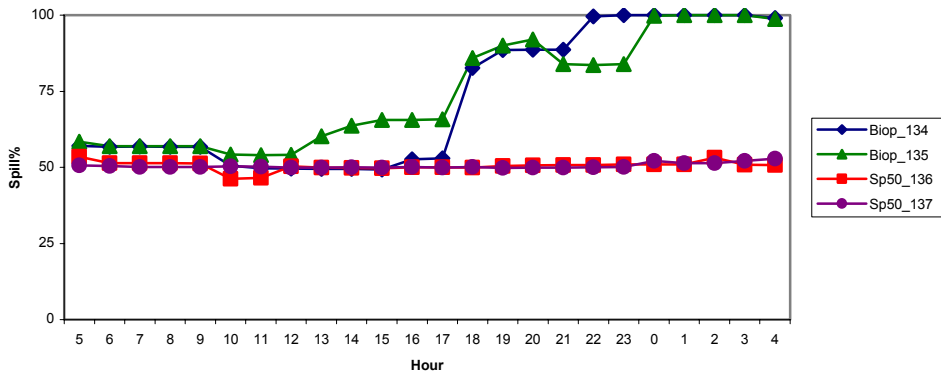


Figure 6. Percent spill during block 6 (spring Biop vs. Spill50).

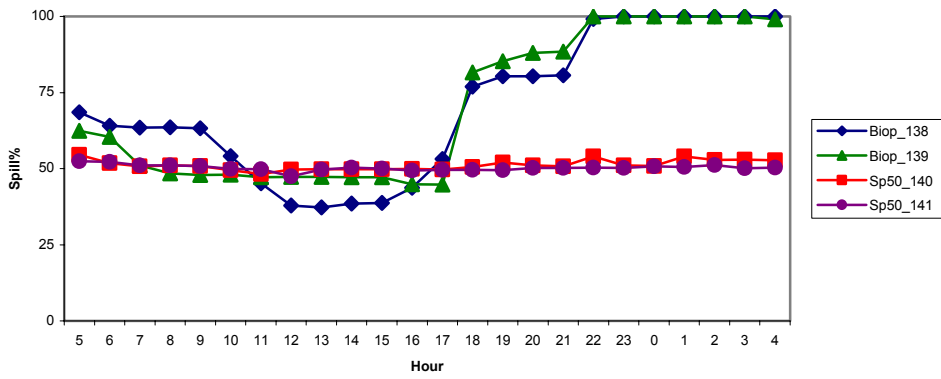


Figure 7. Percent spill during block 7 (spring Biop vs. Spill50).

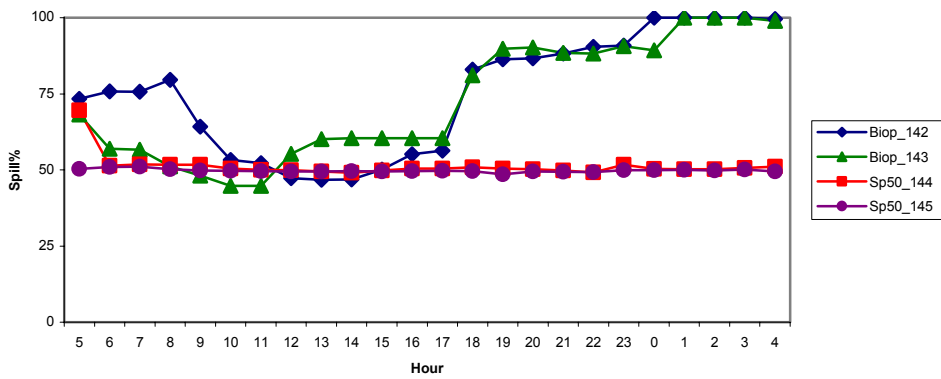


Figure 8. Percent spill during block 8 (spring Biop vs. Spill50).

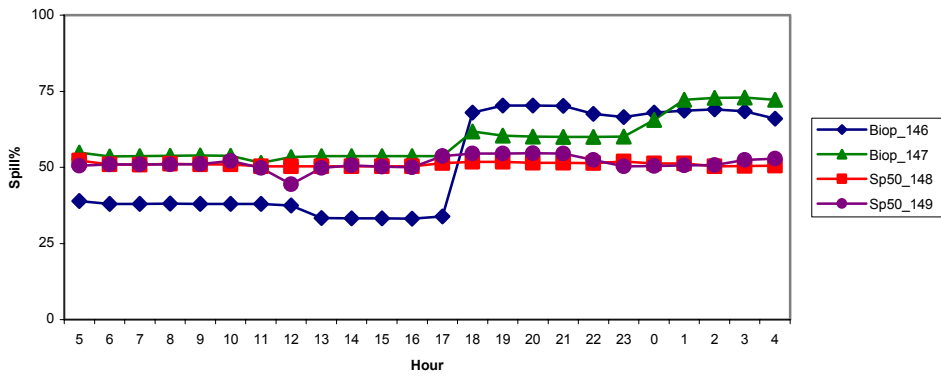


Figure 9. Percent spill during block 9 (spring Biop vs. Spill50). High river flows.

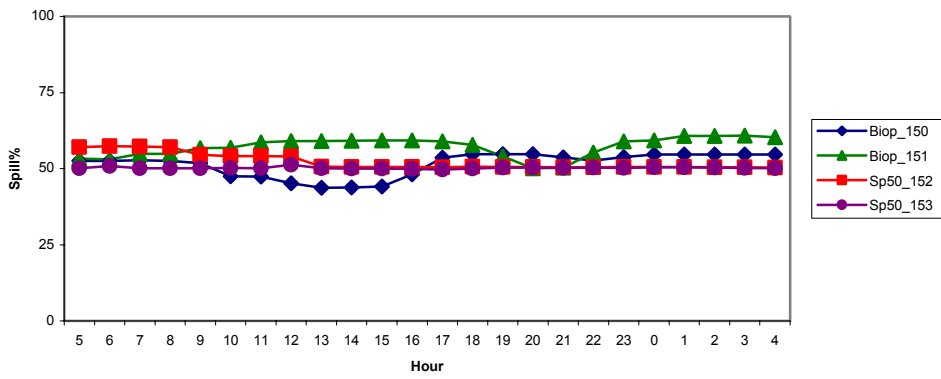


Figure 10. Percent spill during block 10 (spring Biop vs. Spill50). High river flows.

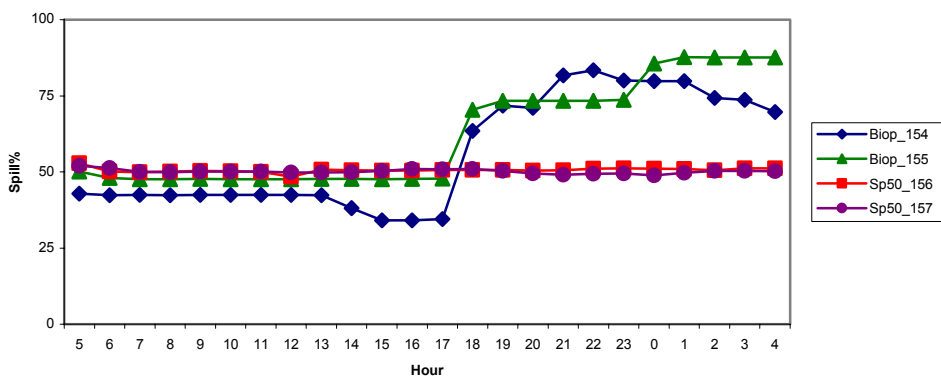


Figure 11. Percent spill during block 11 (spring Biop vs. Spill50).

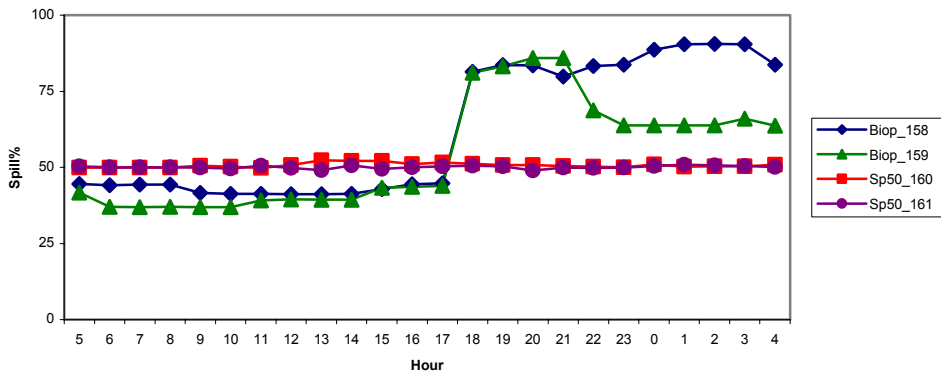


Figure 12. Percent spill during block 12 (summer Biop vs. Spill50).

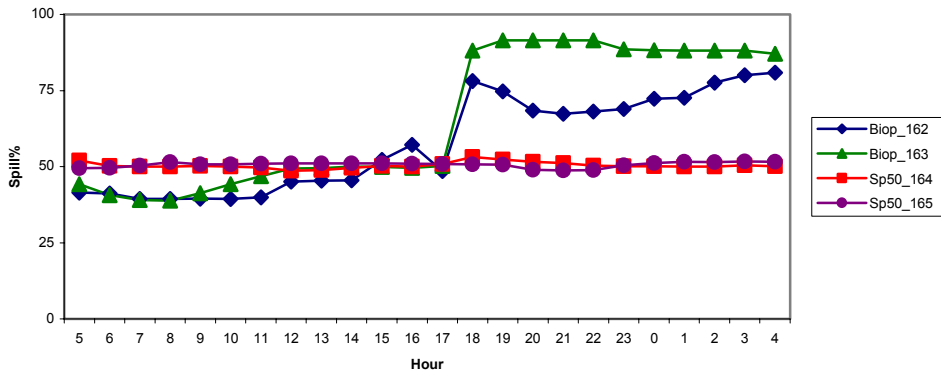


Figure 13. Percent spill during block 13 (summer Biop vs. Spill50).

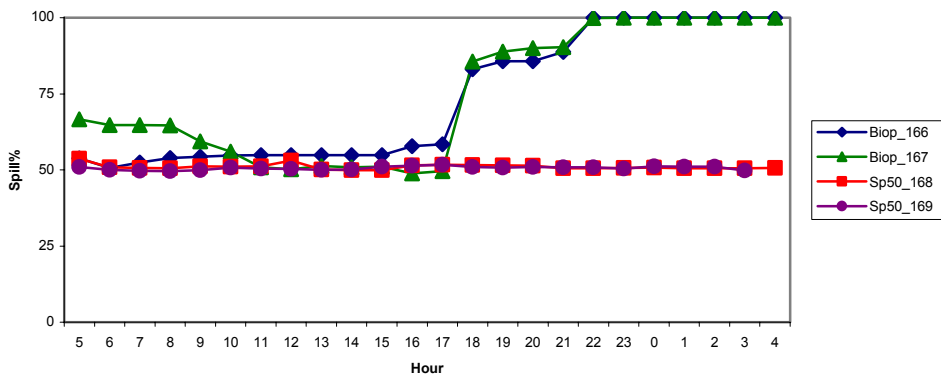


Figure 14. Percent spill during block 14 (summer Biop vs. Spill50).

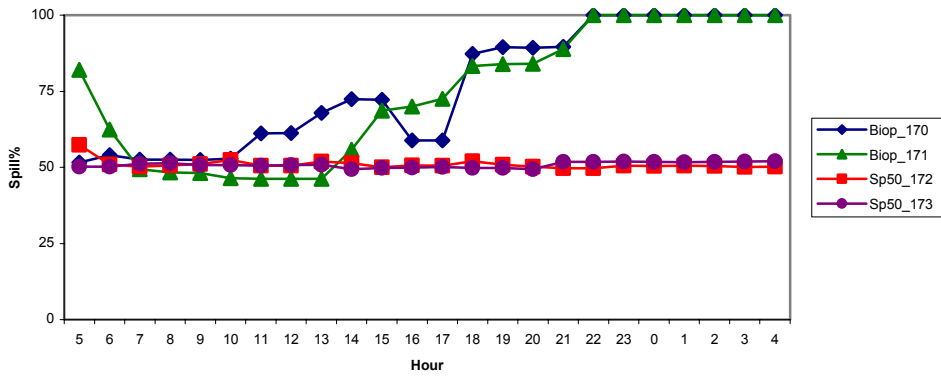


Figure 15. Percent spill during block 15 (summer Biop vs. Spill50).

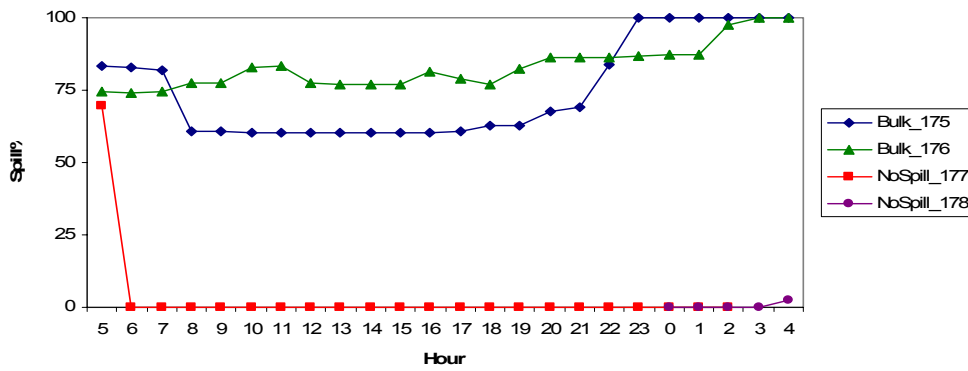


Figure 16. Percent spill during block 17 (summer Bulk vs. NoSpill).

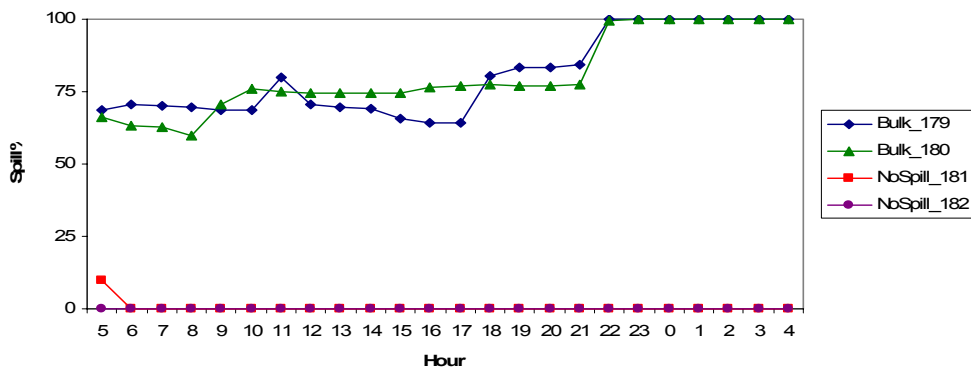


Figure 17. Percent spill during block 18 (summer Bulk vs. NoSpill).

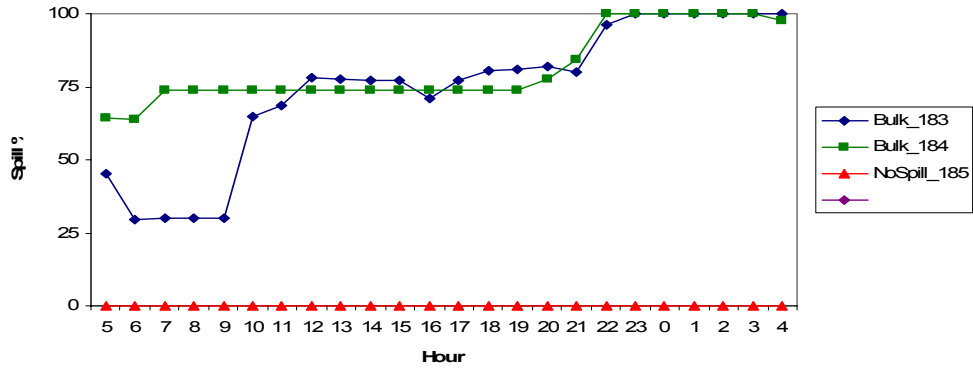


Figure 18. Percent spill during block 19 (summer Bulk vs. NoSpill).

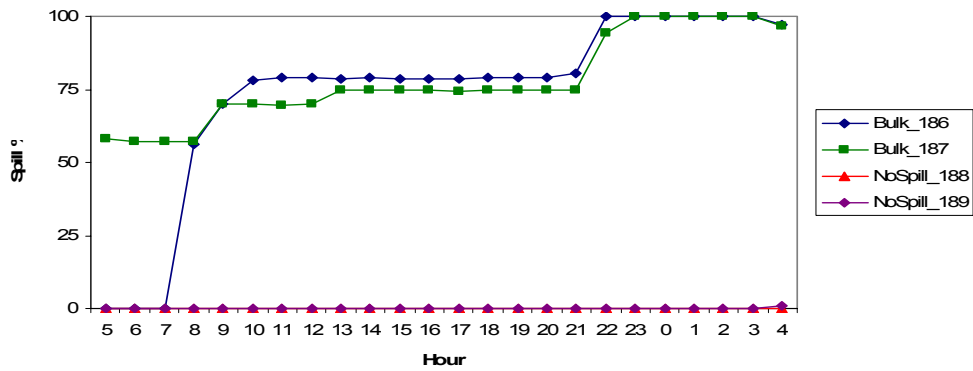


Figure 19. Percent spill during block 20 (summer Bulk vs. NoSpill).

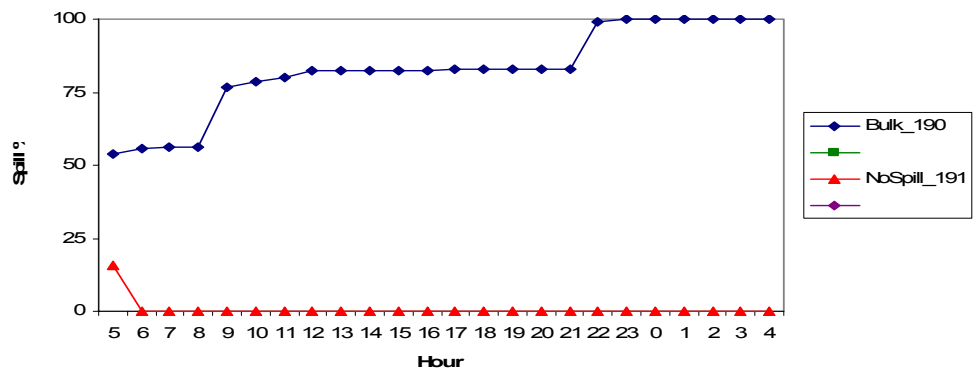


Figure 20. Percent spill during block 21 (summer Bulk vs. NoSpill).

Appendix D

Fish Trajectories by Spill Gate Opening

Appendix D

Fish Trajectories by Spill Gate Opening

The following series of pictures show the spatial relationships between fish trajectories, fish distributions within the water column, and flows at each spill gate opening. The data is further divided into spring and summer along the chinook run timing transition. Features of the plot include the forebay elevation of 438 ft, the top of the spillway crest at elevation 391, and the hydroacoustic transducer at elevation 436. The series of circles and vectors are a combination plot of fish vertical abundance and trajectories along the middle of the hydroacoustic beam. The relative abundance of fish within these 1 m range bins from the transducer is associated with the right-hand side vertical contour legend. The fish vectors are on the same scale as the axes, so that 1 ft of distance along the vector is equivalent to 1 ft/s (the horizontal axis, while not shown, is also at the same scale as the vertical axis). The nominal beamwidth of the transducer is also plotted, and describes the hydroacoustic sample volume (Figure 1).

The fish distribution and trajectory data shown represents only those fish considered to be entrained and expected to pass the dam via the spillway. In addition, these estimates have been corrected for detectability within the beam. The fish speed and direction data were collected with split-beam transducers, while the vertical distribution data represents a combination of single- and split-beam data across the entire spillway. Factors other than spill gate opening and season, such as treatments and diel period, have been pooled.

The flow field was constructed from a computational fluid dynamics model (CFD) to represent the flow through the centerline of a single spill bay—it is 2D and static. The flow field contour key is horizontally oriented across the top of the graph, and the flow vectors have been reduced to a 1/5th scale. The purple lines were formed as forward streamtraces into the CFD flow field from the following release points: the shallow release point was 10 ft above the crest at elevation 401, and the deep release point was 3 ft above the crest at elevation 394. Both release points are directly below the upstream edge of the stoplog slot.

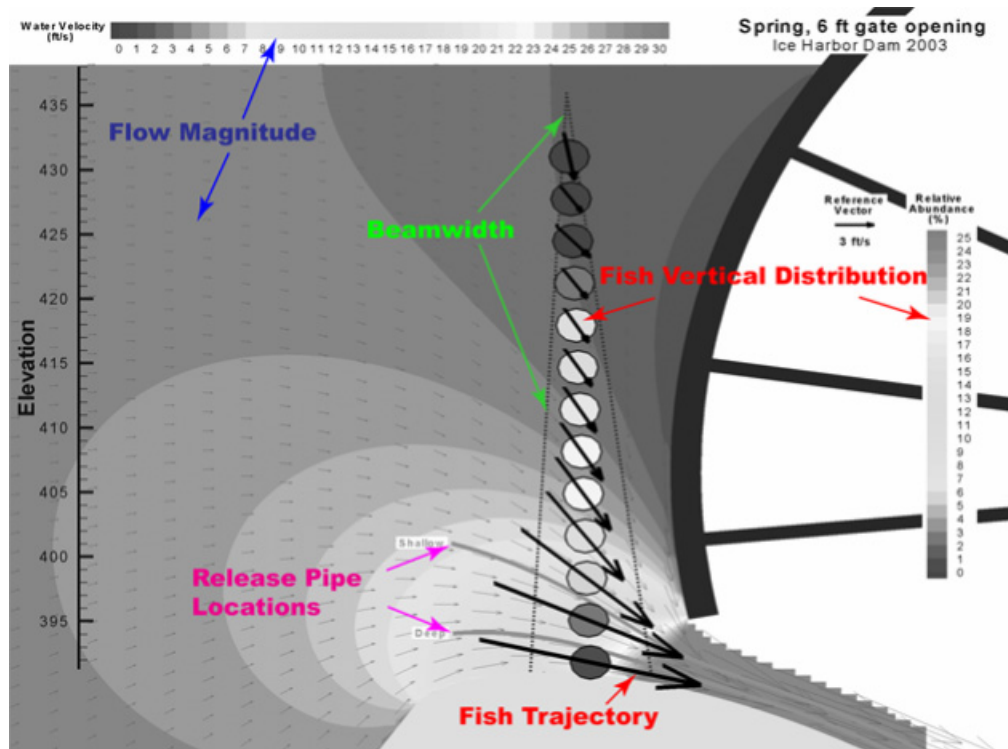


Figure 1. Spill bay plots feature legend.

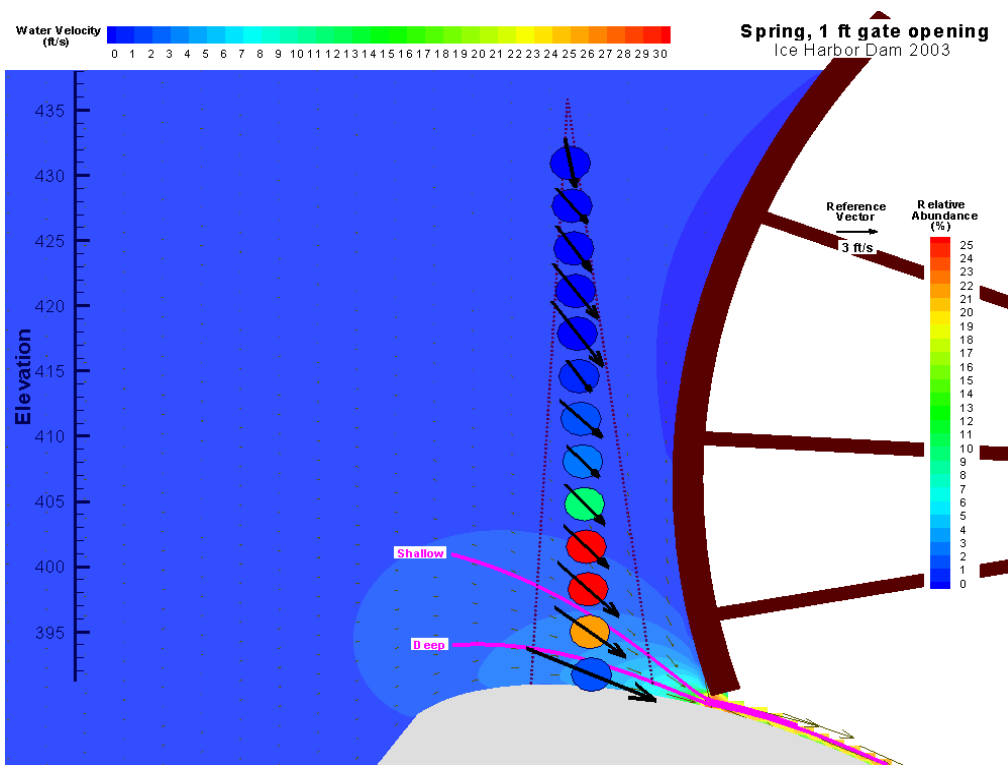


Figure 2. Fish trajectories, vertical distribution, flows, and release pipe locations for 1 ft gate in spring

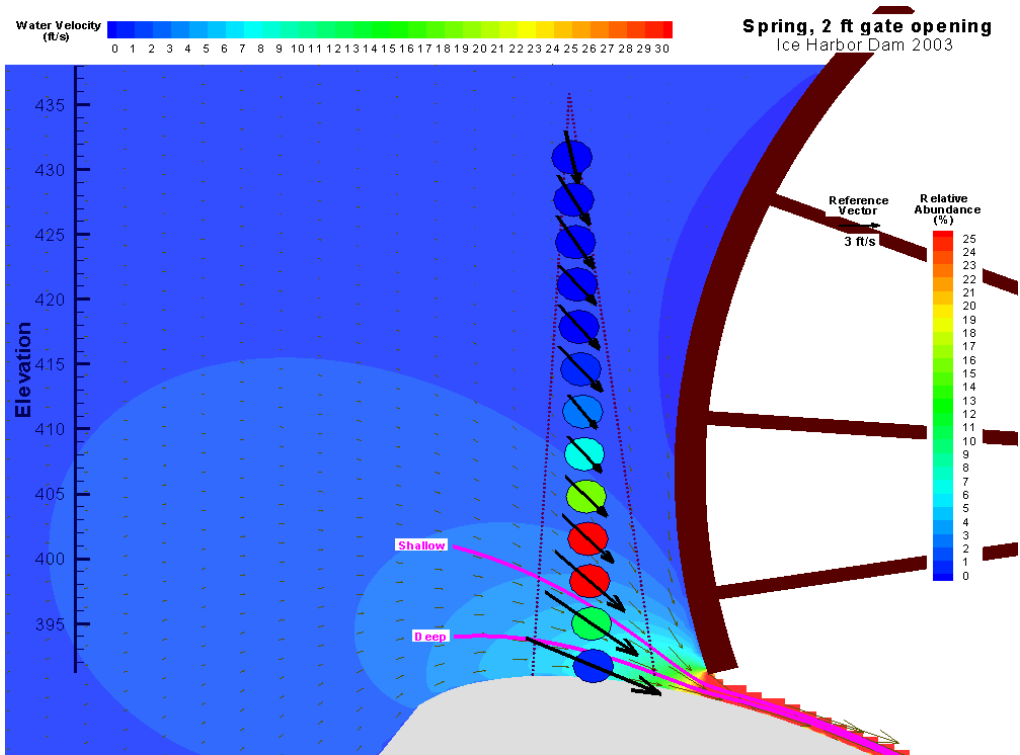


Figure 3. Fish trajectories, vertical distribution, flows, and release pipe locations for 2 ft gate in spring

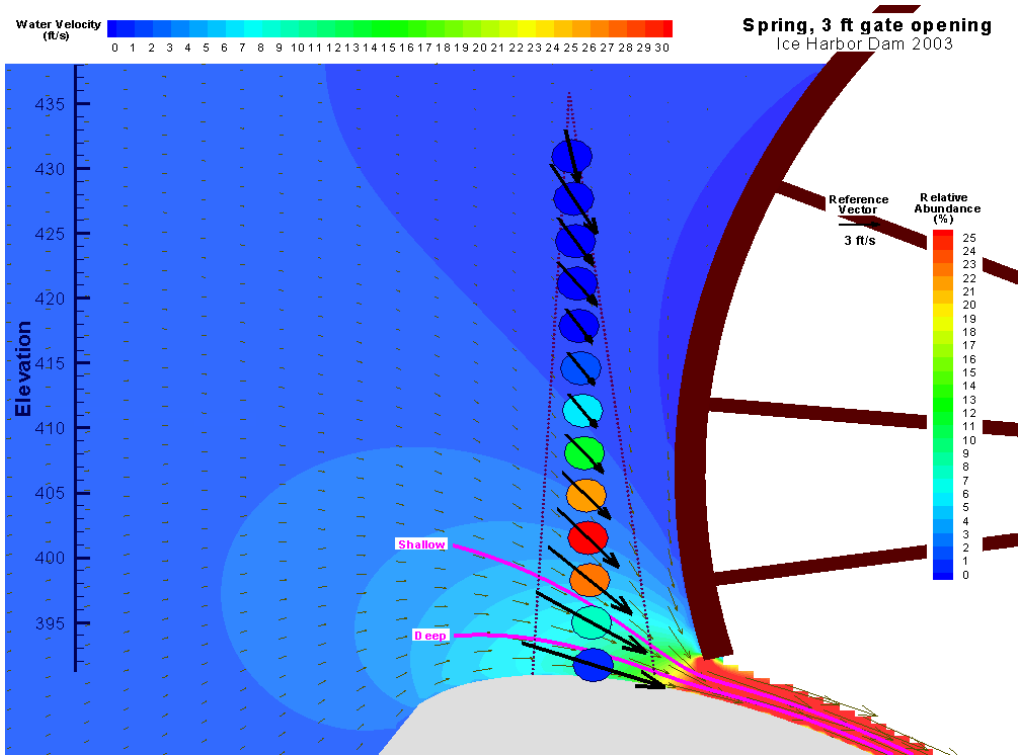


Figure 4. Fish trajectories, vertical distribution, flows, and release pipe locations for 3 ft gate in spring

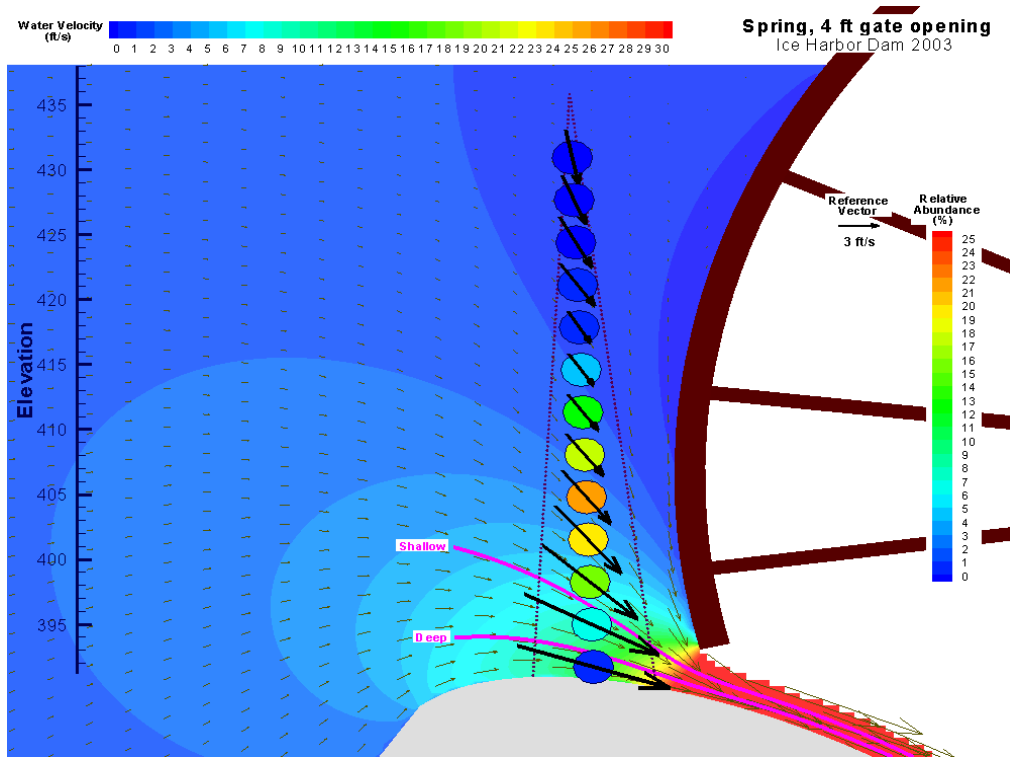


Figure 5. Fish trajectories, vertical distribution, flows, and release pipe locations for 4 ft gate in spring

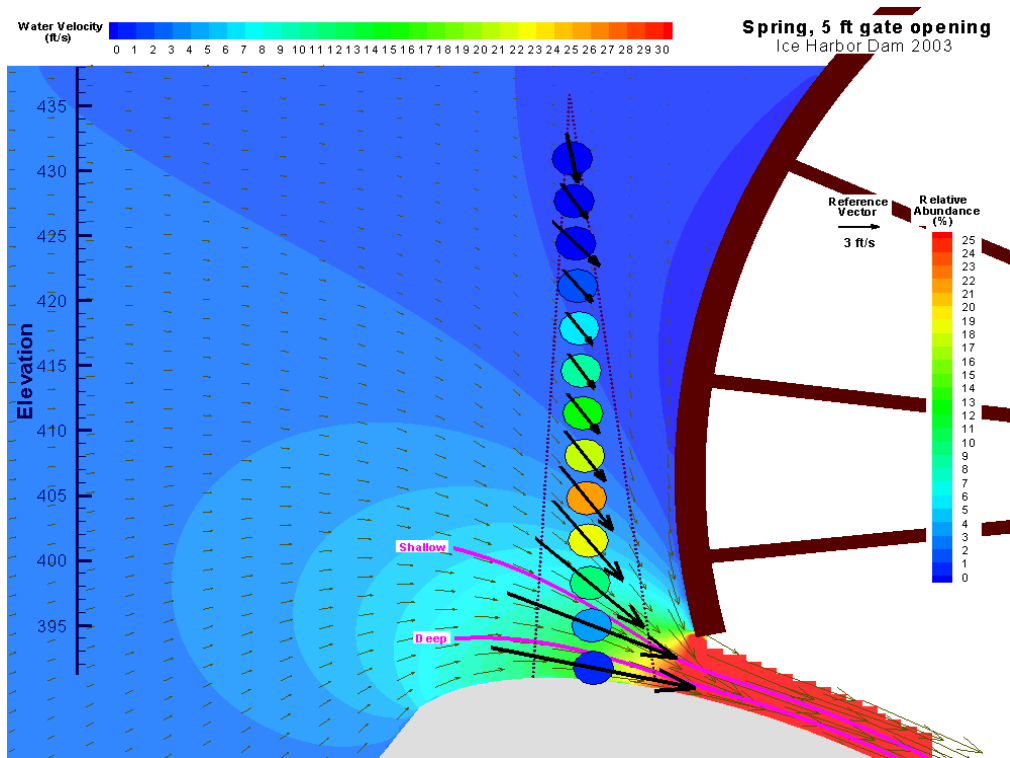


Figure 6. Fish trajectories, vertical distribution, flows, and release pipe locations for 5 ft gate in spring

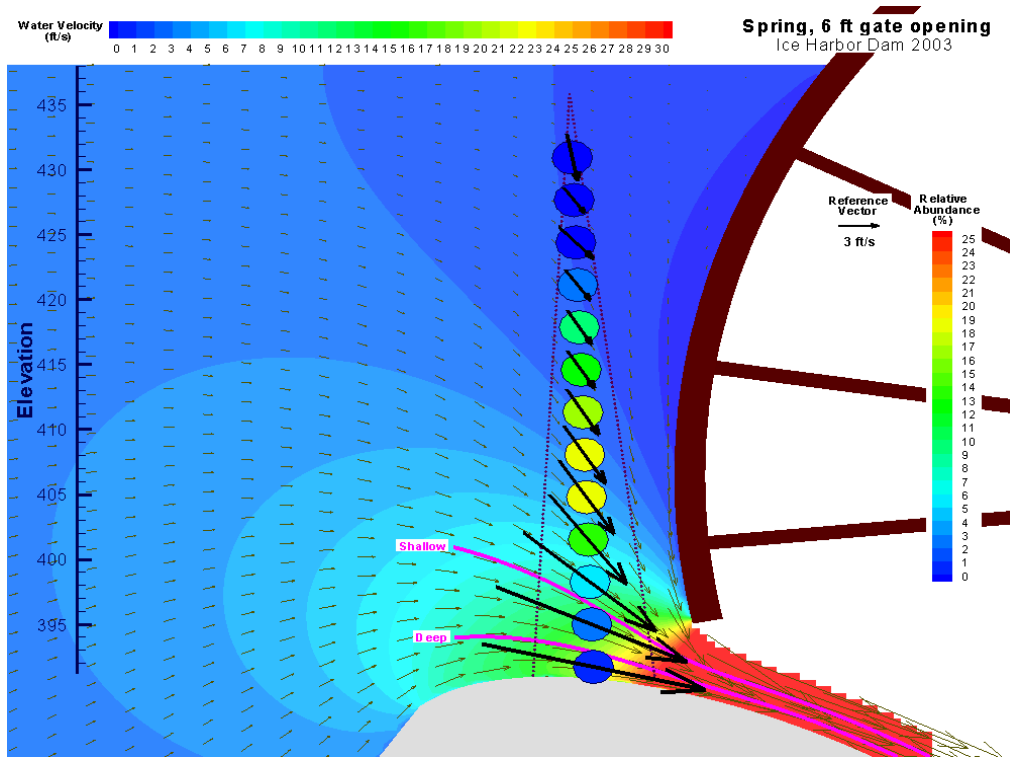


Figure 7. Fish trajectories, vertical distribution, flows, and release pipe locations for 6 ft gate in spring

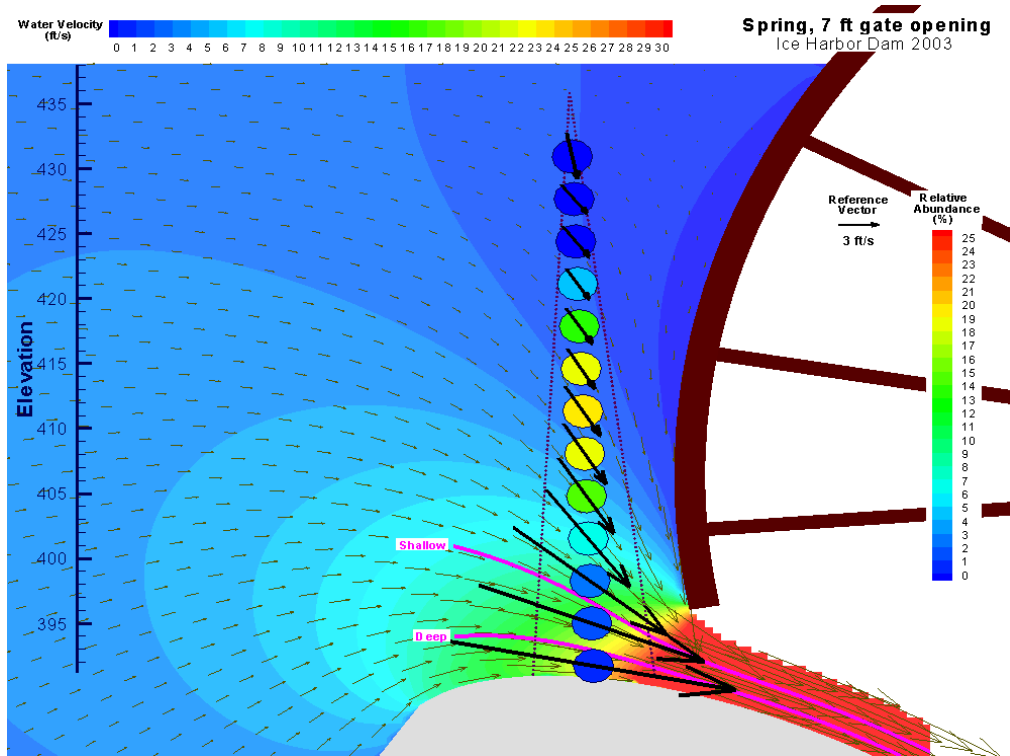


Figure 8. Fish trajectories, vertical distribution, flows, and release pipe locations for 7 ft gate in spring

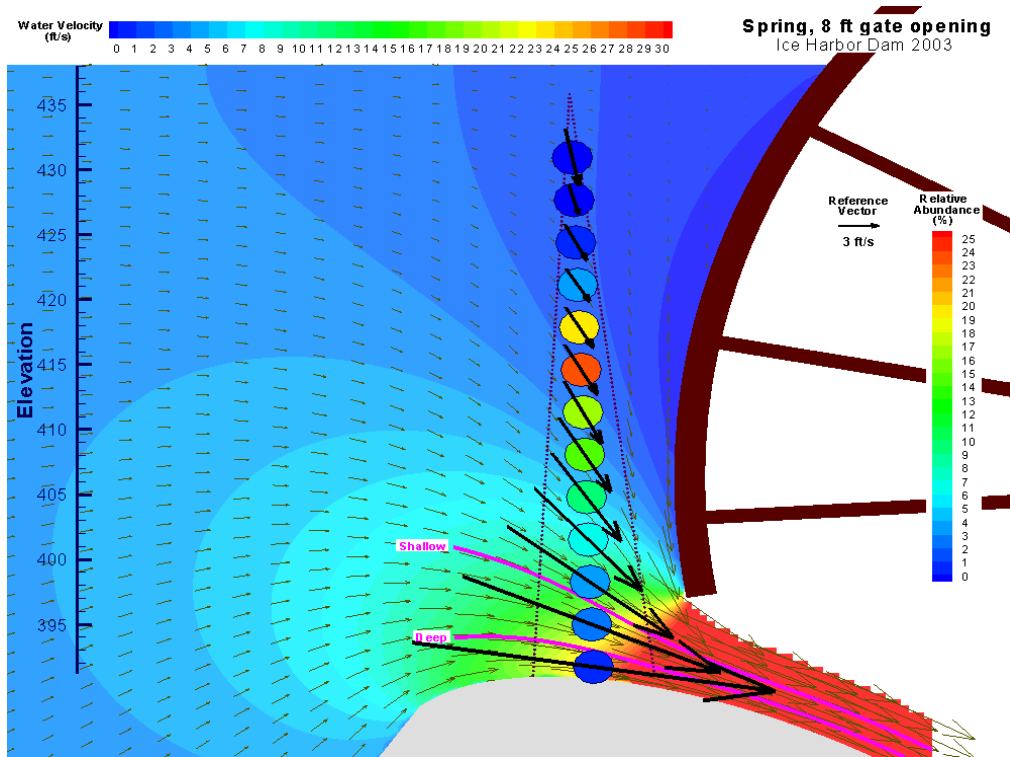


Figure 9. Fish trajectories, vertical distribution, flows, and release pipe locations for 8 ft gate in spring

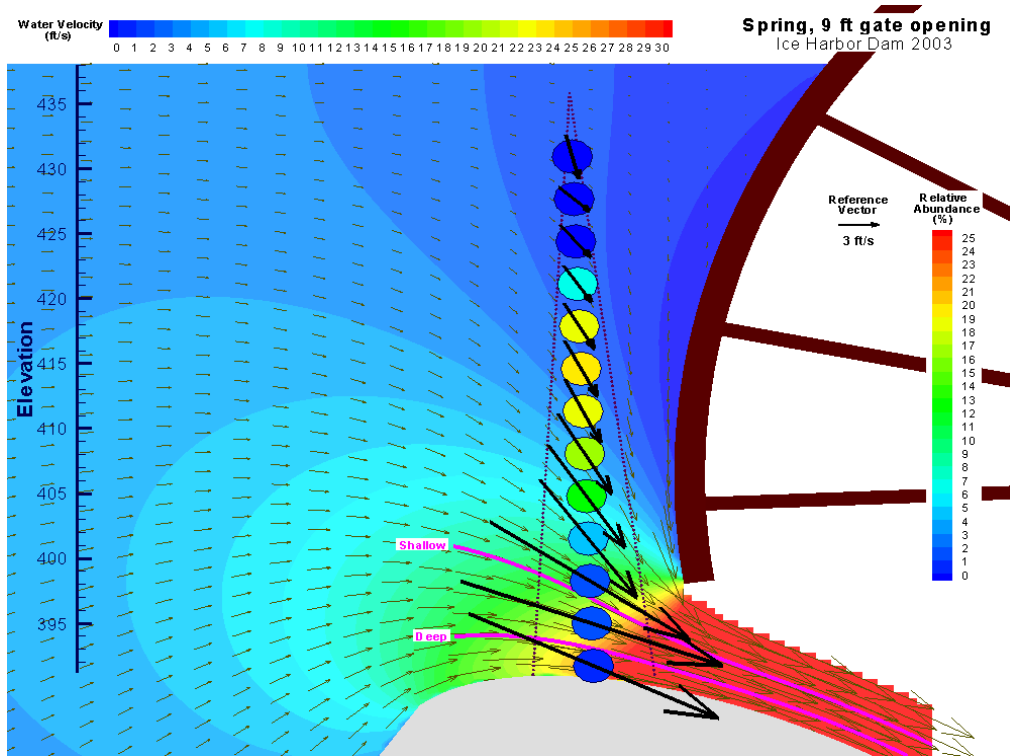


Figure 10. Fish trajectories, vertical distribution, flows, and release pipe locations for 9 ft gate in spring

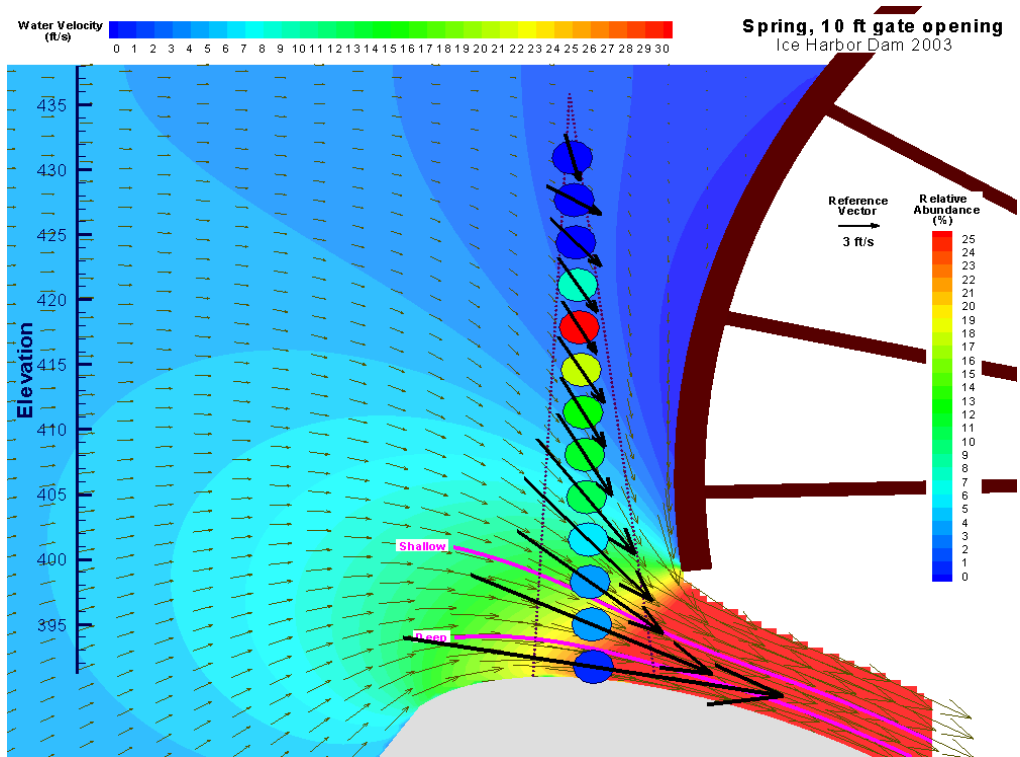


Figure 11. Fish trajectories, vertical distribution, flows, and release pipe locations for 10 ft gate in spring

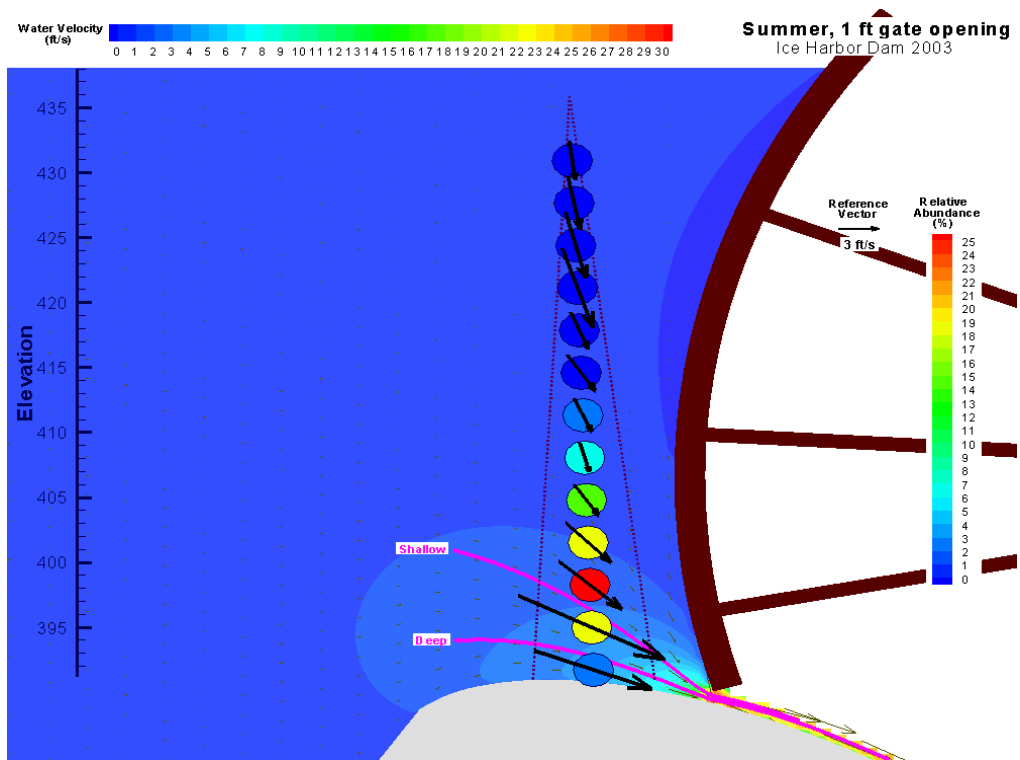


Figure 12. Fish trajectories, vertical distribution, flows, and release pipe locations for 1 ft gate in summer

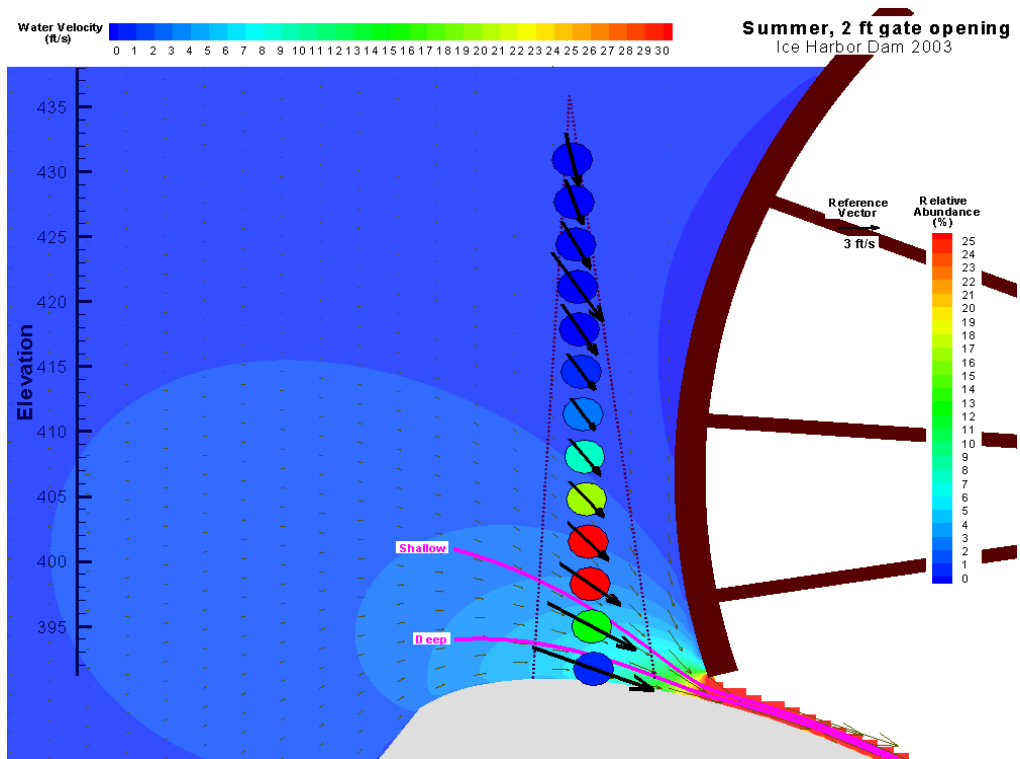


Figure 13. Fish trajectories, vertical distribution, flows, and release pipe locations for 2 ft gate in summer

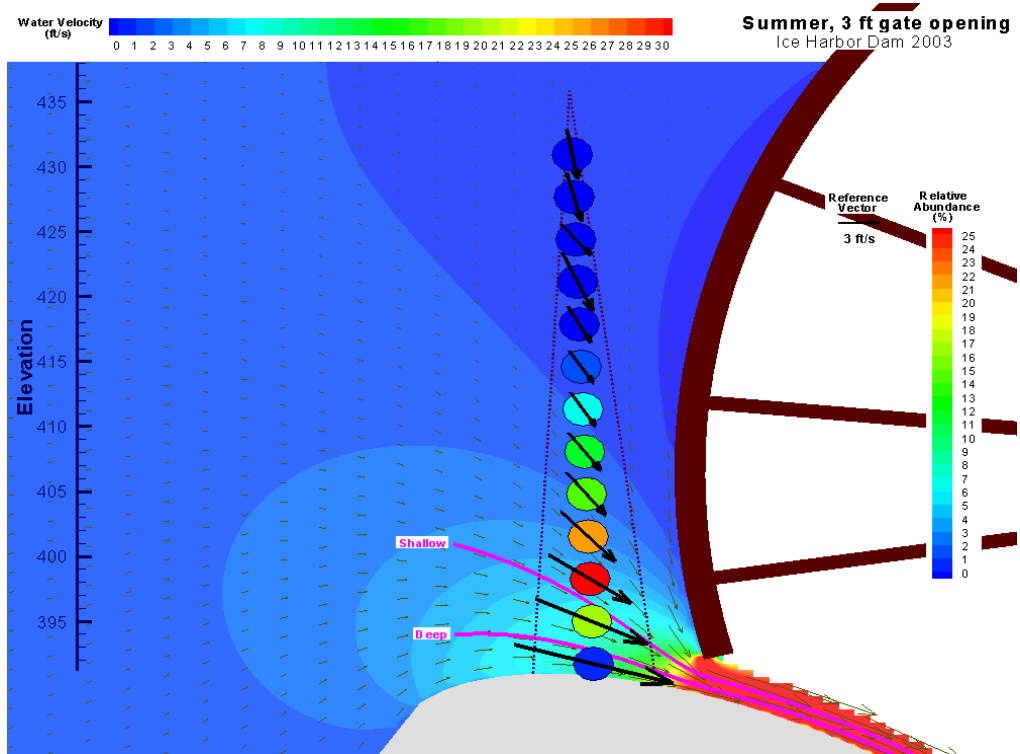


Figure 14. Fish trajectories, vertical distribution, flows, and release pipe locations for 3 ft gate in summer

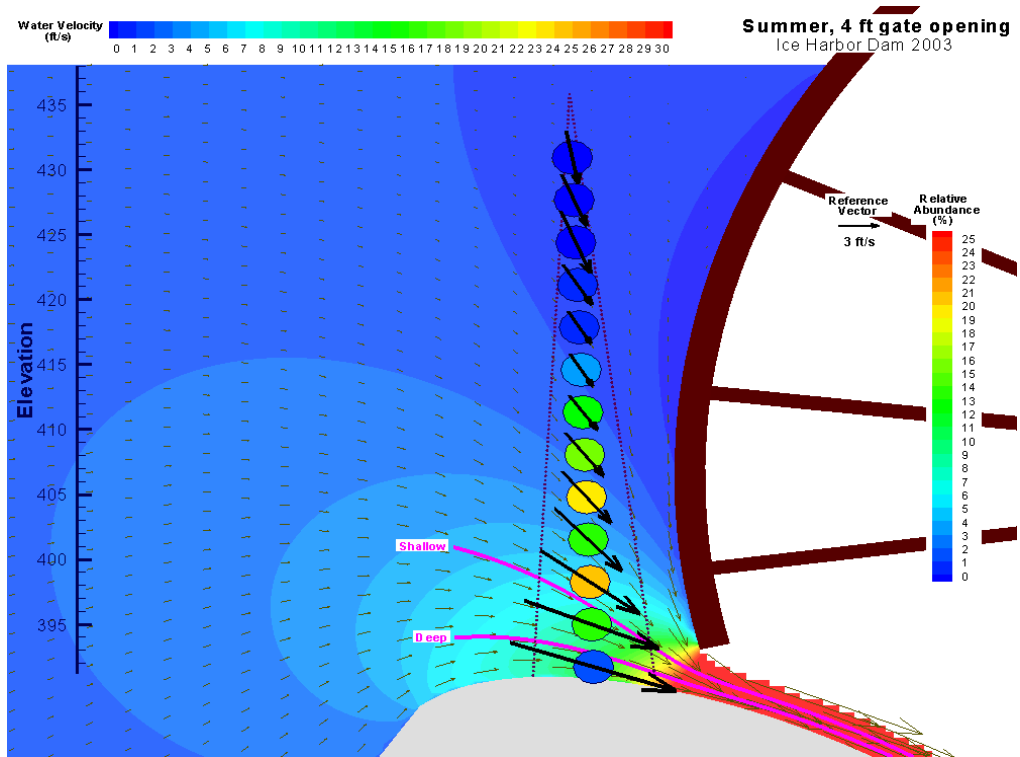


Figure 15. Fish trajectories, vertical distribution, flows, and release pipe locations for 4 ft gate in summer

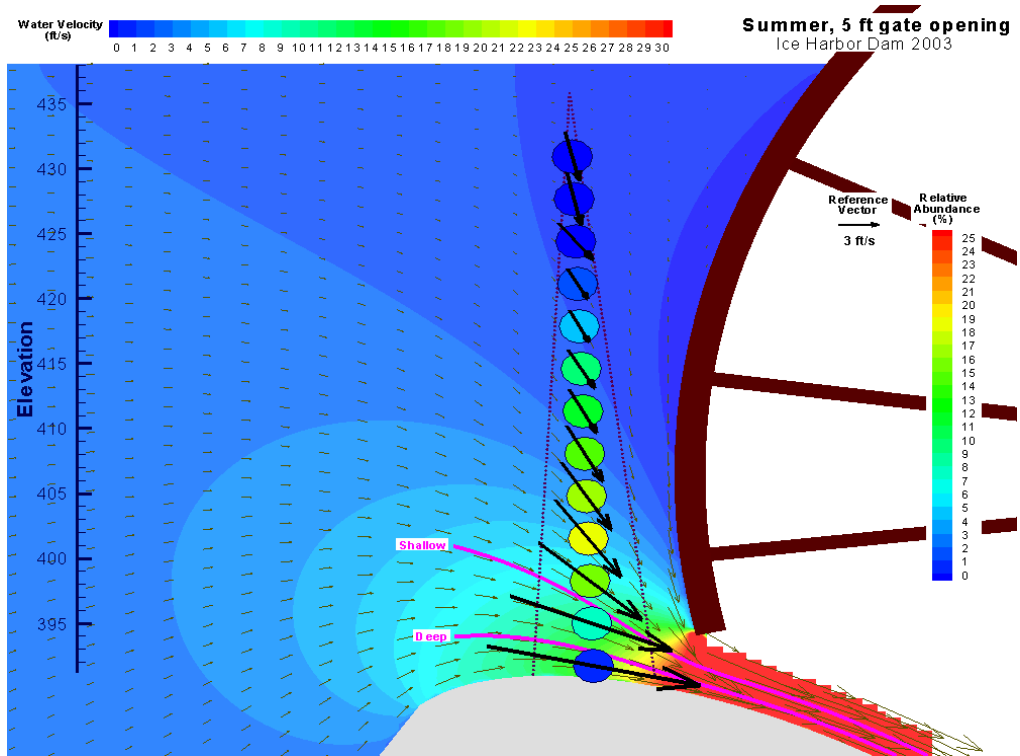


Figure 16. Fish trajectories, vertical distribution, flows, and release pipe locations for 5 ft gate in summer

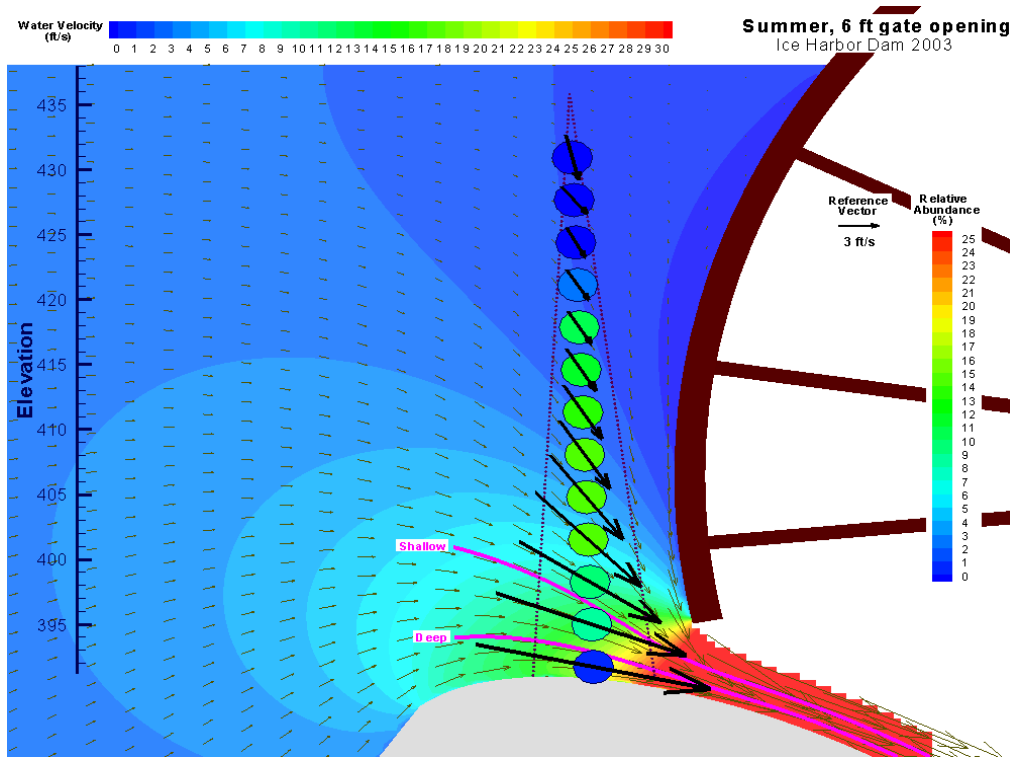


Figure 17. Fish trajectories, vertical distribution, flows, and release pipe locations for 6 ft gate in summer

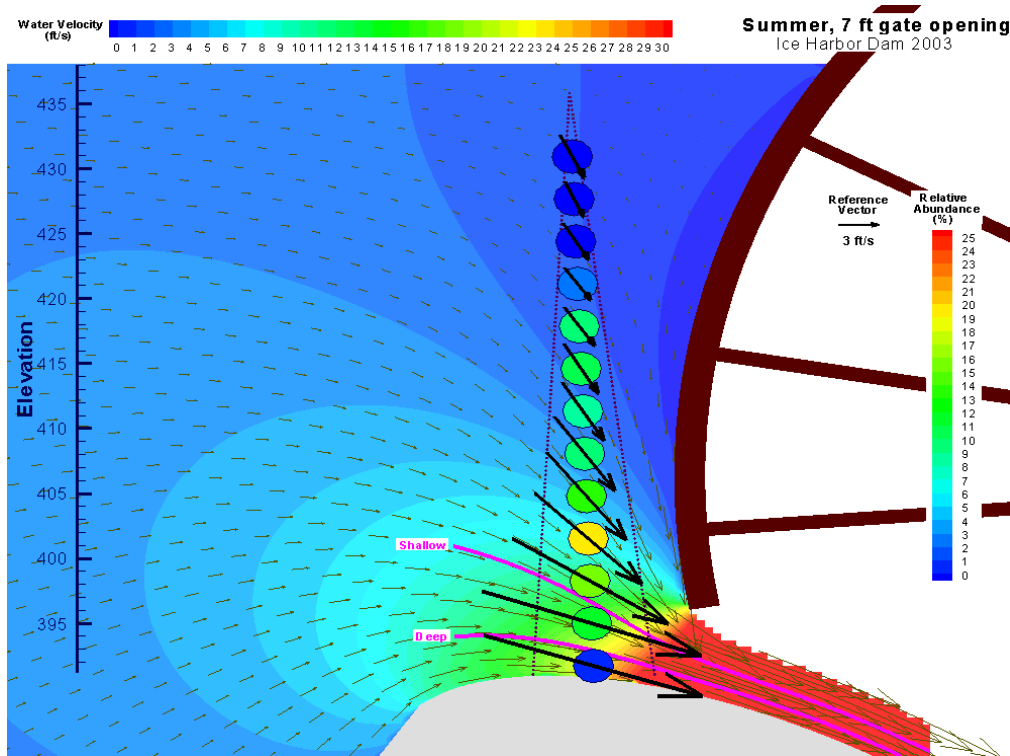


Figure 18. Fish trajectories, vertical distribution, flows, and release pipe locations for 7ft gate in summer

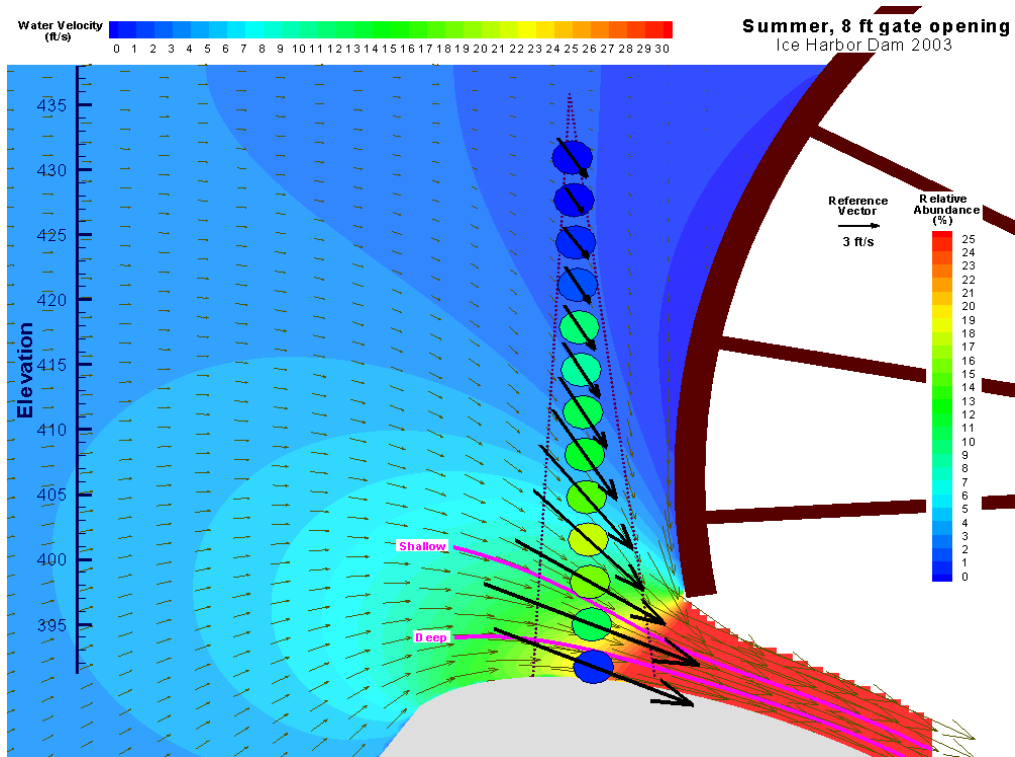


Figure 19. Fish trajectories, vertical distribution, flows, and release pipe locations for 8 ft gate in summer

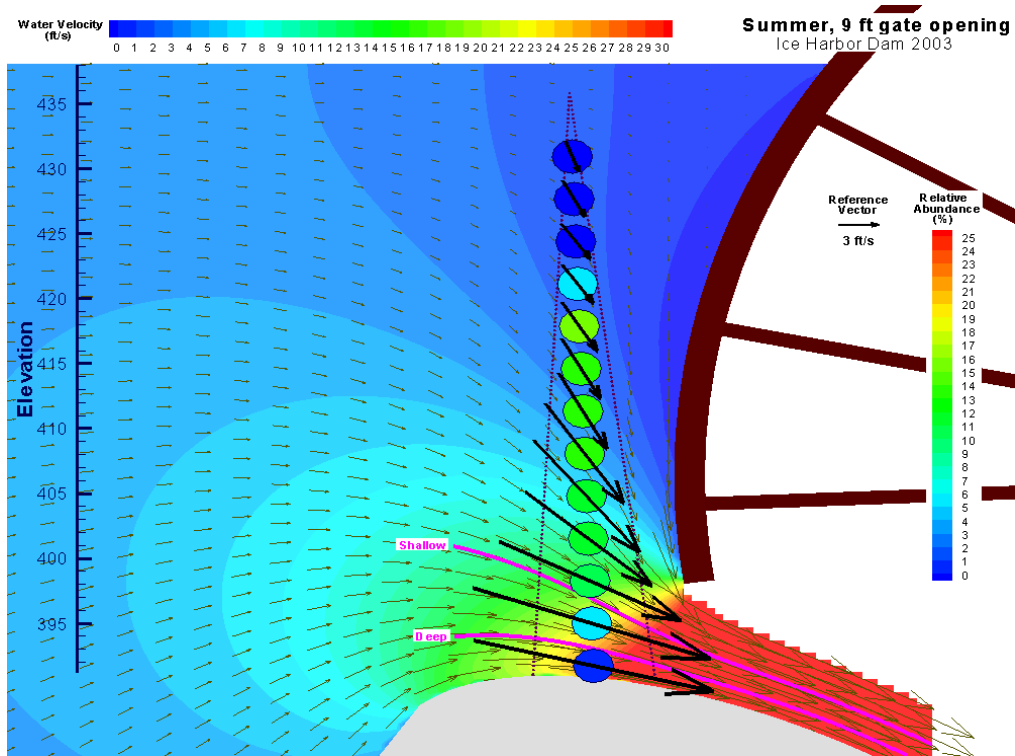


Figure 20. Fish trajectories, vertical distribution, flows, and release pipe locations for 9 ft gate in summer

Appendix E

Vertical Distributions by Season and Diel Period

Appendix E

Vertical Distributions by Season and Diel Period

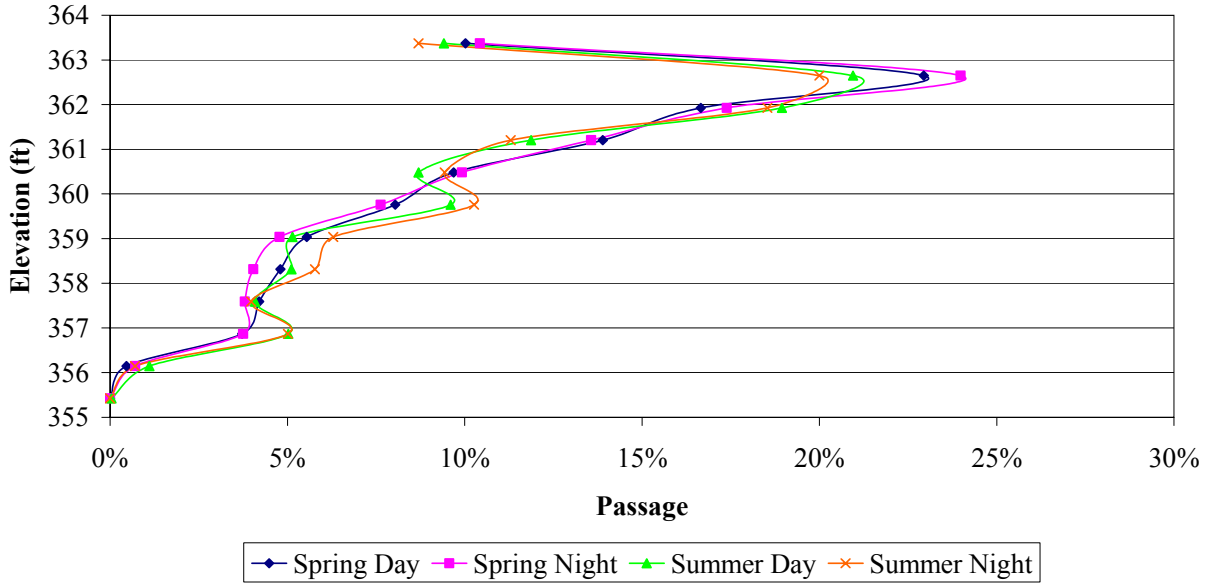


Figure 1. Vertical distribution of guided fish.

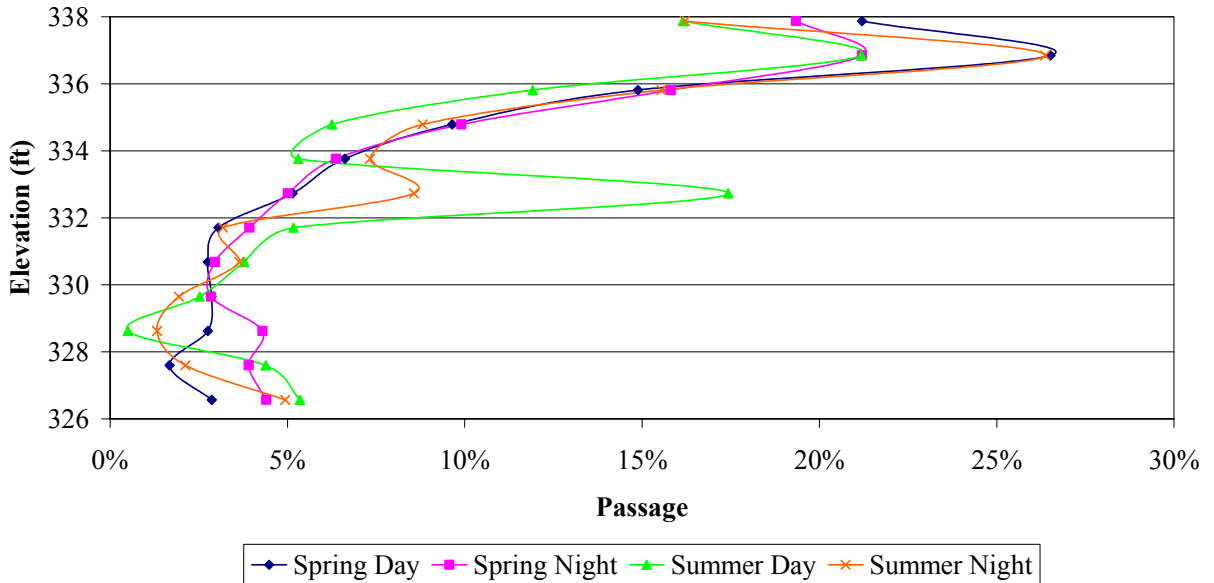


Figure 2. Vertical distribution of unguided fish.

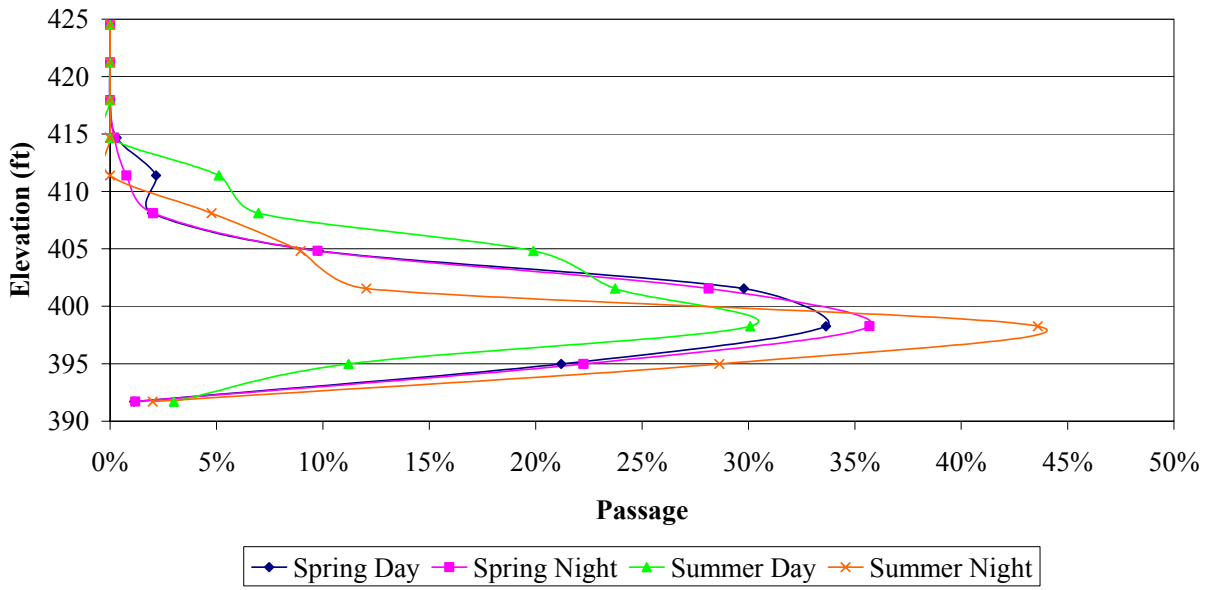


Figure 3. Vertical distribution at a 1 ft spill gate opening.

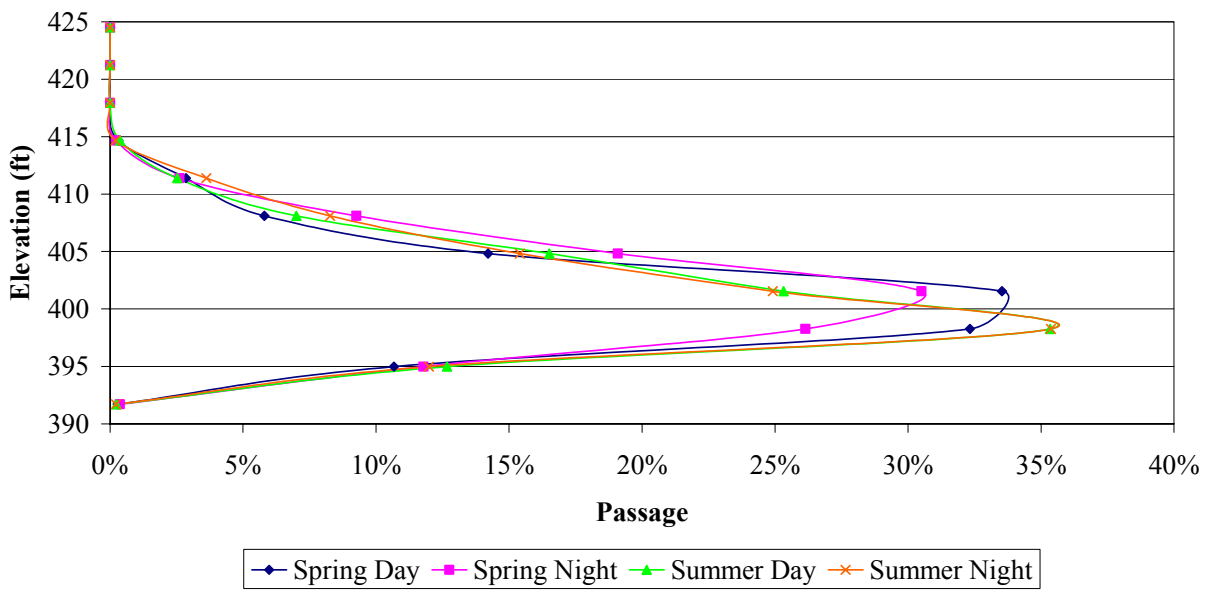


Figure 4. Vertical distribution at a 2 ft spill gate opening.

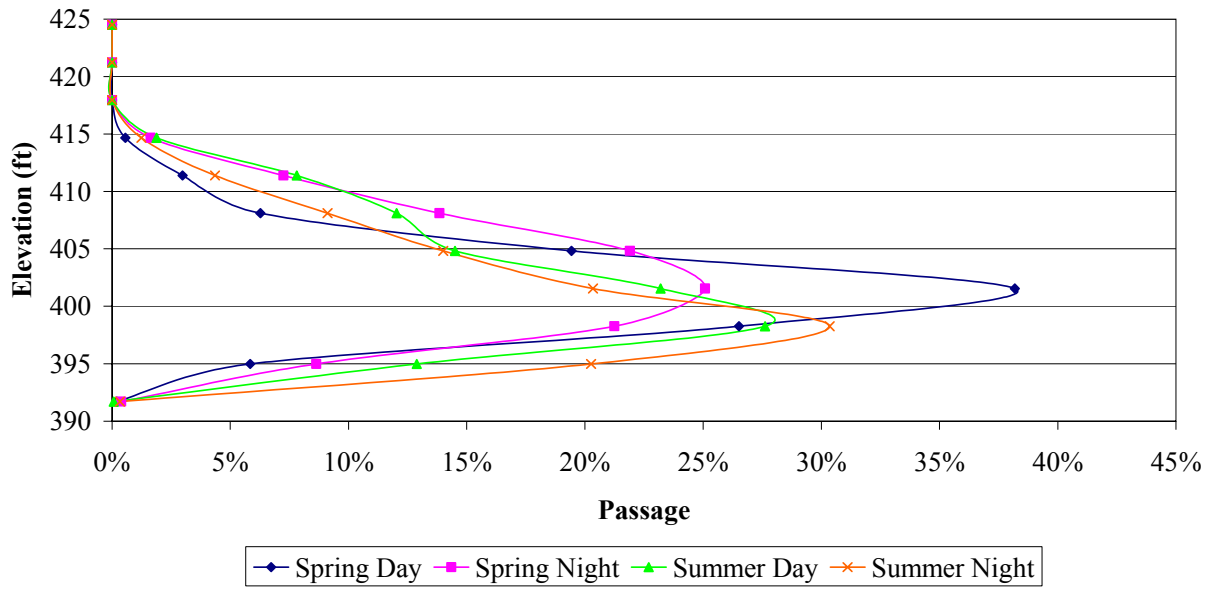


Figure 5. Vertical distribution at a 3 ft spill gate opening.

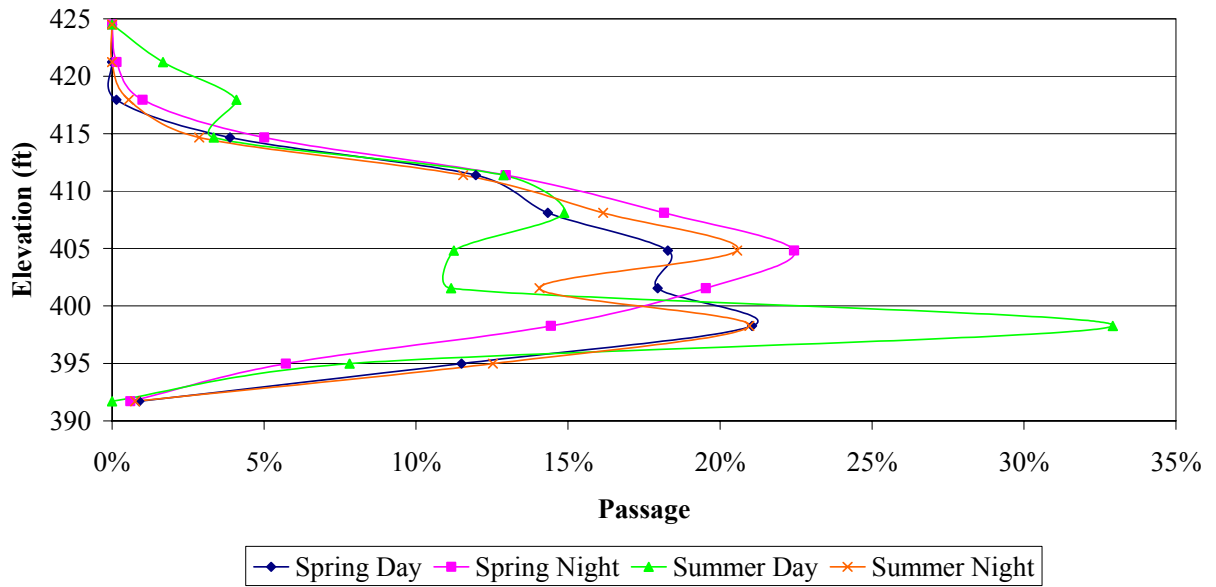


Figure 6. Vertical distribution at a 4 ft spill gate opening.

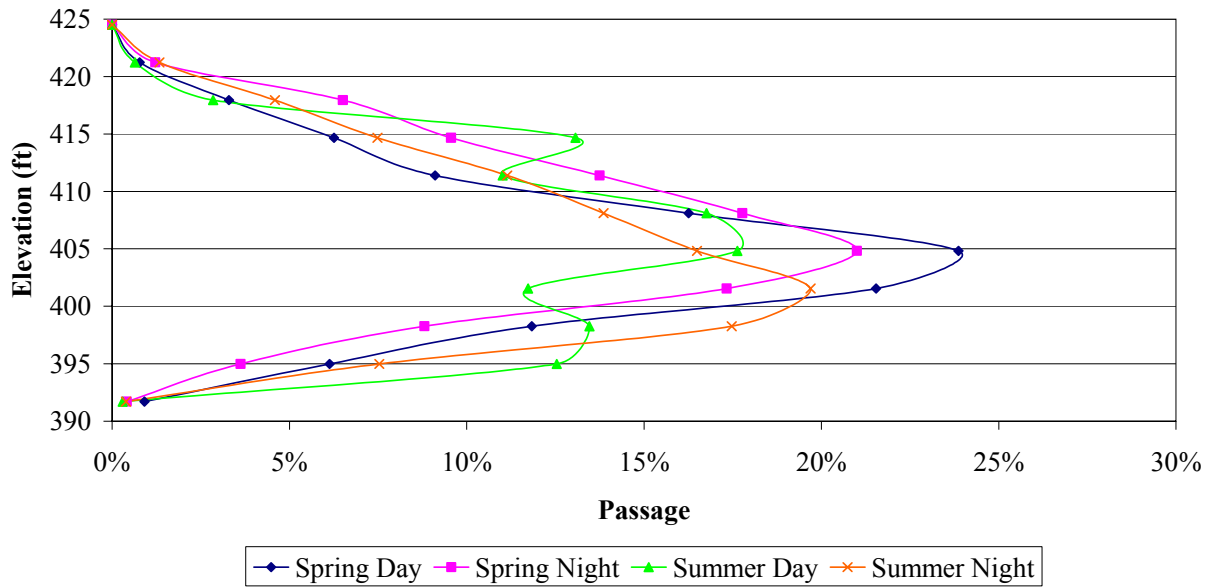


Figure 7. Vertical distribution at a 5 ft spill gate opening.

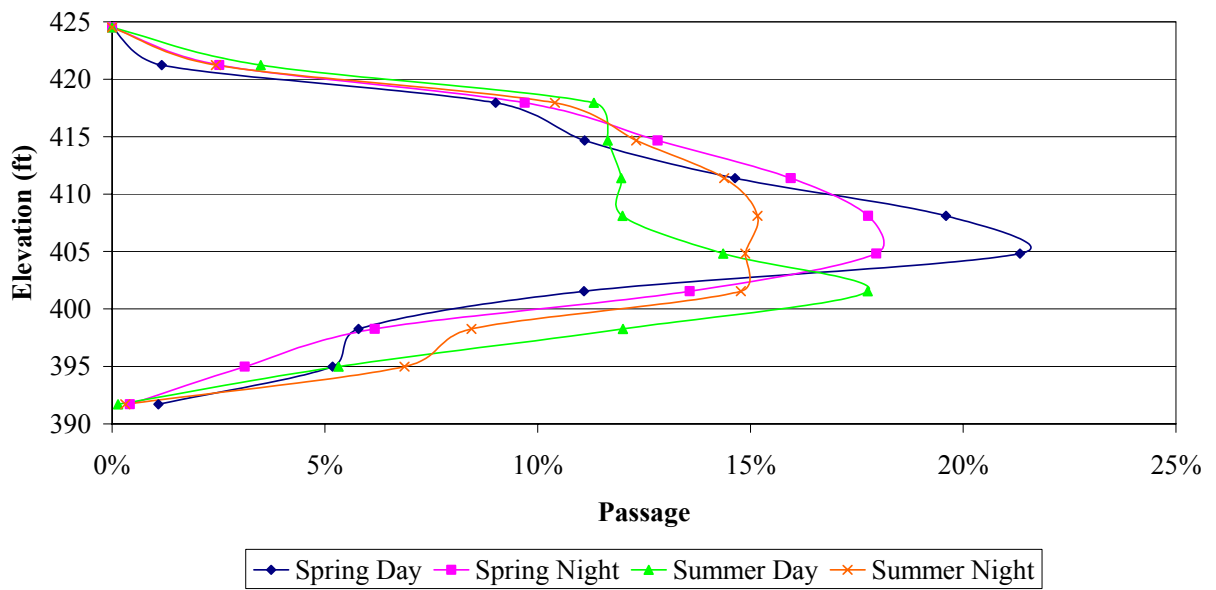


Figure 8. Vertical distribution at a 6 ft spill gate opening.

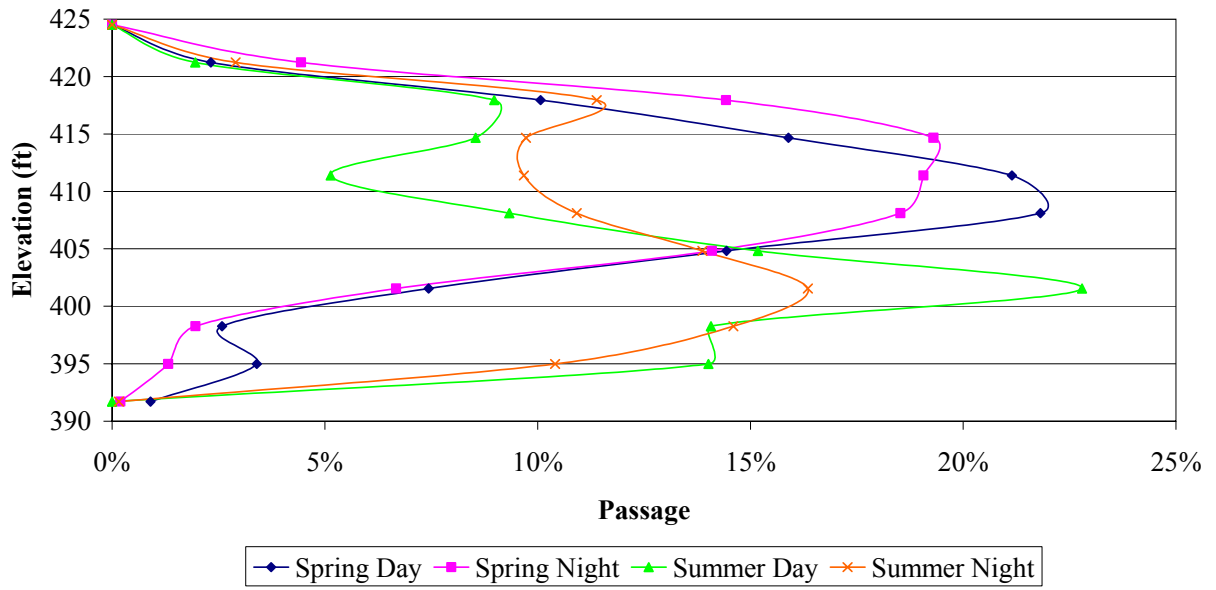


Figure 9. Vertical distribution at a 7 ft spill gate opening.

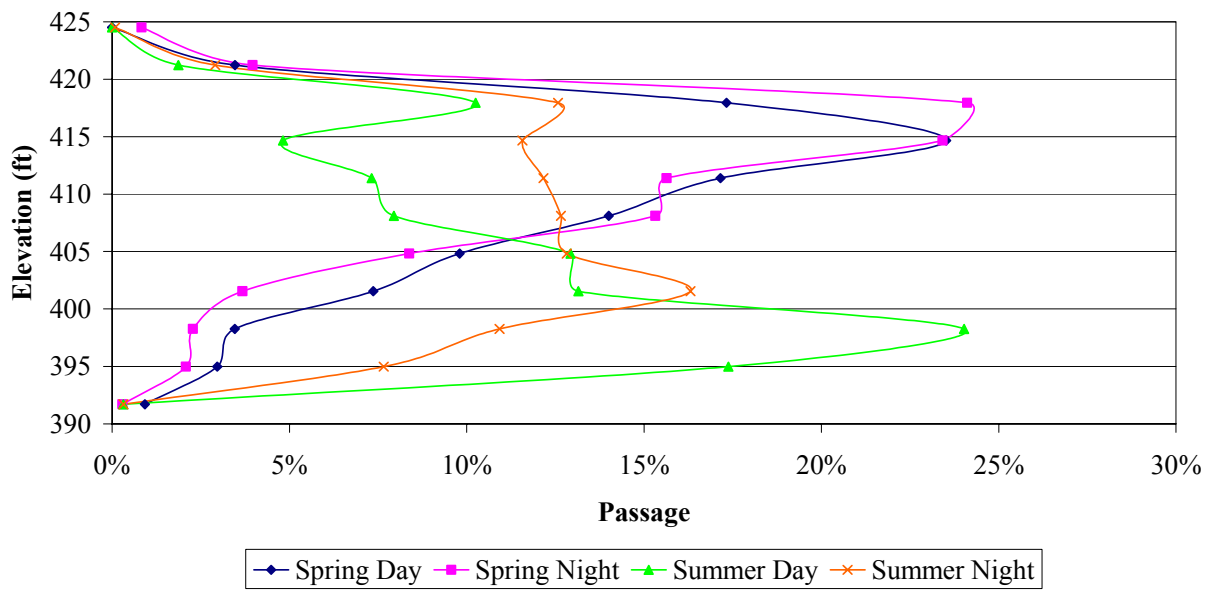


Figure 10. Vertical distribution at an 8 ft spill gate opening.

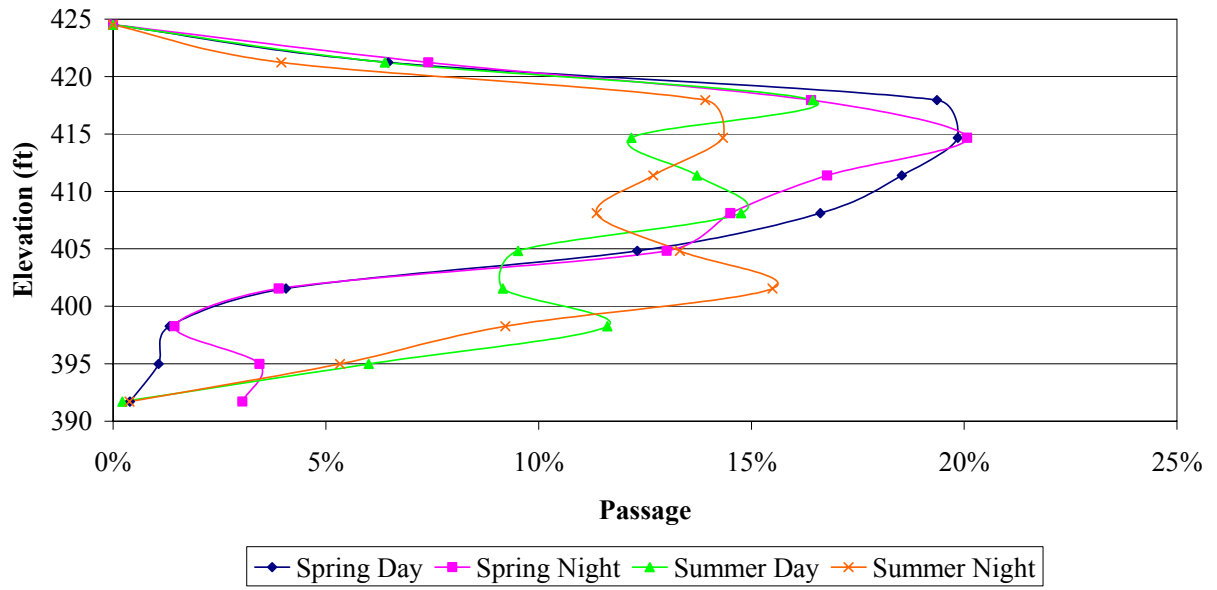


Figure 11. Vertical distribution at a 9 ft spill gate opening.

Appendix F
System Calibrations

Appendix F

System Calibrations

System IHR_X_Powerhouse SPB													Pings/	Min./
Description	S/N	Xducer Type	Channel	Location	Cable Lengths	Length	SN	Mounting	Aiming angle	Elevation	Mux Type	Second	Hr.	
SPB Sounder	20					470	114							
Remote Multiplexer	16													
SPB xducer_1	426	6° split	0	PH 1_A_S	470	940	82	35° from plane of trashrack	uplooker/guided	325 ft.	Slow	25	10	
SPB xducer_2	427	6° split	1	PH 1_A_N	470	940	71	63° from plane of trashrack	uplooker/unguided	325 ft.	Slow	25	10	
SPB xducer_3	428	6° split	2	PH 3_B_S	235	705	113	35° from plane of trashrack	uplooker/guided	325 ft.	Slow	25	10	
SPB xducer_4	400	6° split	3	PH 3_B_N	235	705	41	63° from plane of trashrack	uplooker/unguided	325 ft.	Slow	25	10	
System IHR_Y_Powerhouse SPB													Pings/	Min./
Description	S/N	Xducer Type	Channel	Location	Cable Lengths	Length	SN	Mounting	Aiming angle	Elevation	Mux Type	Second	Hr.	
SPB Sounder	27					470	89							
Remote Multiplexer	17													
SPB xducer_1	441	6° split	0	PH 4_C_S	235	705	74	35° from plane of trashrack	uplooker/guided	325 ft.	Slow	25	10	
SPB xducer_2	430	6° split	1	PH 4_C_N	235	705	111	63° from plane of trashrack	uplooker/unguided	325 ft.	Slow	25	10	
SPB xducer_3	443	6° split	2	PH 6_B_N	235	705	112	35° from plane of trashrack	uplooker/guided	325 ft.	Slow	25	10	
SPB xducer_4	402	6° split	3	PH 6_B_S	235	705	42	63° from plane of trashrack	uplooker/unguided	325 ft.	Slow	25	10	
System IHR_Z_Spillway SPB													Pings/	Min./
Description	S/N	Xducer Type	Channel	Location	Cable Lengths	Length	SN	Mounting	Aiming angle	Elevation	Mux Type	Second	Hr.	
SPB Sounder	12					470	59							
Remote Multiplexer	14													
SPB xducer_1	421	10° split	3	Bay 1_S	157	627	86	2° downstream of vertical	pole-downlooker	435 ft.	Slow	25	10	
SPB xducer_2	412	10° split	1	Bay 2_N	157	627	85	2° downstream of vertical	pole-downlooker	435 ft.	Slow	25	10	
SPB xducer_3	413	10° split	2	Bay 3_M	470	940	80	2° downstream of vertical	pole-downlooker	435 ft.	Slow	25	10	
SPB xducer_4	404	10° split	0	Bay 4_N	470	940	109	2° downstream of vertical	pole-downlooker	435 ft.	Slow	25	10	
System IHR_T_spillway SPB													Pings/	Min./
Description	S/N	Xducer Type	Channel	Location	Cable Lengths	Length	SN	Mounting	Aiming angle	Elevation	Mux Type	Second	Hr.	
SPB Sounder	22					470	24							
Remote Multiplexer	13													
SPB xducer_1	436	10° split	0	Bay 5_S	235	705	48	2° downstream of vertical	pole-downlooker	435 ft.	Slow	25	10	
SPB xducer_2	437	10° split	1	Bay 6_M	235	705	78	2° downstream of vertical	pole-downlooker	435 ft.	Slow	25	10	
SPB xducer_3	406	10° split	2	Bay 8_N	235	705	75	2° downstream of vertical	pole-downlooker	435 ft.	Slow	25	10	
SPB xducer_4	407	10° split	3	Bay 10_S	470	940	81	2° downstream of vertical	pole-downlooker	435 ft.	Slow	25	10	
System IHR_A_Powerhouse SIB													Pings/	Min./
Description	S/N	Xducer Type	Channel	Location	Arm.	Deck	Total	Mounting	Aiming angle	Elevation	Mux Type	Second	Hr.	
SIB Sounder	42													
SIB xducer_1	105	6° single	0	PH 2_C_S	235	500	735	35° from plane of trashrack	uplooker/guided	325 ft.	Slow	25	10	
SIB xducer_2	104	6° single	1	PH 2_C_N	235	500	735	63° from plane of trashrack	uplooker/unguided	325 ft.	Slow	25	10	
SIB xducer_3	111	6° single	2	PH 5_A_N	235	500	735	35° from plane of trashrack	uplooker/guided	325 ft.	Slow	25	10	
SIB xducer_4	112	6° single	3	PH 5_A_S	235	500	735	63° from plane of trashrack	uplooker/unguided	325 ft.	Slow	25	10	
SIB xducer_5	519	10° single	4	Bay 7_S	235	500	735	2° downstream of vertical	pole-downlooker	435 ft.	Slow	25	10	
SIB xducer_6	520	10° single	5	Bay 9_M	235	500	735	2° downstream of vertical	pole-downlooker	435 ft.	Slow	25	10	

Static Transmit Power	Installed System	Channel	Echo-sounder Number	Trans-ducer Number and Phase (if split beams)	Calibrated Cable Length (ft)	Source Level (dB)	Maximum Output Voltage (dB)	Voltage of Largest On-axis Target at 20 dB per Volt (V)	40 logR Receiver Sensitivity (dB)	Target Strength of largest on-axis target of interest (db)	Calculated Receiver gain (dB)	Installed Cable Length (ft)	Difference in Cable Length Between Calibrated Cable and Installed Cable (ft)	Receiver Gain Adjusted for Difference in Cable Length (dB)	Source Level Adjusted for Difference in Cable Length (dB)	Receiver Sensitivity Adjusted for Difference in Cable Length (dB)	Target Strength of Smallest On-axis Target (dB)	Voltage of Smallest On-axis Target (dB)	Voltage of Smallest Target at 20 dB per Volt (V)	
-3	Z		12	404(x)	940	210.79	80	4.0	-113.78	-26	8.99	940	0	8.99	210.79	-113.78	-56	50	2.50	
	Z		12	404(y)	940	210.79	80	4.0	-113.78	-26	8.99	940	0	8.99	210.79	-113.78	-56	50	2.50	
	Z	00	12	404	940	210.79	80	4.0	-113.78	-26	8.99	940	0	8.99	210.79	-113.78	-56	50	2.50	
-3	Z		12	412(x)	627	212.64	80	4.0	-114.68	-26	8.04	627	0	8.04	212.64	-114.68	-56	50	2.50	
	Z		12	412(y)	627	212.62	80	4.0	-114.68	-26	8.06	627	0	8.06	212.62	-114.68	-56	50	2.50	
	Z	01	12	412	627	212.63	80	4.0	-114.68	-26	8.05	627	0	8.05	212.63	-114.68	-56	50	2.50	
-3	Z		12	413(x)	940	209.23	80	4.0	-115.14	-26	11.91	940	0	11.91	209.23	-115.14	-56	50	2.50	
	Z		12	413(y)	940	209.23	80	4.0	-115.14	-26	11.91	940	0	11.91	209.23	-115.14	-56	50	2.50	
	Z	02	12	413	940	209.23	80	4.0	-115.14	-26	11.91	940	0	11.91	209.23	-115.14	-56	50	2.50	
-3	Z		12	421(x)	627	212.84	80	4.0	-114.30	-26	7.46	627	0	7.46	212.84	-114.30	-56	50	2.50	
	Z		12	421(y)	627	212.87	80	4.0	-114.34	-26	7.47	627	0	7.47	212.87	-114.34	-56	50	2.50	
	Z	03	12	421	627	212.86	80	4.0	-114.32	-26	7.46	627	0	7.46	212.86	-114.32	-56	50	2.50	
-3	Z		12	435(x)	627	213.27	80	4.0	-113.36	-26	6.09	627	0	6.09	213.27	-113.36	-56	50	2.50	
	Z		12	435(y)	627	213.28	80	4.0	-113.36	-26	6.08	627	0	6.08	213.28	-113.36	-56	50	2.50	
	Z	spare	12	435	627	213.28	80	4.0	-113.36	-26	6.08	627	0	6.08	213.28	-113.36	-56	50	2.50	
-3	Z		12	435(x)	940	210.19	80	4.0	-113.50	-26	9.31	940	0	9.31	210.19	-113.50	-56	50	2.50	
	Z		12	435(y)	940	210.19	80	4.0	-113.52	-26	9.33	940	0	9.33	210.19	-113.52	-56	50	2.50	
	Z	spare	12	435	940	210.19	80	4.0	-113.51	-26	9.32	940	0	9.32	210.19	-113.51	-56	50	2.50	
-3	Z		12	413(x)	705	212.53	80	4.0	-114.32	-26	7.79	705	0	7.79	212.53	-114.32	-56	50	2.50	
	Z		12	413(y)	705	212.49	80	4.0	-114.32	-26	7.83	705	0	7.83	212.49	-114.32	-56	50	2.50	
	Z	spare	12	413	705	212.51	80	4.0	-114.32	-26	7.81	705	0	7.81	212.51	-114.32	-56	50	2.50	
***Sys Z transducers are 6 degree (?) transducers w/ 10 degree lenses																				
-4	X		20	426(x)	705	217.63	90	4.5	-108.44	-26	6.81	940	-235	8.91	216.73	-109.64	-56	60	3.00	
	X		20	426(y)	705	217.65	90	4.5	-108.44	-26	6.79	940	-235	8.89	216.75	-109.64	-56	60	3.00	
	X	00	20	426	705	217.64	90	4.5	-108.44	-26	6.80	940	-235	8.90	216.74	-109.64	-56	60	3.00	
-4	X		20	427(x)	705	217.77	90	4.5	-108.06	-26	6.29	940	-235	8.39	216.87	-109.26	-56	60	3.00	
	X		20	427(y)	705	217.76	90	4.5	-108.04	-26	6.28	940	-235	8.38	216.86	-109.24	-56	60	3.00	
	X	01	20	427	705	217.77	90	4.5	-108.05	-26	6.28	940	-235	8.39	216.86	-109.25	-56	60	3.00	
-4	X		20	428(x)	705	217.54	90	4.5	-108.56	-26	7.02	705	0	7.02	217.54	-108.56	-56	60	3.00	
	X		20	428(y)	705	217.53	90	4.5	-108.58	-26	7.05	705	0	7.05	217.53	-108.58	-56	60	3.00	
	X	02	20	428	705	217.54	90	4.5	-108.57	-26	7.03	705	0	7.03	217.54	-108.57	-56	60	3.00	
-4	X		20	441(x)	705	217.23	90	4.5	-107.28	-26	6.05	705	0	6.05	217.23	-107.28	-56	60	3.00	
	X		20	441(y)	705	217.24	90	4.5	-107.24	-26	6.00	705	0	6.00	217.24	-107.24	-56	60	3.00	
	X	Spare	20	441	705	217.24	90	4.5	-107.26	-26	6.02	705	0	6.02	217.24	-107.26	-56	60	3.00	
-4	X		20	400(x)	705	216.80	90	4.5	-108.68	-26	7.88	705	0	7.88	216.80	-108.68	-56	60	3.00	
	X		20	400(y)	705	216.83	90	4.5	-108.64	-26	7.81	705	0	7.81	216.83	-108.64	-56	60	3.00	
	X	03	20	400	705	216.82	90	4.5	-108.66	-26	7.84	705	0	7.84	216.82	-108.66	-56	60	3.00	
-4	X		20	401(x)	705	216.68	90	4.5	-108.44	-26	7.76	705	0	7.76	216.68	-108.44	-56	60	3.00	
	X		20	401(y)	705	216.70	90	4.5	-108.42	-26	7.72	705	0	7.72	216.70	-108.42	-56	60	3.00	
	X	Spare	20	401	705	216.69	90	4.5	-108.43	-26	7.74	705	0	7.74	216.69	-108.43	-56	60	3.00	

Static Transmit Power	Installed System	Channel	Echo-sounder Number	Trans-ducer Number and Phase (if split beams)	Calibrated Cable Length (ft)	Source Level (dB)	Maximum Output Voltage (dB)	Voltage of Largest On-axis Target at 20 dB per Volt (V)	40 logR Receiver Sensitivity (dB)	Target Strength of largest on-axis target of interest (db)	Calculated Receiver gain (dB)	Installed Cable Length (ft)	Difference in Cable Length Between Calibrated Cable and Installed Cable (ft)	Receiver Gain Adjusted for Difference in Cable Length (dB)	Source Level Adjusted for Difference in Cable Length (dB)	Receiver Sensitivity Adjusted for Difference in Cable Length (dB)	Target Strength of Smallest On-axis Target (dB)	Voltage of Smallest On-axis Target (dB)	Voltage of Smallest On-axis Target at 20 dB per Volt (V)
-4	Y		27	429(x)	705	217.98	90	4.5	-107.86	-26	5.88	705	0	5.88	217.98	-107.86	-56	60	3.00
	Y		27	429(y)	705	218.00	90	4.5	-107.88	-26	5.88	705	0	5.88	218.00	-107.88	-56	60	3.00
	Y	00	27	429	705	217.99	90	4.5	-107.87	-26	5.88	705	0	5.88	217.99	-107.87	-56	60	3.00
-4	Y		27	430(x)	705	217.90	90	4.5	-108.26	-26	6.36	705	0	6.36	217.90	-108.26	-56	60	3.00
	Y		27	430(y)	705	217.90	90	4.5	-108.26	-26	6.36	705	0	6.36	217.90	-108.26	-56	60	3.00
	Y	01	27	430	705	217.90	90	4.5	-108.26	-26	6.36	705	0	6.36	217.90	-108.26	-56	60	3.00
-4	Y		27	443(x)	705	217.26	90	4.5	-108.18	-26	6.92	705	0	6.92	217.26	-108.18	-56	60	3.00
	Y		27	443(y)	705	217.25	90	4.5	-108.22	-26	6.97	705	0	6.97	217.25	-108.22	-56	60	3.00
	Y	02	27	443	705	217.26	90	4.5	-108.20	-26	6.94	705	0	6.94	217.26	-108.20	-56	60	3.00
-4	Y		27	402(x)	705	217.07	90	4.5	-108.72	-26	7.65	705	0	7.65	217.07	-108.72	-56	60	3.00
	Y		27	402(y)	705	217.07	90	4.5	-108.72	-26	7.65	705	0	7.65	217.07	-108.72	-56	60	3.00
	Y	03	27	402	705	217.07	90	4.5	-108.72	-26	7.65	705	0	7.65	217.07	-108.72	-56	60	3.00
-4	Y		27	441(x)	705	217.22	90	4.5	-107.28	-26	6.06	705	0	6.06	217.22	-107.28	-56	60	3.00
	Y		27	441(y)	705	217.22	90	4.5	-107.28	-26	6.06	705	0	6.06	217.22	-107.28	-56	60	3.00
	Y	Spare	27	441	705	217.22	90	4.5	-107.28	-26	6.06	705	0	6.06	217.22	-107.28	-56	60	3.00
-4	Y		27	403(x)	705	216.92	90	4.5	-108.00	-26	7.08	705	0	7.08	216.92	-108.00	-56	60	3.00
	Y		27	403(y)	705	216.92	90	4.5	-108.02	-26	7.10	705	0	7.10	216.92	-108.02	-56	60	3.00
	Y	Spare	27	403	705	216.92	90	4.5	-108.01	-26	7.09	705	0	7.09	216.92	-108.01	-56	60	3.00
-4	Y		27	405(x)	705	217.12	90	4.5	-108.02	-26	6.90	705	0	6.90	217.12	-108.02	-56	60	3.00
	Y		27	405(y)	705	217.14	90	4.5	-108.04	-26	6.90	705	0	6.90	217.14	-108.04	-56	60	3.00
	Y	Spare	27	405	705	217.13	90	4.5	-108.03	-26	6.90	705	0	6.90	217.13	-108.03	-56	60	3.00
-3	T		22	436(x)	705	215.46	80	4.0	-112.74	-26	3.28	705	0	3.28	215.46	-112.74	-56	50	2.50
	T		22	436(y)	705	215.48	80	4.0	-112.76	-26	3.28	705	0	3.28	215.48	-112.76	-56	50	2.50
	T	00	22	436	705	215.47	80	4.0	-112.75	-26	3.28	705	0	3.28	215.47	-112.75	-56	50	2.50
-3	T		22	437(x)	705	215.30	80	4.0	-113.26	-26	3.96	705	0	3.96	215.30	-113.26	-56	50	2.50
	T		22	437(y)	705	215.29	80	4.0	-113.28	-26	3.99	705	0	3.99	215.29	-113.28	-56	50	2.50
	T	01	22	437	705	215.30	80	4.0	-113.27	-26	3.97	705	0	3.97	215.30	-113.27	-56	50	2.50
-3	T		22	406(x)	705	214.44	80	4.0	-113.62	-26	5.18	705	0	5.18	214.44	-113.62	-56	50	2.50
	T		22	406(y)	705	214.43	80	4.0	-113.64	-26	5.21	705	0	5.21	214.43	-113.64	-56	50	2.50
	T	02	22	406	705	214.44	80	4.0	-113.63	-26	5.19	705	0	5.19	214.44	-113.63	-56	50	2.50
-3	T		22	407(x)	940	211.18	80	4.0	-115.12	-26	9.94	940	0	9.94	211.18	-115.12	-56	50	2.50
	T		22	407(y)	940	211.19	80	4.0	-115.10	-26	9.91	940	0	9.91	211.19	-115.10	-56	50	2.50
	T	03	22	407	940	211.19	80	4.0	-115.11	-26	9.92	940	0	9.92	211.19	-115.11	-56	50	2.50

Installed System	Channel	Echo-sounder Number	Transducer Number and Phase (if split beams)	Calibrated Cable Length (ft)	Source Level (dB) - 5 dB Static Transmit	Maximum Output Voltage (dB)	Voltage of Largest On-axis Target at 20 dB per Volt (V)	40 logR Receiver Sensitivity (dB)	Target Strength of largest on-axis target of interest (db)	Calculated Receiver gain (dB)	Installed Cable Length (ft)	Difference in Cable Length							Voltage of Smallest On-axis Target at 20 dB per Volt (V)
												Difference Between Calibrated Cable and Installed Cable (ft)	Receiver Gain Adjusted for Difference in Cable Length (dB)	Source Level Adjusted for Difference in Cable Length (dB)	Receiver Sensitivity Adjusted for Difference in Cable Length (dB)	Target Strength of Smallest On-axis Target (dB)	Voltage of Smallest On-axis Target (dB)		
A	0	42	105	985	214.89	90	4.5	-104.18	-26	5.29	735	250	3.69	216.17	-103.85	-56	60	3.00	
A	1	42	104	985	215.00	90	4.5	-104.02	-26	5.02	735	250	3.42	216.28	-103.69	-56	60	3.00	
A	2	42	111	735	216.63	90	4.5	-104.86	-26	4.23	735	0	4.23	216.63	-104.86	-56	60	3.00	
A	3	42	112	735	216.66	90	4.5	-104.72	-26	4.06	735	0	4.06	216.66	-104.72	-56	60	3.00	
A		42	116	735	216.39	90	4.5	-105.40	-26	5.01	500	235	3.51	217.59	-105.09	-56	60	3.00	
A		42	110	735	216.68	90	4.5	-104.92	-26	4.24	500	235	2.74	217.88	-104.61	-56	60	3.00	
A		42	114	985	215.24	90	4.5	-104.36	-26	5.12	750	235	3.62	216.44	-104.05	-56	60	3.00	
A		42	115	735	216.75	90	4.5	-104.54	-26	3.79	500	235	2.29	217.95	-104.23	-56	60	3.00	
A		42	108	735	216.51	90	4.5	-105.02	-26	4.51	500	235	3.01	217.71	-104.71	-56	60	3.00	
A	4	42	519	735	216.49	90	4.5	-104.46	-26	3.97	735	0	3.97	216.49	-104.46	-56	60	3.00	
A		42	520	735	216.72	90	4.5	-104.36	-26	3.64	735	0	3.64	216.72	-104.36	-56	60	3.00	
A	5	42	521	985	214.23	90	4.5	-104.02	-26	5.79	735	250	4.19	215.51	-103.69	-56	60	3.00	

Appendix G
Equipment Diagrams

Appendix G

Equipment Diagrams

Complete schematics of the hydroacoustic equipment are shown below. The physical layout of each structure (powerhouse and spillway) is followed by wiring diagrams for each system. Cabling and connections are also shown for overall study reproducibility.

2003 Ice Harbor Dam Powerhouse Hydroacoustic System Layout

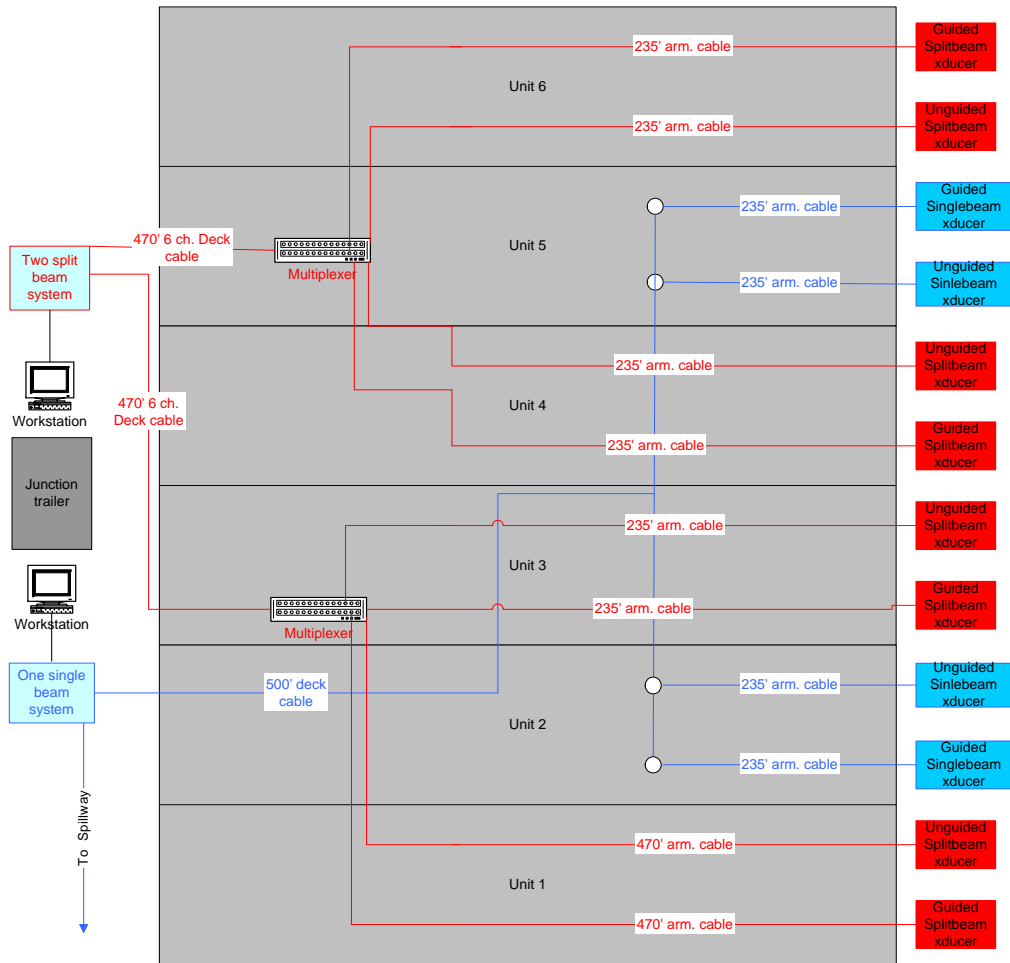


Figure 1. Physical layout of the hydroacoustic deployment at the powerhouse.

**Ice Harbor Dam Powerhouse
Splitbeam System "X" at Units 1 and 3**

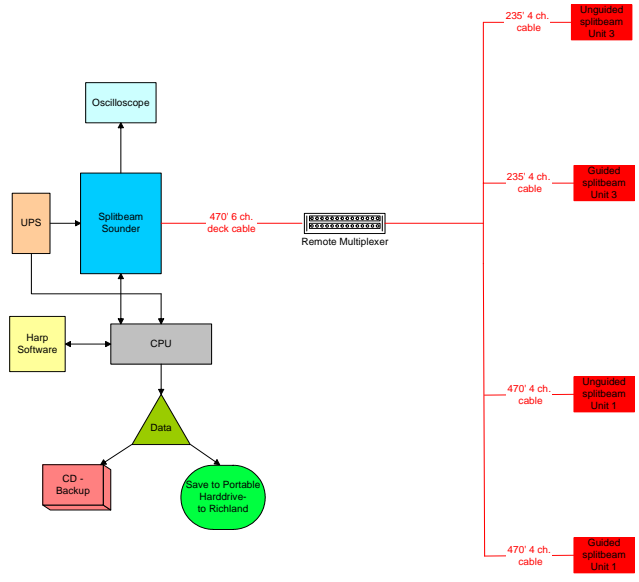


Figure 2. Wiring diagram of System X.

**Ice Harbor Dam Powerhouse
Splitbeam System "Y" at Units 4 and 6**

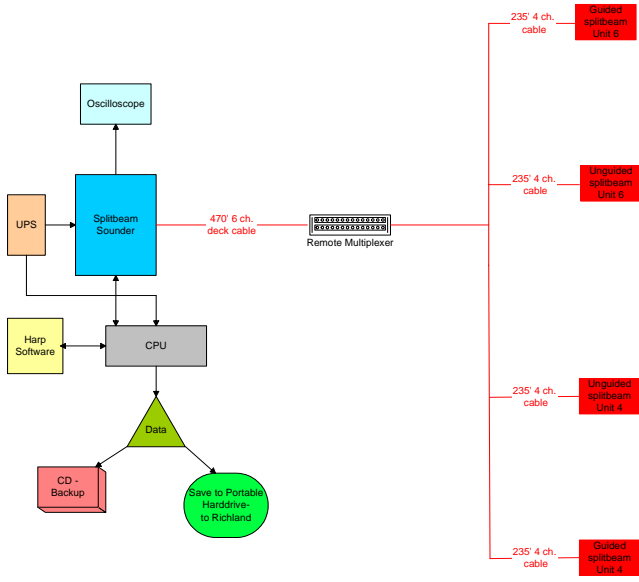


Figure 3. Wiring diagram of System Y.

Ice Harbor Dam Singlebeam System "A" at Units 2 and 5 and Spillbays 7 and 9

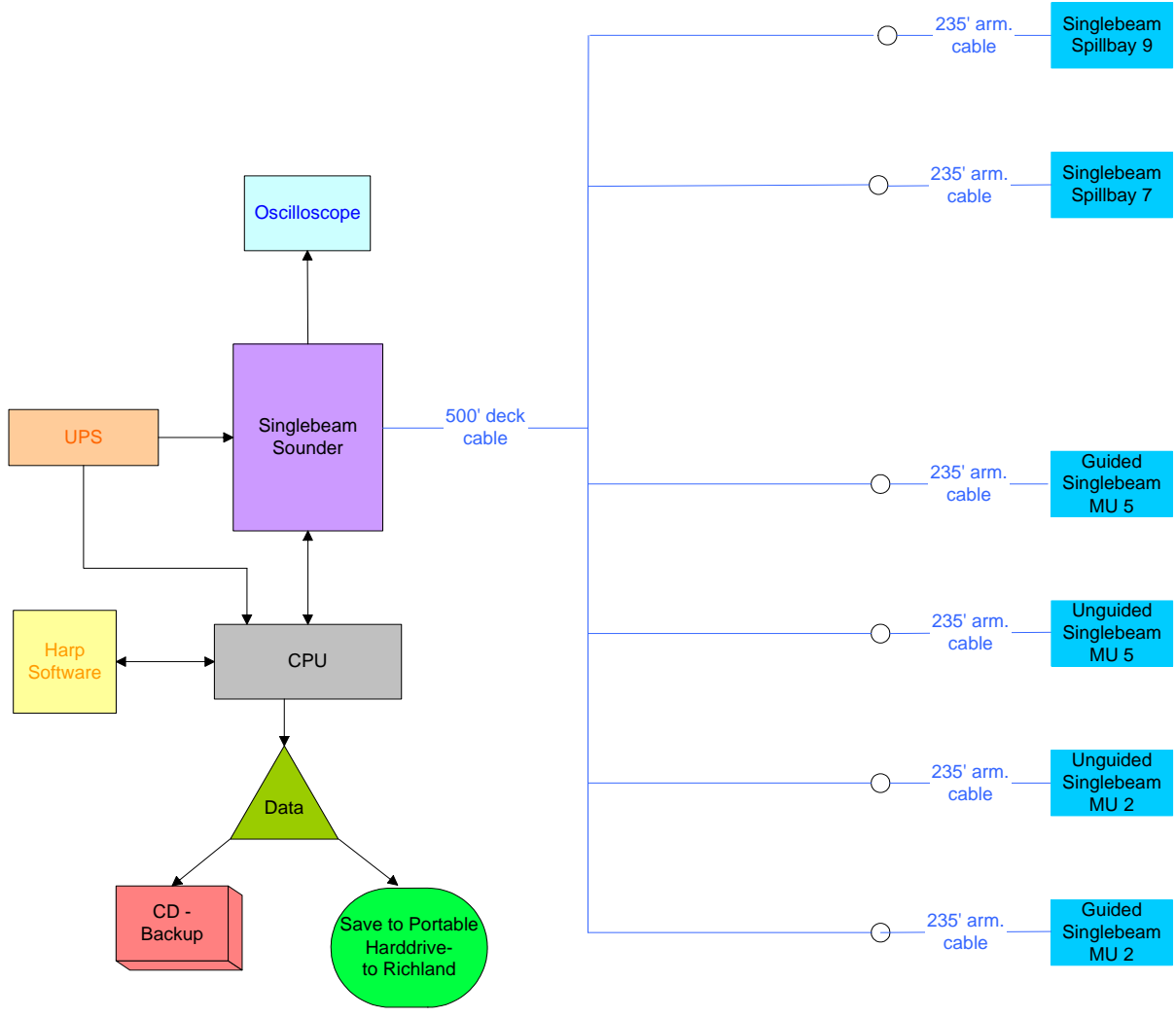


Figure 4. Wiring diagram of System A.

2003 Ice Harbor Dam Spillway
Hydroacoustic System Layout

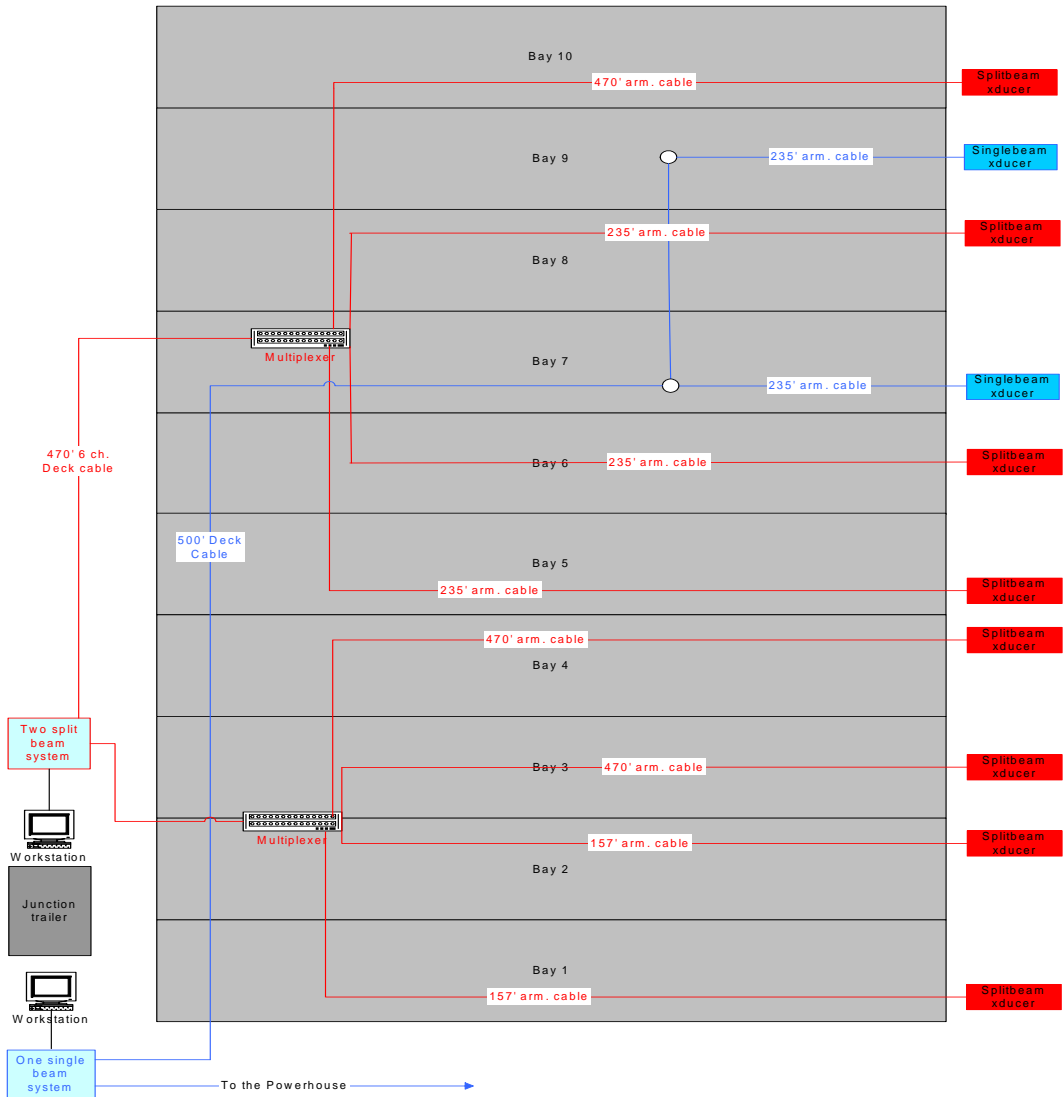


Figure 5. Physical layout of the hydroacoustic deployment at the spillway.

**Ice Harbor Dam Spillway
Splitbeam System "Z" at Spillbay 1, 2, 3, and 4**

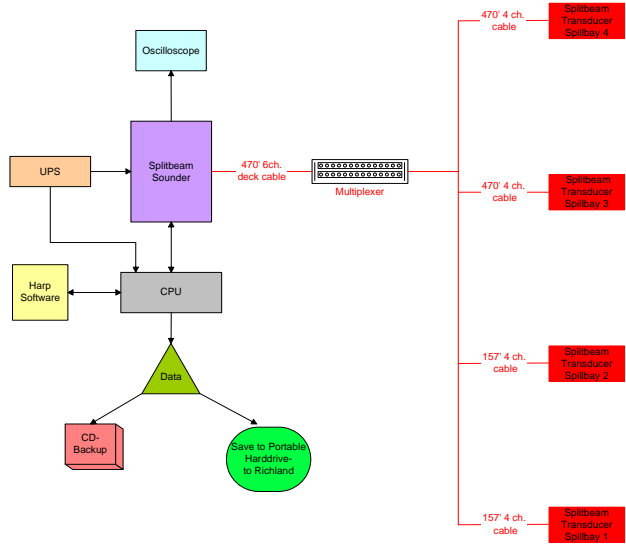


Figure 6. Wiring diagram of System Z.

**Ice Harbor Dam Spillway
Splitbeam System "T" at Spillbay 5, 6, 8, and 10**

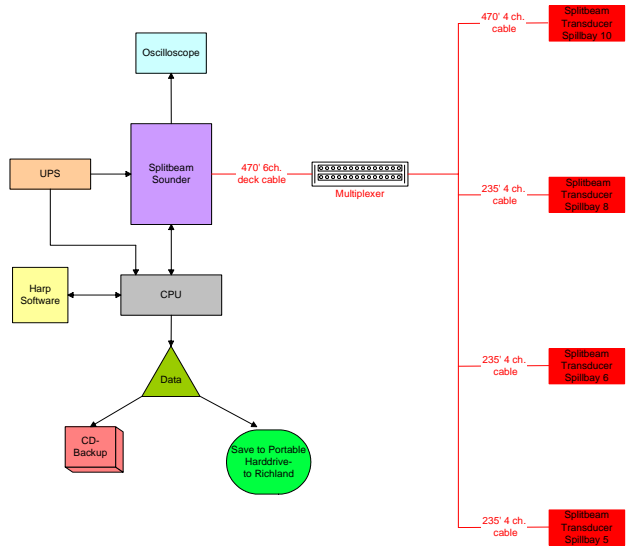


Figure 7. Wiring diagram of System T.